

MODELING PERMIAN PETROLEUM SYSTEM OF NORTHEAST  
NETHERLANDS: HYDROCARBON GENERATION AND MIGRATION

A THESIS SUBMITTED TO  
THE GRADUATE SCHOOL OF NATURAL AND APPLIED SCIENCES  
OF  
MIDDLE EAST TECHNICAL UNIVERSITY

BY

ESRA MERT-GAUTHIER

IN PARTIAL FULFILLMENT OF THE REQUIREMENTS  
FOR  
THE DEGREE OF MASTER OF SCIENCE  
IN  
GEOLOGICAL ENGINEERING

SEPTEMBER 2010

Approval of the thesis:

**MODELING PERMIAN PETROLEUM SYSTEM OF NORTHEAST  
NETHERLANDS: HYDROCARBON GENERATION AND MIGRATION**

submitted by **ESRA MERT-GAUTHIER** in partial fulfillment of the requirements  
for the degree of **Master of Science in Geological Engineering Department,**  
**Middle East Technical University** by,

Prof. Dr. Canan Özgen  
Dean, **Graduate School of Natural and Applied Sciences** \_\_\_\_\_

Prof. Dr. Zeki Çamur  
Head of Department, **Geological Engineering** \_\_\_\_\_

Assoc. Prof. Dr. Nuretdin Kaymakçı  
Supervisor, **Geological Engineering Dept., METU** \_\_\_\_\_

Assist. Prof. Dr. A. Arda Özacar  
Co-Supervisor, **Geological Engineering Dept., METU** \_\_\_\_\_

**Examining Committee Members:**

Prof. Dr. Erdin Bozkurt  
Geological Engineering Dept., METU \_\_\_\_\_

Assoc. Prof. Dr. Nuretdin Kaymakçı  
Geological Engineering Dept., METU \_\_\_\_\_

Assist. Prof. Dr. A. Arda Özacar  
Geological Engineering Dept., METU \_\_\_\_\_

Dr. Özgür Sipahioğlu  
TPAO \_\_\_\_\_

Dr. Sadun Arzuman  
Schlumberger \_\_\_\_\_

**Date: 17.09.2010**

**I hereby declare that all information in this document has been obtained and presented in accordance with academic rules and ethical conduct. I also declare that, as required by these rules and conduct, I have fully cited and referenced all material and results that are not original to this work.**

Name, Last name: Esra Mert-Gauthier

Signature:

# **ABSTRACT**

## **MODELING PERMIAN PETROLEUM SYSTEM OF NETHERLANDS: HYDROCARBON GENERATION AND MIGRATION**

Mert-Gauthier, Esra

M.Sc., Department of Geological Engineering

Supervisor: Assoc. Prof. Dr. Nuretdin Kaymakçı

Co-Supervisor: Assist. Prof. Dr. A. Arda Özacar

September 2010, 76 pages

Groningen Gas Field is located within the southern part of the South Permian Basin in the northeast Netherlands. Since several wells have been producing from the Carboniferous-Permian Petroleum System, the field is considered as mature for hydrocarbon exploration. More detailed work is necessary to evaluate further exploration and development opportunities. Thus, evaluation of the subsurface has been carried out as part of the petroleum system concept by using the basin modeling.

In this study, seismic interpretation was performed by using 3-dimensional seismic and borehole data with Petrel software in order to understand stratigraphy and structural settings of the area. PetroMod basin analysis software has been used for 1-dimensional and 2-dimensional basin modeling study by integrating interpreted geophysical, geological and geochemical data.

Results show that the most recognized traps were formed during pre-Zechstein, and the major generation-migration and accumulation of hydrocarbon commenced during Middle Jurassic and continues to the present time. Since the timing of main hydrocarbon generation varies spatially and has begun after trap formation, both early and late migration enhances the potential of the porous Upper Rotliegend reservoirs. Prospective hydrocarbon traps may occur in the southwestern regions of the basin due to shallower depth of burial. On the other hand, all local structural highs that formed as a result of salt movement create potential traps in the region.

Keywords: Petroleum system, basin modeling, Groningen Gas Field, Netherlands

# ÖZ

## KUZEYDOĞU HOLLANDA, PERMİYEN PETROL SİSTEMİ MODELLEMESİ: HİDROKARBON OLUŞUMU VE GÖÇÜ

Mert-Gauthier, Esra

Yüksek Lisans, Jeoloji Mühendisliği Bölümü

Tez Yöneticisi: Doç. Dr. Nuretdin Kaymakçı

Ortak Tez Yöneticisi: Yrd. Doç. Dr. A. Arda Özacar

Eylül 2010, 76 sayfa

Groningen Gaz Sahası, Güney Permiyen Havzası'nın güneyinde, Hollanda'nın kuzeydoğusunda yer almaktadır. Karbonifer-Permiyen Petrol Sistemi'nden üretim yapan birçok kuyu olduğu için, saha hidrokarbon aramacılığı açısından olgun kabul edilmektedir. İlerideki aramacılık ve üretim fırsatlarını değerlendirmek için daha ayrıntılı çalışmalar yapılması gerekmektedir. Bu nedenle havza, petrol sistemi konsepti çerçevesinde havza modelleme kullanılarak değerlendirilmiştir.

Bu çalışmada, 3 boyutlu sismik ve sondaj verileri kullanılarak, Petrel programı ile bölgenin stratigrafi ve yapısal jeolojisini anlamak için sismik yorumlama yapılmıştır. Petromod programı ile jeofizik, jeoloji ve jeokimya verileri birleştirilerek 1 ve 2 boyutlu havza modellemesi yapılmıştır.

Sonuçlar, kapanımların büyük çoğunluğunun Zechstein öncesi birimlerde olduğunu, hidrokarbon oluşum, göç ve kapanlanmasının Orta Jura döneminde başlayıp günümüze kadar devam ettiğini göstermektedir. Hidrokarbon oluşumunun zirve yaptığı zaman alansal olarak değişiklik gösterdiği için ve kapanım oluşumundan sonraki bir zamana denk geldiği için, hem erken hem de geç göçler, gözenekli Üst Rotliegend rezervuarının potansiyelini arttırmıştır. Hidrokarbon kapanımlarının, daha az derin olan havzanın güneybatısında oluşması muhtemeldir. Diğer yandan, tuzun hareketi sonucu oluşan tüm yapısal yükseltiler bölgede kapanım oluşturma potansiyeline sahiptir.

Anahtar kelimeler: Petrol sistemi, havza modelleme, Groningen Gaz Sahası, Hollanda

## ACKNOWLEDGEMENTS

I would like to thank to my supervisor Assoc. Prof. Dr. Nuretdin Kaymakçı for his constructive comments and essential advices throughout my M.S. studies.

I appreciate the invaluable contributions of Sadun Arzuman, Kıvanç Yücel, İbrahim Youssef Mriheel, Ömer Aksu, Candida Menezes de Jesus and Victor Hugo Guimaraes Pinto.

Special thanks are extended to my managers Paulo Moreira de Carvalho and Hercules Tadeu Ferreira da Silva for their concrete support and allowing me to use Petrobras resources to complete my thesis.

Furthermore, I acknowledge the committee of the thesis, Prof. Dr. Erdin Bozkurt and Assist. Prof. Dr. A. Arda Özacar Bozkurt (Middle East Technical University), Dr. Özgür Sipahioğlu (Turkish Petroleum Company) and Dr. Sadun Arzuman (Schlumberger) for their thoughtful comments and suggestions.

I am also grateful to my parents Nazmiye and Musa Mert for being with me whenever I need and for their patience and encouragement.

Finally the one, who carries the real load of my hard days, share the best moments and support whatever I do with his artistic way, my husband Matthieu Gauthier deserves the most appreciation.

# TABLE OF CONTENTS

ABSTRACT .....	iv
ÖZ .....	v
ACKNOWLEDGEMENTS .....	vi
TABLE OF CONTENTS .....	vii
LIST OF TABLES .....	ix
LIST OF FIGURES .....	x
CHAPTERS	
1. INTRODUCTION .....	1
1.1 Purpose and Scope .....	1
1.2 Location .....	2
1.3 Exploration History and Previous Studies .....	4
1.4 Available Data and Methodology .....	5
1.5 Geological Background: Tectonic Setting and Basin Evolution .....	8
2. PETROLUEM SYSTEMS .....	13
2.1 Source Rocks .....	16
2.2 Reservoir Rocks .....	18
2.3 Seal Rocks .....	19
2.4 Overburden Rocks .....	21
2.5 Trap and Play Types .....	22
3. DATA .....	24
3.1 Seismic Data .....	24
3.2 Seismic Interpretation .....	26
4. 1D MATURITY MODELING .....	35

4.1	Introduction and Data Processing .....	35
4.2	Inputs of the Model.....	37
4.2.1	Geological Data.....	37
4.2.2	Geochemical and Thermal Data.....	38
4.2.3	Boundary Conditions .....	38
4.3	Calibrations.....	39
4.4	Sensitivity Analysis .....	43
4.4.1	Kinetic Model Selection.....	43
4.4.2	Source Rock Thickness Selection .....	45
4.5	1D Modeling Results .....	47
5.	2D BASIN MODELING.....	49
5.1	Introduction and Data Processing .....	49
5.2	Inputs of the Model.....	50
5.2.1	Geophysical, Geological and Geochemical Data .....	50
5.2.2	Simulation – Model Run .....	54
5.3	2D Model Results .....	54
6.	SUMMARY AND CONCLUSIONS .....	59
	REFERENCES .....	61
	APPENDICES.....	64
	A: Literature Data Used in the Model.....	64
	B: Interpreted Horizons Maps.....	69

## LIST OF TABLES

### TABLES

<b>Table 3.1.</b> Interval velocities used for the time to depth conversion of the seismic volume (Van Dalfsen et al., 2006).....	<b>26</b>
<b>Table 4.1.</b> Stratigraphic and age data from wells RDW-1 and USQ-1 (intervals are same as Figure 3.2, Q stands for Quaternary).....	<b>37</b>
<b>Table 4.2.</b> Boundary conditions.....	<b>39</b>
<b>Table 4.3.</b> Vitrinite reflectance ( $R_o$ ) values used for calibration (NL Oil and Gas Portal, on-line, 2009). ....	<b>41</b>
<b>Table 4.4.</b> Obtained and calibrated paleo-heat flow values (*Verweij, 2003) (HF: Heat flow).....	<b>41</b>
<b>Table 5.1.</b> Classification of petroleum (Hantschel and Kauerauf, 2009).....	<b>57</b>

# LIST OF FIGURES

## FIGURES

<b>Figure 1.1.</b> The location and facies distribution of North German Basin in Northwest Europe, which comprises North and South Permian basins (modified from Geluk, 2007). .....	<b>2</b>
<b>Figure 1.2.</b> Location of the study area over tectonic map of Netherlands (Modified from Gent et al., 2008; Limburg Group was removed).....	<b>3</b>
<b>Figure 1.3.</b> Location of 3D seismic data and boreholes in the study area (inline and crossline interval is 25m). ....	<b>6</b>
<b>Figure 1.4.</b> Flow chart indicating steps of the study. ....	<b>7</b>
<b>Figure 1.5.</b> Generalized columnar section and major tectonic events in the northern Netherlands (modified from Geluk 2007). Red box indicates the units present in the study area.....	<b>9</b>
<b>Figure 1.6</b> Stratigraphic scheme for the Upper Carboniferous (Silesian) deposits in the eastern Netherlands (after Van Adrichem Boogaert & Kouwe, 1994). Note that these units are the main source rocks in the region. ....	<b>12</b>
<b>Figure 2.1.</b> Generalized stratigraphical chart of Southern Northern Sea sector of the Northwest German Basin (modified after Boigk 1981, Van Adrichem Boogaert 1993, Bachmann & Hoffmann 1997 in IHS 2009). The Carboniferous-Rotliegend Petroleum System which is the main concern of this study is indicated with a red box.....	<b>14</b>
<b>Figure 2.2.</b> Events chart for the Carboniferous-Rotliegend Petroleum System in South Permian Basin (Gautier, 2003). ....	<b>15</b>
<b>Figure 2.3.</b> Subcrop of source rocks and cross-section along line XY (adopted from Buggenum & den Hartog Jager, 2007). ....	<b>17</b>
<b>Figure 2.4.</b> Facies distribution (a) and isopach map (b) of Upper Rotliegend Group. CNB: Central Netherlands Basin; WNB: West Netherlands Basin; TIJH: Texel-	

IJsselmeer High; MNSH: Mid North Sea High; RFH: Ringkøbing-Fyn High. Study area is indicated with red rectangle. Black arrow shows North (adopted from Gerling et al., 1999a).....	18
<b>Figure 2.5.</b> Facies distribution and characteristics of Zechstein Group. The facies in the study area is indicated with yellow rectangle (Geluk, 2007). .....	19
<b>Figure 2.6.</b> Subcrop map below the Zechstein Upper Claystone Formation showing distribution of Zechstein cycles (after Geluk 2007). Zechstein is absent in yellow areas. Study area is indicated with blue rectangle. GH: Groningen High, MNSH: Mid North Sea High, RO: Rotliegend Group. Black arrow shows North.....	20
<b>Figure 2.7.</b> Play type and overburden rocks of the study area. Red box indicates the units present in the study area. Note that Jurassic Altona Group is absent in the study area (modified from Geluk 2007). .....	21
<b>Figure 2.8.</b> Depth to the base of overburden rocks. Green rectangle indicates the study area. Note that it is also equal to the isopach of the overburden. ....	22
<b>Figure 2.9.</b> Northwest German Basin, chart showing cumulative liquid and gas reserves per play between 1934 and 2009. Stt: stratigraphic; Str: structural (IHS, 2009). .....	23
<b>Figure 3.1.</b> Interval velocity vs. lithology cross plot. The lithologies are overlapping. Therefore, direct identification from the P-wave velocities is difficult. Thus, additional information is necessary for discrimination (Veeken, 2007). .....	25
<b>Figure 3.2.</b> (a-b) Inline 373, (c-d) inline 523, (e-f) inline 698, raw and interpreted seismic sections. Note that inline and crossline intervals are 25 m.....	27
<b>Figure 3.3.</b> (a-b) Crossline 645, (c-d) crossline 764, (e-f) crossline 1014, raw and interpreted seismic sections. Note that inline and crossline intervals are 25 m. ....	28
<b>Figure 3.4.</b> Major unconformities in the study area (Abbreviations and location of the seismic section are same as Figure 3.2). .....	29
<b>Figure 3.5.</b> (a) Perspective view of alignments of Permian faults, arrow shows North and (b) a representative cross-section illustrating the Permian and younger faults. Location of the seismic section is same as Figures 3.2.....	30

<b>Figure 3.6.</b> (a) Inline 523 and (b) crossline 1014 in time and depth respectively. Location and scale of the seismic sections are same as Figure 3.2. ....	<b>31</b>
<b>Figure 3.7.</b> Velocity model maps (a) top Carboniferous, (b) top Rotliegend, (c) top Permian, (d) top Rijnland, (e) top Chalk and (f) top North Sea Group. Green arrow shows North.....	<b>32</b>
<b>Figure 3.8.</b> Time and depth maps of interpreted horizons (a-c) time maps of Top Permian (top Zechstein), top Rotliegend, and top Carboniferous and (d-f) depth maps of same horizons, respectively. Horizontal axes are x5 exaggerated. Green arrows show North (see Appendix B, for their higher resolution versions).....	<b>33</b>
<b>Figure 3.9.</b> (a-c) Time maps of base Rijnland, Chalk and North Sea Groups and (d-f) their corresponding depth maps. Arrows show North (see Appendix B for their higher resolution versions).....	<b>34</b>
<b>Figure 4.1.</b> Map showing the Groningen Gas Field and study area. Boreholes used in the model are highlighted by circles (IHS, 2009).....	<b>36</b>
<b>Figure 4.2.</b> Porosity calibration of RDW-1 well.....	<b>40</b>
<b>Figure 4.3.</b> Heat-flow calibration with temperature; (a) before calibration, (b) after calibration.....	<b>40</b>
<b>Figure 4.4.</b> Maturity-paleoheat flow match of RDW-1 before and after calibration respectively.....	<b>42</b>
<b>Figure 4.5.</b> Maturity-paleoheat flow match of USQ-1 before and after calibration respectively.....	<b>42</b>
<b>Figure 4.6.</b> Burial history and hydrocarbon zones with kinetic model of Ungerer (1990). .....	<b>44</b>
<b>Figure 4.7.</b> Burial history and hydrocarbon zones with kinetic model of Behar et al. (1997). ....	<b>44</b>
<b>Figure 4.8.</b> Burial history and hydrocarbon zones with kinetic model of Vandenbroucke et al. (1999).....	<b>45</b>
<b>Figure 4.9.</b> Burial history and hydrocarbon zones with 700 m source rock thickness. ....	<b>46</b>

<b>Figure 4.10.</b> Burial history and hydrocarbon zones with 1250 m source rock thickness. .....	<b>46</b>
<b>Figure 4.11.</b> Burial history and hydrocarbon zones with 2100 m source rock thickness. .....	<b>47</b>
<b>Figure 4.12.</b> Burial history and hydrocarbon zones.....	<b>48</b>
<b>Figure 4.13.</b> Graph showing time of total generated and expelled hydrocarbon from RDW-1 well. Note that the main hydrocarbon generation is during the Jurassic rifting phase and the main expulsion is during Alpine collision.....	<b>48</b>
<b>Figure 5.1:</b> Data processing sequence in PetroBuilder (PetroMod, Tutorial Version 11, 2009). .....	<b>49</b>
<b>Figure 5.2.</b> Crossline 1014 used for modeling purpose, pre-grid and grid-based sections respectively (abbreviations are same as Figure 3.2).....	<b>51</b>
<b>Figure 5.3.</b> Erosion building (Red zigzag lines show unconformities).....	<b>52</b>
<b>Figure 5.4.</b> Simulation preview showing the evolution of the basin in time.....	<b>53</b>
<b>Figure 5.5.</b> 2D model results of hydrocarbon zonation and accumulations in geological time. ....	<b>55</b>
<b>Figure 5.6.</b> Accumulations in reservoir and surface conditions respectively.....	<b>56</b>
<b>Figure 5.7.</b> Graph showing total hydrocarbon generated and expelled as a result of 2D model.....	<b>57</b>
<b>Figure 5.8.</b> Migration pathways and accumulation of hydrocarbon. Red arrows show the up-dip migration. ....	<b>58</b>
<b>Figure 6.1.</b> Petroleum system event chart of the study area.....	<b>60</b>

# CHAPTER 1

## INTRODUCTION

### 1.1 Purpose and Scope

An understanding of the basin evolution and related petroleum system is essential in hydrocarbon exploration and exploitation. Petroleum system starts with deposition of sedimentary rocks into a basin and continues with subsequent accommodation, burial and deformation. Basin modeling involves in numerically reconstruction of rock packages until the hydrocarbon network forms which is then modeled as petroleum system (Magoon, 2009).

Quantitative basin analysis and modeling help to understand the timing, depth and extend of hydrocarbon generation and migration, which provide constraints for the hydrocarbon potential of a basin. In this regard, the aim of this thesis is to evaluate the petroleum potential of a part of Groningen Gas Field located within the southern part of the South Permian Basin in the northeast Netherlands (Figure 1.1) and to provide a geological model to serve as a guide for the future exploration programs.

The main objectives are:

- to investigate the thermal maturation history of the study area,
- to determine the timing of hydrocarbon generation and expulsion,
- to interpret the hydrocarbon migration and possible accumulations,
- to integrate the results with the previous works.

Although numerous exploration and production wells have been drilled, continuous new discoveries indicate great potential of significant amount of hydrocarbon, especially gas, yet to be found (Jager and Geluk, 2007). Therefore, this study intends to provide new insights for future exploration programs in the region.

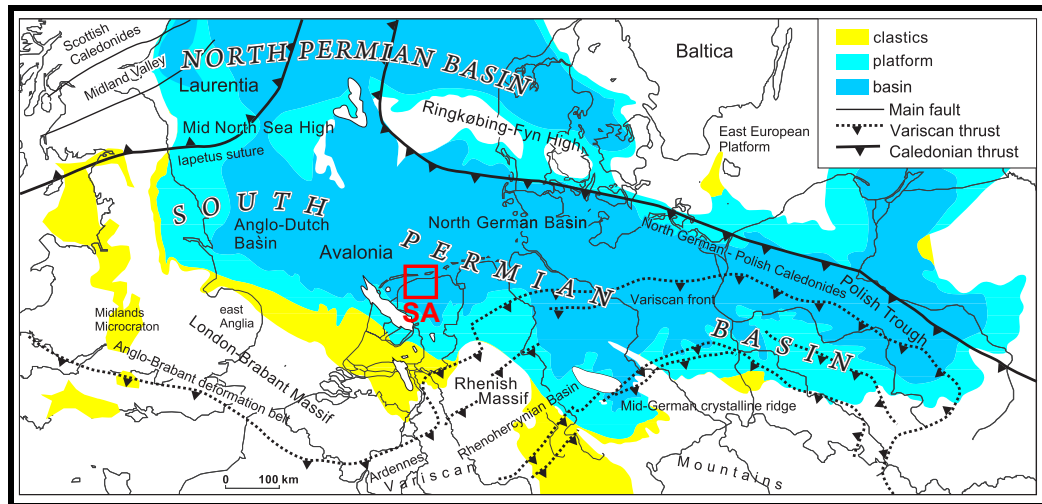
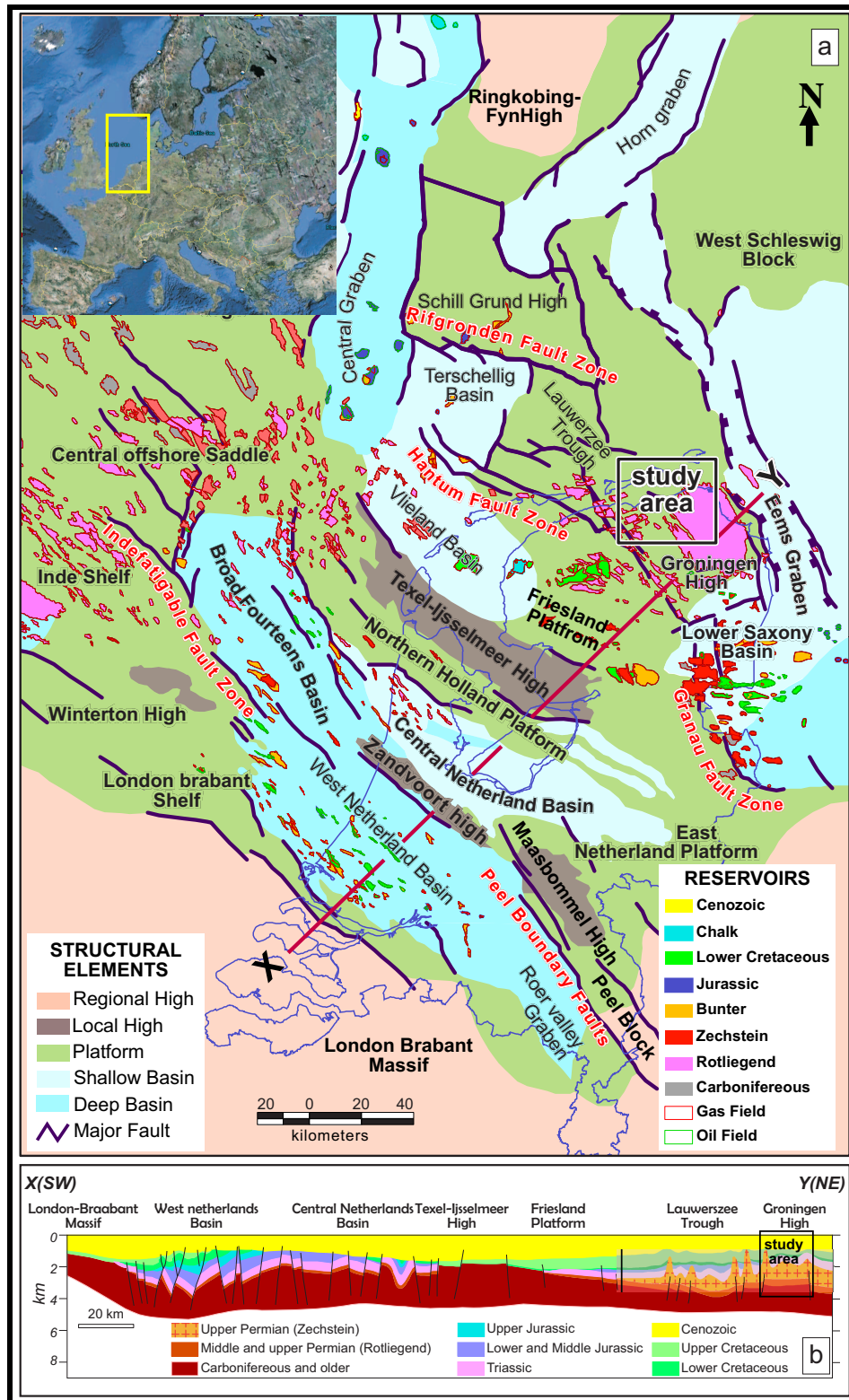


**Figure 1.1.** The location and facies distribution of North German Basin in Northwest Europe, which comprises North and South Permian basins (modified from Geluk, 2007).

## 1.2 Location

Geographically, the study area is located in the northeastern corner of the Netherlands near its border with Germany. Geologically, it is located at the northern part of the Groningen High, which is bounded by the Ems Graben to the east, the Lower Saxony Basin to the south, and the Lauwerzee Trough to the West (Figure 1.2).



### **1.3 Exploration History and Previous Studies**

Groningen Field is located in South Permian Basin (Figure 1.1), which contains several production wells and must be considered fully mature for hydrocarbon exploration. The exploration studies have been started in 1952 in the area. The first discovery was Slochteren-1 well in 1959. In 1965, availability of new seismic and facies interpretation led to realize that different production wells in the area had been producing from the same structure. From 1969 to 1988, interpretation of fault orientations and reservoir depths were perfected which improved the estimation of connected hydrocarbon volumes. After 1993, prediction of reservoir properties such as porosity and net pay from seismic inversion became possible with the better imaging below salt dome (Grötsch and Steenbrink, 2009). Despite its over exploration, new opportunities still exist in the field with the help of advances in computer and information technology (Geluk, 2007).

There were not a lot of scientific publications about the region until 2000s since petroleum companies had not released confidential data. However, due to new petroleum laws in the Netherlands and United Kingdom, much of the data were disclosed and abundant literature information were accumulated, since then. These also include online data portals from which well, seismic and company reports became available digitally such as Netherlands Oil and Gas Portal ([www.nlog.nl](http://www.nlog.nl)).

There are hundreds of publications in the literature related to geology and petroleum geology of the Netherlands and the North Sea. However, the most important one within the concern of this thesis include Gautier (2003) who studied the Carboniferous-Rotliegend Petroleum System. Other related publications are Cornford (1998), Glennie (1998), Gerling et al. (1999a), Van Wees et al. (2000), Geluk (2007), Jager and Geluk (2007), Kombrink (2008), Gent et al. (2008) and Grötsch and Steenbrink (2009).

Apart from the geology of the study area, the previous works related to Petroleum System and Basin Modeling concepts include Magoon and Dow (1994), Allen and Allen (2005), Hantschel and Kaurauf (2009). The other important works are Tissot et al. (1987), Burnham and Sweeney (1991), Waples (1994), Burrus et al. (1995) and Archard et al. (1998).

#### **1.4 Available Data and Methodology**

Basin modeling is a new research area, arose in the late seventies, and developed during the late eighties and early nineties with the ongoing improvements in computing and 3-dimensional visualization. It is now well established, and widely used in petroleum exploration (Burrus et al., 1995). The objective of the basin modeling is to reduce risk in exploration by a better integration of geological, geophysical and geochemical data.

The 3-dimensional seismic data with an aerial distribution of around 400 km<sup>2</sup> in SEG-Y format (survey L3nam1988N) and borehole information from 9 wells (ODP-1, PBN-1, RDW-1, UHM-1, UHZ-1, USQ1, WRF-1, WSM-1 and ZND) in ASCII and LIS-LAS formats obtained from the Netherlands Oil and Gas Portal (NLOG) provided by Geological Survey of Netherlands (TNO-NITG) (Figure 1.3). A conceptual model of regional geological history was constructed during the seismic interpretation stage together with the utilization of literature information. This helped to understand the depositional, erosional and thermal history of the study area.

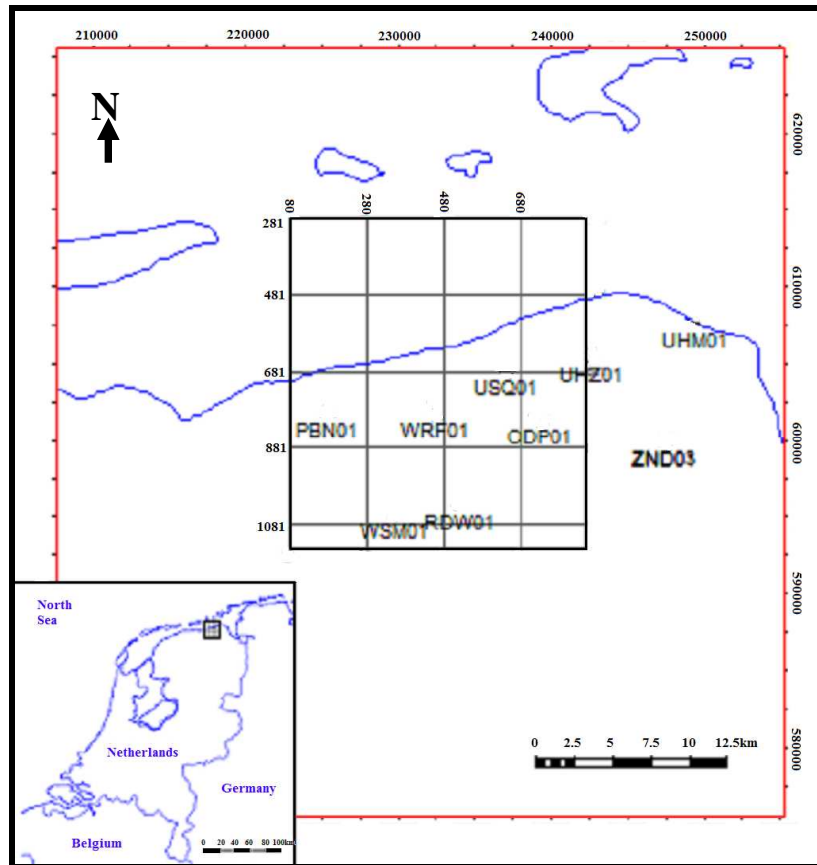


**Figure 1.3.** Location of 3D seismic data and boreholes in the study area (inline and crossline interval is 25m).

The study has been conducted in 4 steps:

- 1) Seismic interpretation aided by formation tops from the borehole data and literature,
- 2) 1-Dimensional (1D) Maturity Modeling,
- 3) 2-Dimensional (2D) Basin Modeling,
- 4) Validation and evaluation of results.

In summary, the workflow of the study is as below on Figure 1.4.

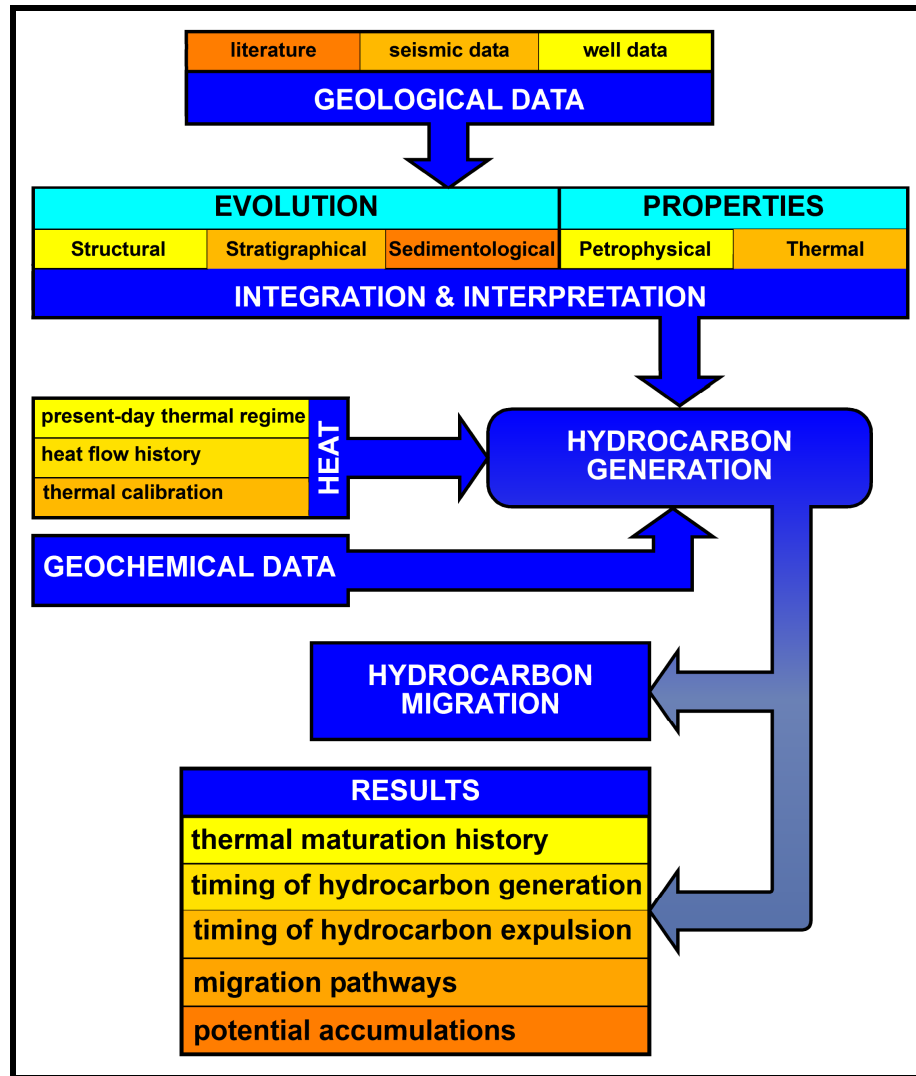


**Figure 1.4.** Flow chart indicating steps of the study.

Petrel seismic to simulations and PetroMod petroleum systems modeling software of Schlumberger were used for the seismic interpretation and hydrocarbon potential evaluation purposes.

## **1.5 Geological Background: Tectonic Setting and Basin Evolution**

The main controlling events that give rise to petroleum generation, migration and accumulation are largely the result from structural, stratigraphical and sedimentary processes that took place during geological history.

The present-day basin configuration in the study area results from poly-phase Late Paleozoic to Recent lithospheric deformation (Figure 1.4). The main tectonic events that affected the area are:

- following the Caledonian orogenies, the Variscan orogeny resulted in the formation of Pangea supercontinent during the Paleozoic,
- Mesozoic rifting gave way to the break-up of Pangea,
- Late Cretaceous to Tertiary Alpine inversion resulted from Africa and Europe collision,
- Oligocene to Recent development of the Rhine Graben rift system was developed approximately parallel to the basement faults indicative of their reactivation (Jager, 2007).

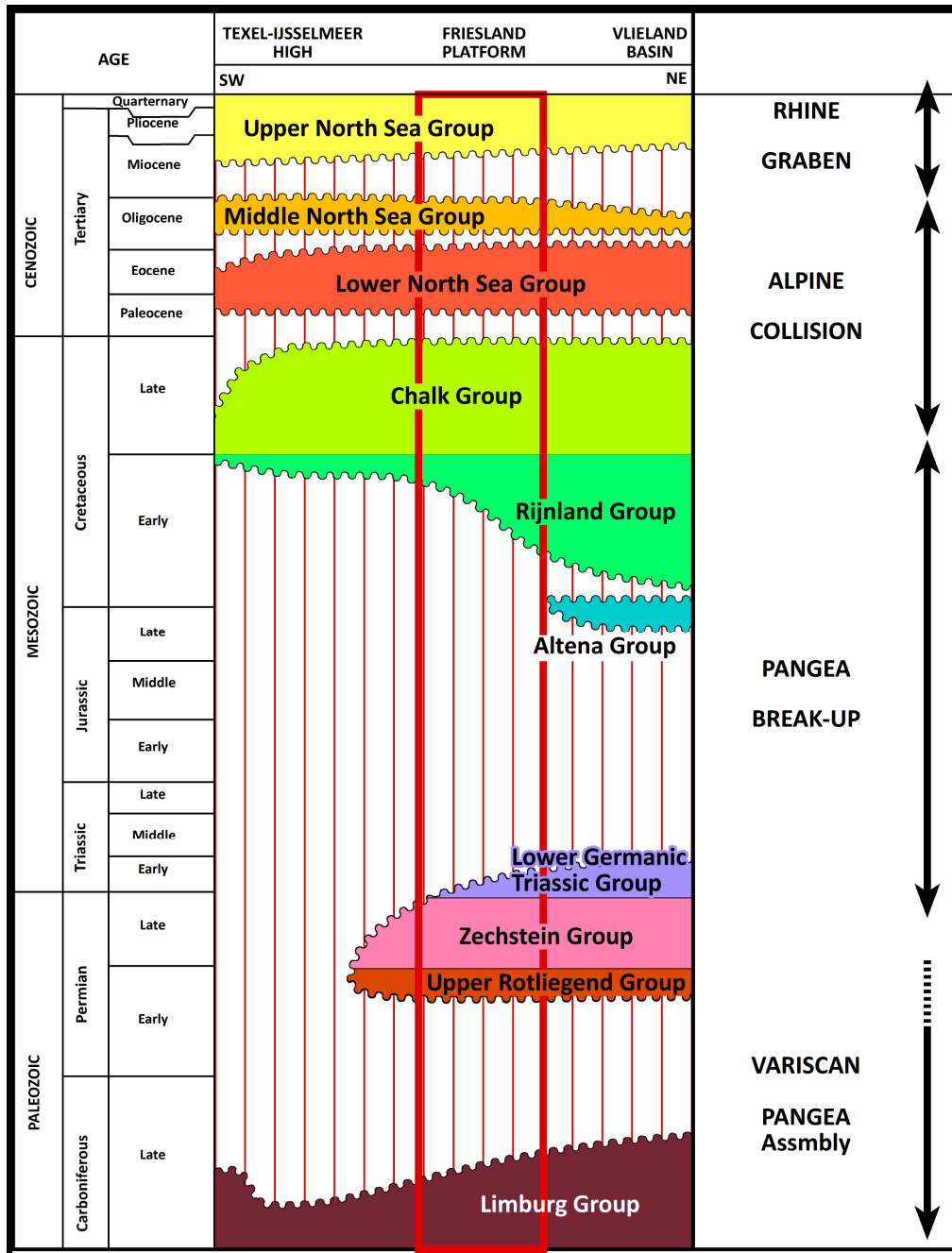


**Figure 1.5.** Generalized columnar section and major tectonic events in the northern Netherlands (modified from Geluk 2007). Red box indicates the units present in the study area.

Gondwana-derived Avalonia paleo-continent constitutes the basement of the basin in the study area (Figure 1.1). More than half amount of the sediments in the South Permian Basin was deposited over the basement during the period of Late Silurian to Early Permian (Jager, 2007). These rocks are rarely penetrated by boreholes because of high depth of burial, on the other hand, they are well-imaged on seismic data.

### **Carboniferous to Permian**

The Carboniferous Limburg Group which includes marine to lacustrine Namurian and coastal-plane and fluvial-plane Westphalian successions with coal seams (Figure 1.5), constitutes the main source rocks in the basin and they have little sign of syn-sedimentary tectonics. There is a small scale extensional faulting observed diminishing through the north of Netherlands where the study area is located (Jager, 2007).

During Late Carboniferous to Early Permian, a system of post-orogenic wrench faults caused differential subsidence and resulted in local graben formation and contemporaneous major uplift and erosion. This gave way to the development of major unconformity in the Early Permian times called Base Permian Unconformity (Gautier, 2003).

A thick succession of fluvial and aeolian sandstones of Rotliegend Group was deposited unconformably over Paleozoic sediments. It was followed by thick evaporitic sequences and interbedded carbonates of Zechstein during regional thermal subsidence (Van Wees et al., 2000) (Figure 1.4).

A broad epicontinental sag basin, the Northwest German Basin, was formed in Late Permian. This basin is a part of South Permian basin which is stretching throughout northern Europe from Great Britain to Poland. The study area is located within the Northwest German Basin, southern margin of the South Permian Basin (Figure 1.1).

### **Triassic to Present-day**

The Early Triassic is characterized by rifting which gave way to the break up of Pangea (Ziegler, 1982; Geluk, 2007; Jager, 2007). By the end of Triassic the Zechstein Salt started to move and resulted in salt halokinesis controlled by thickness variations of Zechstein in the area. According to the seismic-based structural

reconstruction studies of Gent et al. (2008), Permian Zechstein evaporates and carbonates were faulted by the same event as the Top Rotliegend, and no syn-tectonic deposition is observed during the Late Permian to Middle Triassic. During post-rift thermal subsidence, Triassic sandstone and clay-siltstone was deposited conformably over Zechstein Group mostly within the mini basins bounded by salt structures (Jager, 2007).

The Groningen Block (i.e. the study area) was relatively stable since Late Jurassic when the North Netherlands High was formed and resulted in an unconformity. Due to this uplift event, the Jurassic, Triassic and locally Permian sediments were deeply truncated (Jager, 2007; Gent et al., 2008; IHS, 2009). Thus, preserved Triassic units and Lower Cretaceous deposits of the Groningen Block are relatively thin due to Late Jurassic erosion and non-deposition.

The Upper Cretaceous Chalk Group is one of the most extensive unit in the region and consists mainly of carbonates and marls. During the Late Cretaceous (Subhercynian tectonic phase), parts of the chalks were locally eroded (Jager, 2007; Ziegler, 1982). During Late Cretaceous tectonic compressional events exerted by collision of Africa-Eurasia, salt structures were laterally squeezed and strongly deformed (Baldschuhn et al. (1998), NITG (2000) in Geluk, 2007). Although Laramide inversion (Latest Cretaceous) caused intense uplift, associated with truncation, erosion and fault reactivation in the surrounding areas, the northwest corner of the Groningen Block remained relatively stable with only minor regional uplift (Ziegler, 1982; Gras and Geluk, 1999; Gent et al., 2008).

The Cenozoic North Sea Supergroup, deposited from the Early Paleocene onwards is mainly siliciclastic unconformably overlying Upper Cretaceous Chalk Group. The Cenozoic basin evolution was under the effect of Rhine Graben Rifting (Van Adrichem-Boogaert and Kouwe, 1993–1997; Gent et al., 2008).

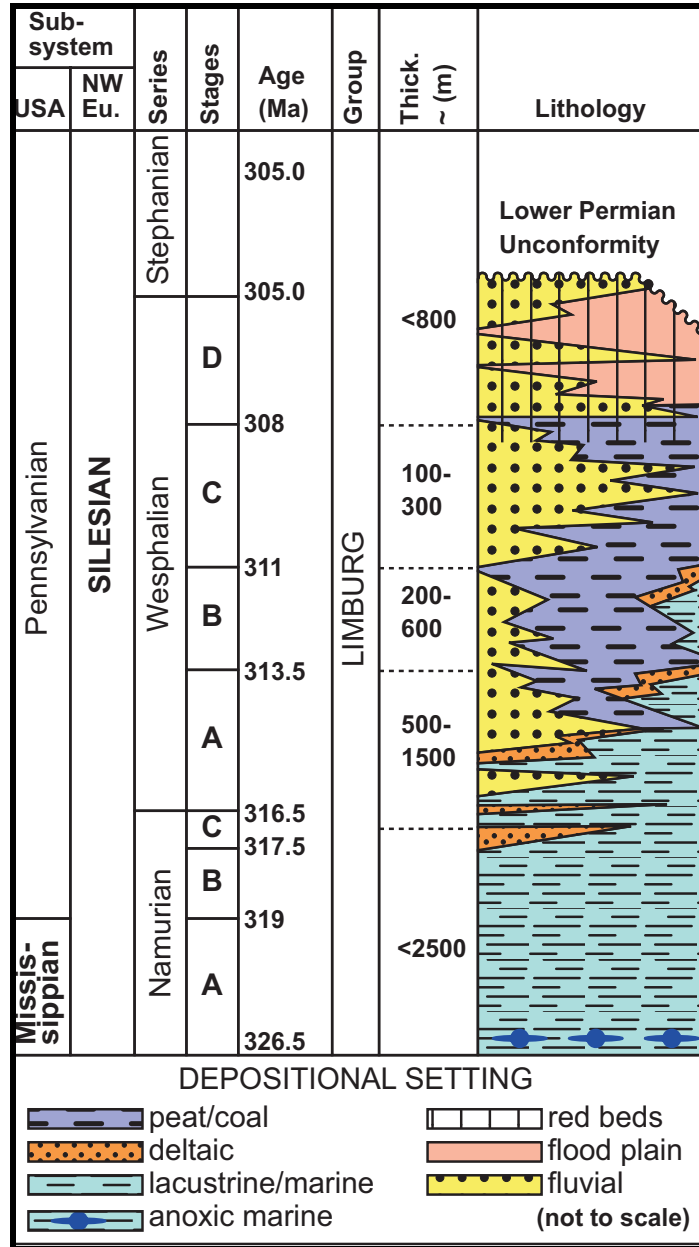


**Figure 1.6** Stratigraphic scheme for the Upper Carboniferous (Silesian) deposits in the eastern Netherlands (after Van Adrichem Boogaert & Kouwe, 1994). Note that these units are the main source rocks in the region.

## CHAPTER 2

### PETROLUUM SYSTEMS

There are three proven petroleum systems recognized in the Northwest German Basin (Figures 2.1):

- The Carboniferous–Rotliegend Petroleum System which is effective in the study area, that accounts for about 90% of discovered hydrocarbons,
- The Posidonia–Mesozoic-Paleogene Petroleum System that is responsible for over 80% of the oil accumulations in the basin and
- The minor Bueckeberg–Upper Jurassic-Lower Cretaceous Petroleum System that is responsible for a number of small oil and gas accumulations in the western part of the basin (IHS, 2009).

The Carboniferous-Rotliegend Petroleum System consists of the thick Upper Carboniferous Namurian and Westphalian successions with abundant coal measures as source rocks for gas, good Rotliegend sandstone reservoirs, and the excellent seal of the Zechstein evaporates (Gautier, 2003). In the study area, there are no Jurassic rocks and sign of any related hydrocarbon system (Jager, 2007). The younger petroleum systems are not present in the study area; therefore, it is crucial to determine the timing of generation, migration and accumulation of the Carboniferous source rock and reservoir quality of Rotliegend in order to evaluate the hydrocarbon potential of the region.

It has long been known that there is only one source rock in Carboniferous and several potential reservoir intervals both in Carboniferous (Kombrink, 2008) and in the overburden all of which have been deposited after or contemporaneously with the source rock (Figure 2.1). The position and timing of seal rocks and trap formations are best fit with the Carboniferous-Rotliegend Petroleum System.

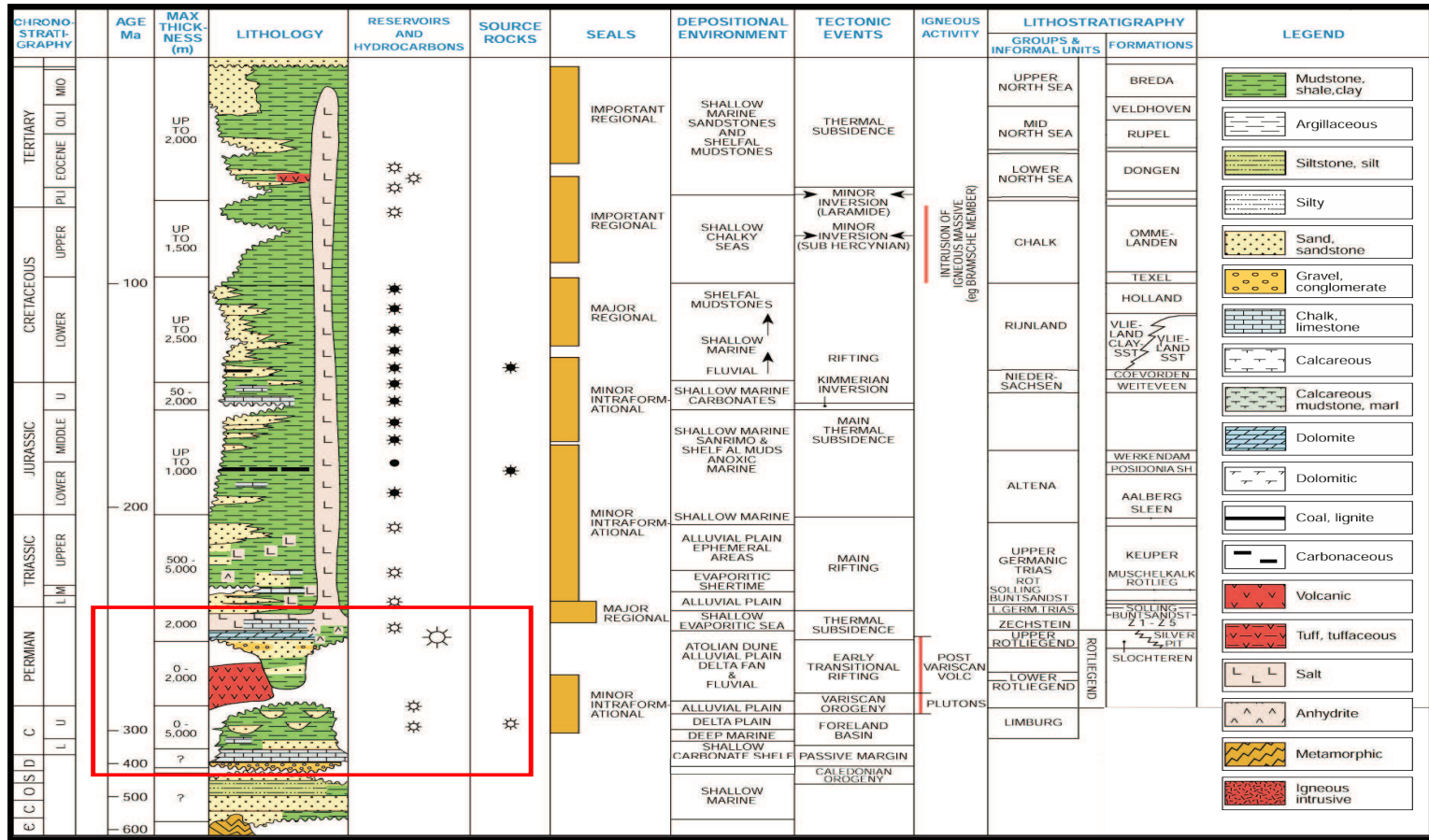


**Figure 2.1.** Generalized stratigraphical chart of Southern Northern Sea sector of the Northwest German Basin (modified after Boigk 1981, Van Adrichem Boogaert 1993, Bachmann & Hoffmann 1997 in IHS 2009). The Carboniferous-Rotliegend Petroleum System which is the main concern of this study is indicated with a red box.

According to the study of Gautier (2003), the critical moment which indicates spatially and temporarily the generation-migration-accumulation of most of the hydrocarbons, is at the Permian-Triassic boundary (248 Ma) which is the main concern of this study (Figure 2.2).

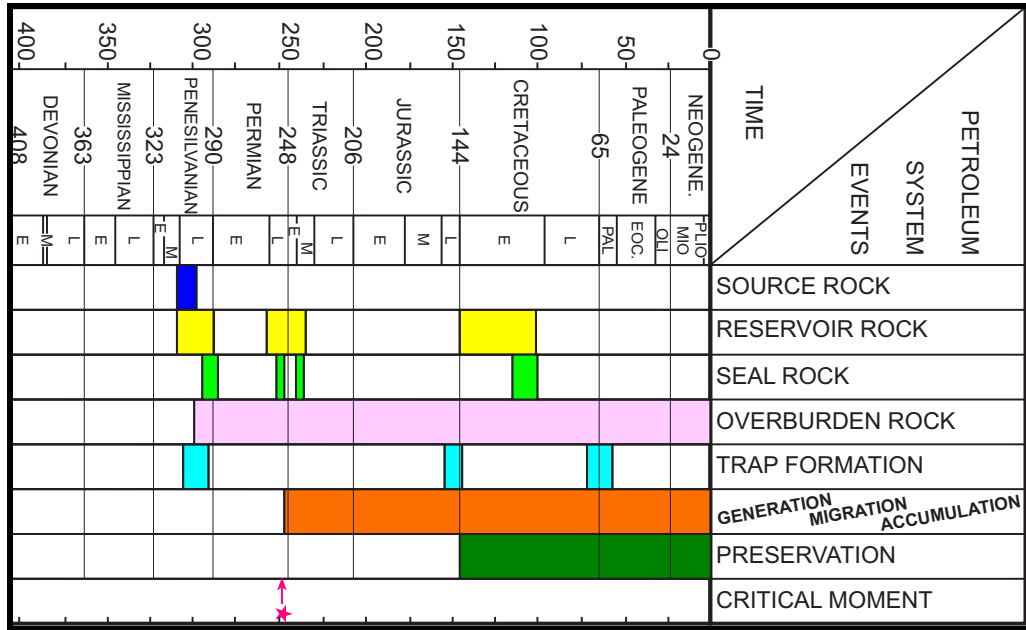


**Figure 2.2.** Events chart for the Carboniferous-Rotliegend Petroleum System in South Permian Basin (Gautier, 2003).

Carboniferous-Rotliegend Petroleum System still holds undiscovered conventional resources of 22 to 184 million barrels of oil (MMBO) and 3.6 to 14.9 trillion cubic feet of natural gas (TCFG). Of these amounts, 1.9 TCFG are predicted in onshore areas (Gautier, 2003).

In order to understand the petroleum system of the study area, brief descriptions of petroleum system elements are given in the next section.

## 2.1 Source Rocks

The principal source rocks of the gas in the study area are the Upper Carboniferous, Westphalian coals and carbonaceous shales that consist of upward-coarsening deltaic rocks overlain by fluvial deposits (Figure 1.5) (Gautier, 2003; Buggenum and den Hartog Jager, 2007). The source rock is kerogen type III. Westphalian succession has been separated into units A, B, C and D for the ease of basin-wide correlation.

The cumulative thickness of the coal is several tens of meters. They occur mostly in Westphalian B accounting for about 3 percent of the total stratigraphic sequence which is assumed to be 1000 to 3000 m thick (Lutz et al., 1975). Carbonaceous shales account for the larger portion (Cornford, 1998). The Westphalian source rock thickness was locally reduced as a result of Early Permian uplift and erosion. Such that, Westphalian C and D were totally, Westphalian B was partly eroded around the study area (Figure 2.3).

High maturity values were measured in the Westphalian in some wells on the Groningen High (Kettel (1983) in Jager, 2007) suggesting that the source rock was affected from several heat pulses in this area. It is likely to have occurred as a result of the main Early Permian erosion, and caused the high vitrinite reflectance directly below the Base Permian Unconformity. Jager (2007) argued that the source rock capacity of coal measures within the Westphalian succession was sufficient to provide hydrocarbon to large Groningen gas field, up to the spill point.

Secondary source rock for gas is basal Namurian organic rich shales (Gerling et al., 1999a; Gerling et al., 1999b). In most places these source rock became overmature during pre-Kimmerian burial. Thus, Namurian is thought to be the source of nitrogen charge, which is mainly expelled at higher temperatures than hydrocarbon gas (Jager and Geluk, 2007).

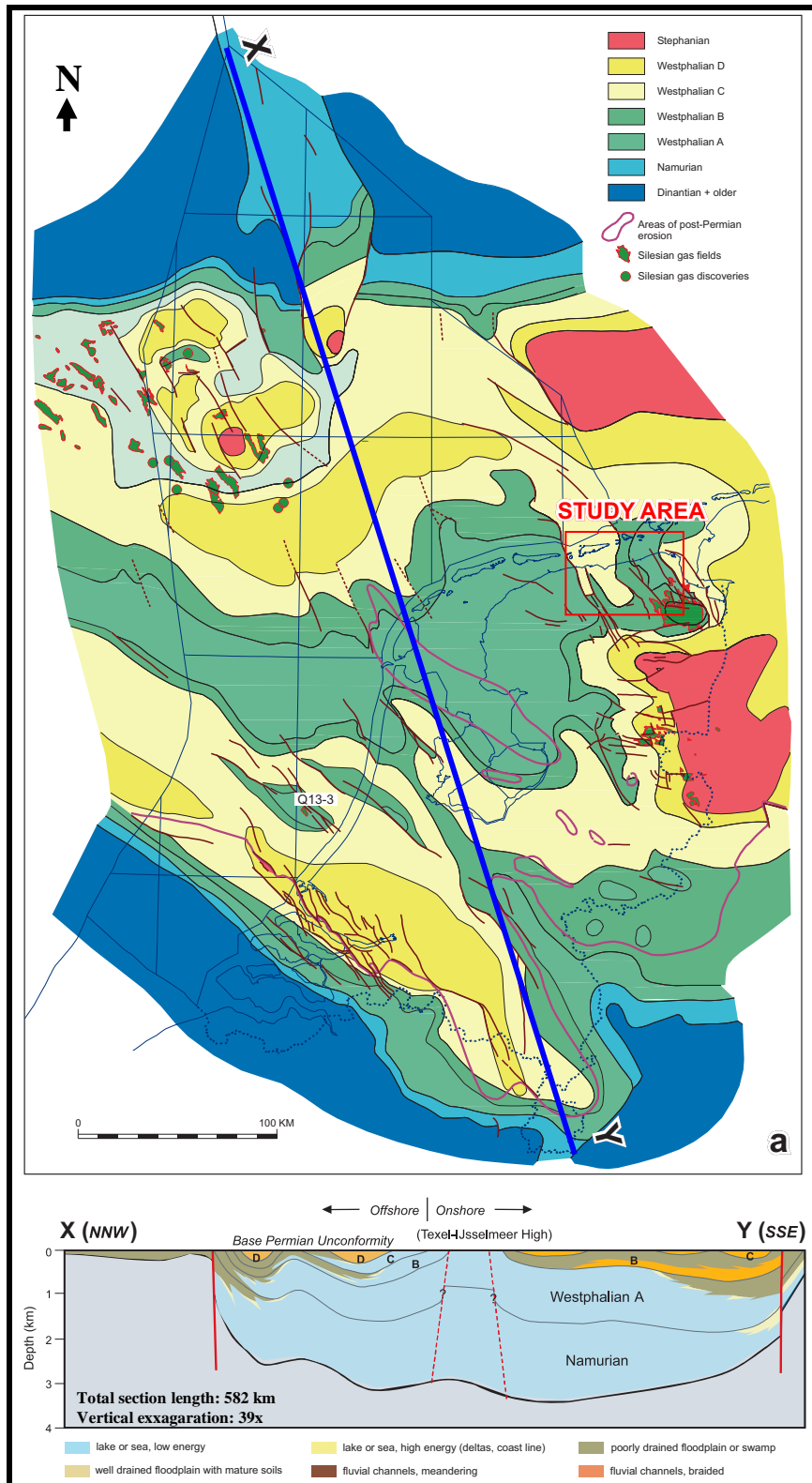


**Figure 2.3.** Subcrop of source rocks and cross-section along line XY (adopted from Buggenum & den Hartog Jager, 2007).

## 2.2 Reservoir Rocks

The Upper Rotliegend reservoir interval consists of fluvial (wadi) and aeolian sands alternation. The sediments were deposited in basin margin alluvial fans whose surfaces were above the water table. Those sandstones accumulated above the water table display the best preservation of porosity and permeability since diagenesis did not decrease the reservoir quality as it did on fluvial sandstones. Accordingly, most commercial gas accumulations are found in aeolian dune deposits (Glennie, 1998; Gautier 2003). Average thickness of the Upper Rotliegend Group in the study area is 283 m based on nearby exploration wells (Figure 2.4).

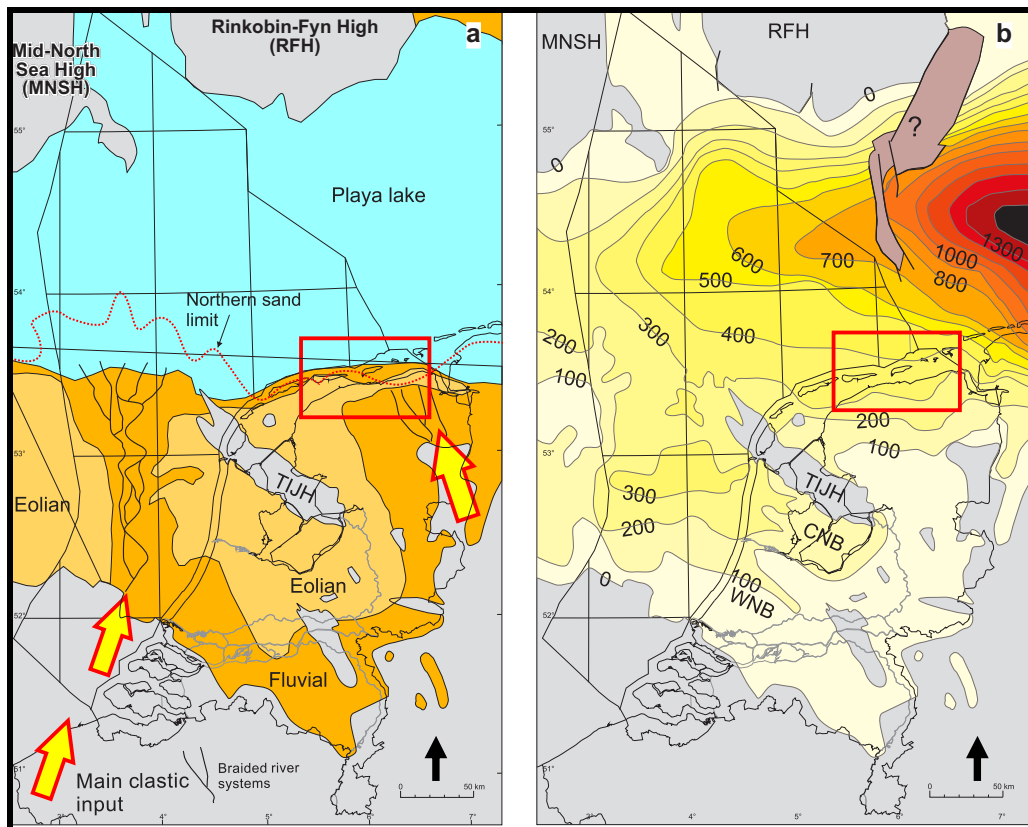


**Figure 2.4.** Facies distribution (a) and isopach map (b) of Upper Rotliegend Group. CNB: Central Netherlands Basin; WNB: West Netherlands Basin; TIJH: Texel-IJsselmeer High; MNSH: Mid North Sea High; RFH: Ringkøbing-Fyn High. Study area is indicated with red rectangle. Black arrow shows North (adopted from Gerling et al., 1999a).

### 2.3 Seal Rocks

The main seal rock for the Carboniferous-Permian Petroleum System is the Zechstein Group. It comprises minor and four major (Z1 to Z4) cycles of evaporite deposition all of which can be observed in the wells of the study area (Figure 2.5) and most of which are penetrated by the exploration wells in the study area (Figure 2.6). In the study area, it comprises intercalations of carbonate, anhydrite, salt and clay sequences. The first three evaporite cycles (Z<sub>1</sub>-Z<sub>3</sub>) are bounded by the carbonate rocks having neritic platform and slope facies. In some areas (e.g. West Netherlands Basin) these carbonates also constitute reservoir rocks together with the Rotliegend Group. In other areas, Zechstein is the seal for nearly all gas accumulations in Rotliegend reservoirs. Evaporitic deposits within the Rotliegend may also be the seal for gas in Carboniferous reservoirs (Gautier, 2003). Based on wells in the study area, average thickness of the Zechstein is 767 m.

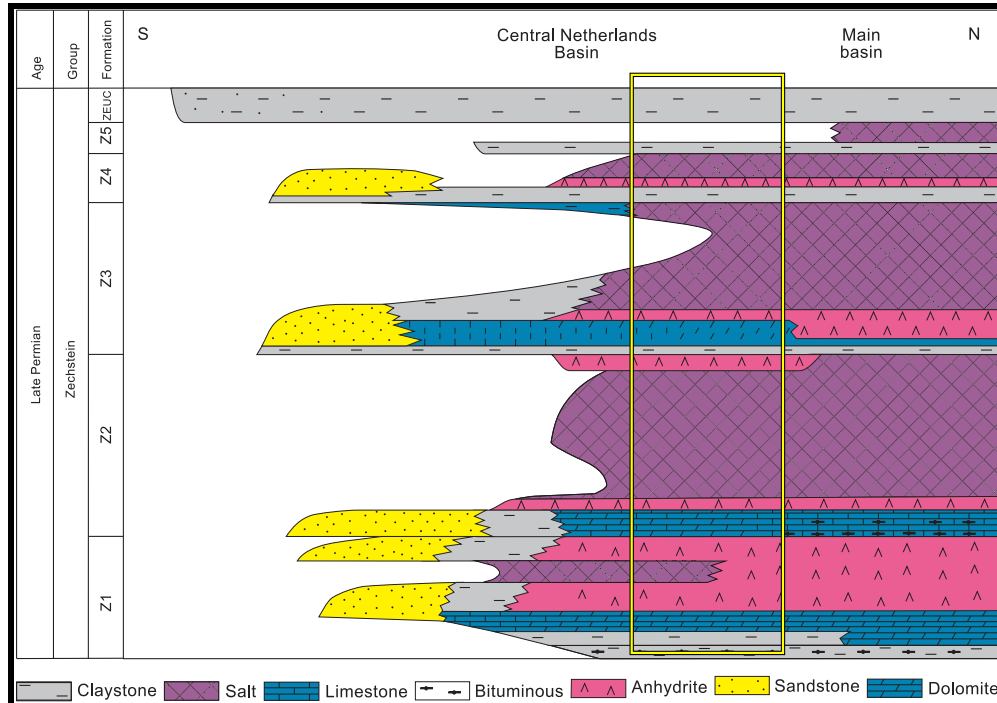


**Figure 2.5.** Facies distribution and characteristics of Zechstein Group. The facies in the study area is indicated with yellow rectangle (Geluk, 2007).

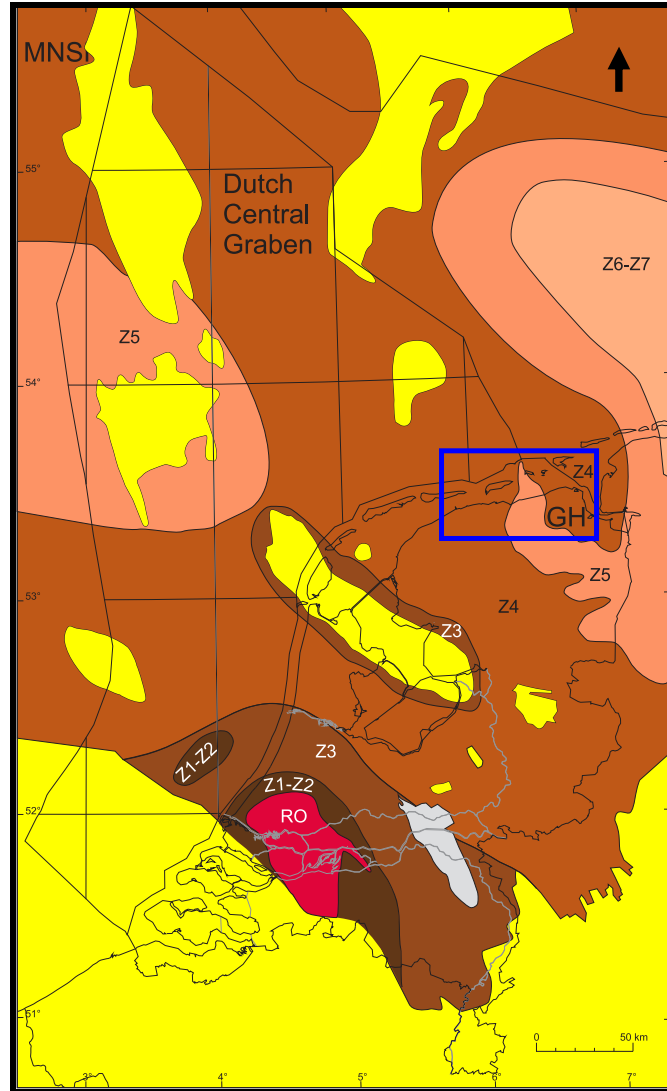


**Figure 2.6.** Subcrop map below the Zechstein Upper Claystone Formation showing distribution of Zechstein cycles (after Geluk 2007). Zechstein is absent in yellow areas. Study area is indicated with blue rectangle. GH: Groningen High, MNSH: Mid North Sea High, RO: Rotliegend Group. Black arrow shows North.

## 2.4 Overburden Rocks

Overburden rocks include Upper Germanic Triassic Group with 279 m average thickness. It is unconformably overlain by the Lower Cretaceous Rijnland Group with 115 m average thickness. In turn, it is overlain by Upper Cretaceous Chalk Group with 780 m average thickness and Cenozoic North Sea Supergroup, deposited from the Early Paleocene onwards and has 735 m average thickness within the study area. In this study, the Jurassic Altena Group is not encountered in the exploration wells (Figure 2.7). Depth map to the base of overburden units is illustrated in Figure 2.8.

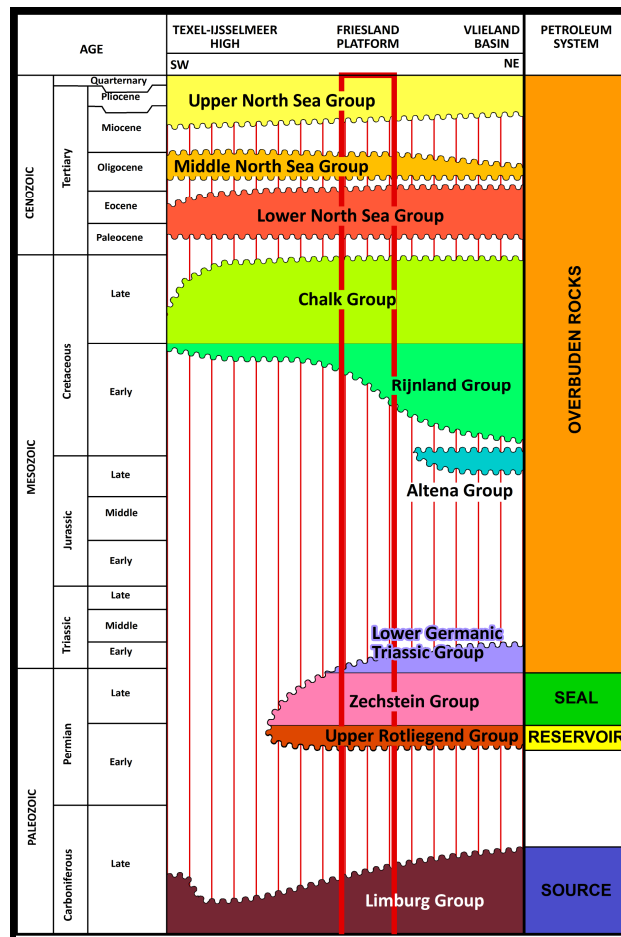


**Figure 2.7.** Play type and overburden rocks of the study area. Red box indicates the units present in the study area. Note that Jurassic Altena Group is absent in the study area (modified from Geluk 2007).

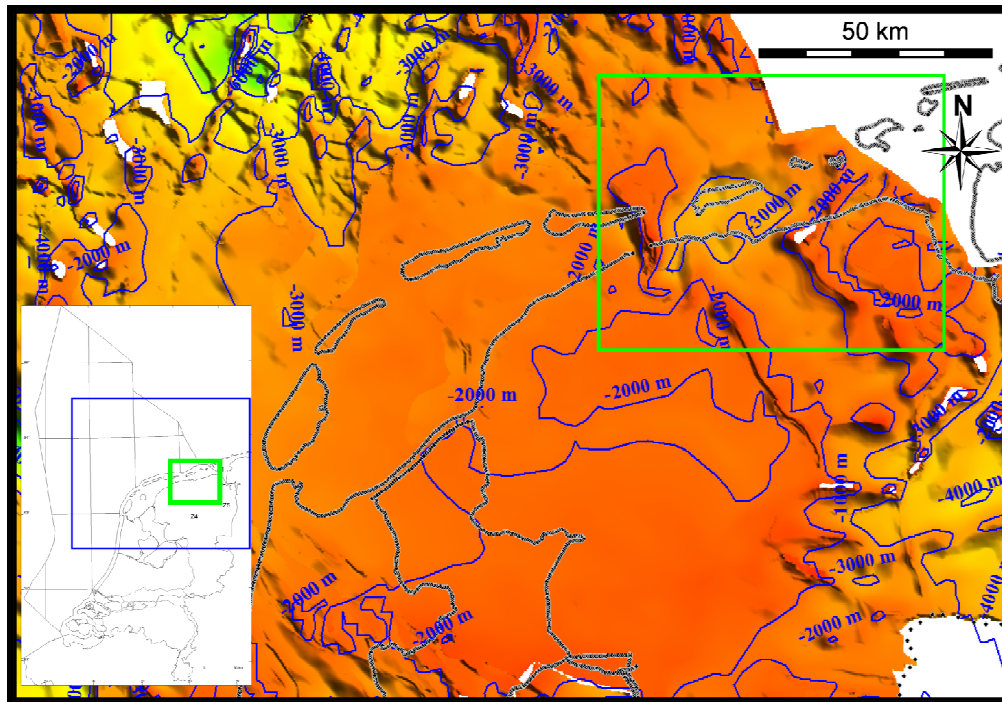


**Figure 2.8.** Depth to the base of overburden rocks. Green rectangle indicates the study area. Note that it is also equal to the isopach of the overburden.

## 2.5 Trap and Play Types

Nearly 75% of gas has been discovered in the Rotliegend Structural Play in Northwest German Basin (Figure 2.9). The fluvio-aeolian sandstone reservoirs of Rotliegend were formed in tilted fault blocks beneath the overlying Zechstein seal during the Variscan orogeny (Late Carboniferous - Permian phases) which is the main concern of this study.

Zechstein structural/stratigraphic play is another significant gas play where shelf margin carbonate reservoir is sealed by evaporites within tilted fault blocks (IHS, 2009). Traps also would be provided by permeability barriers caused by lithological discontinuities (Gautier, 2003).

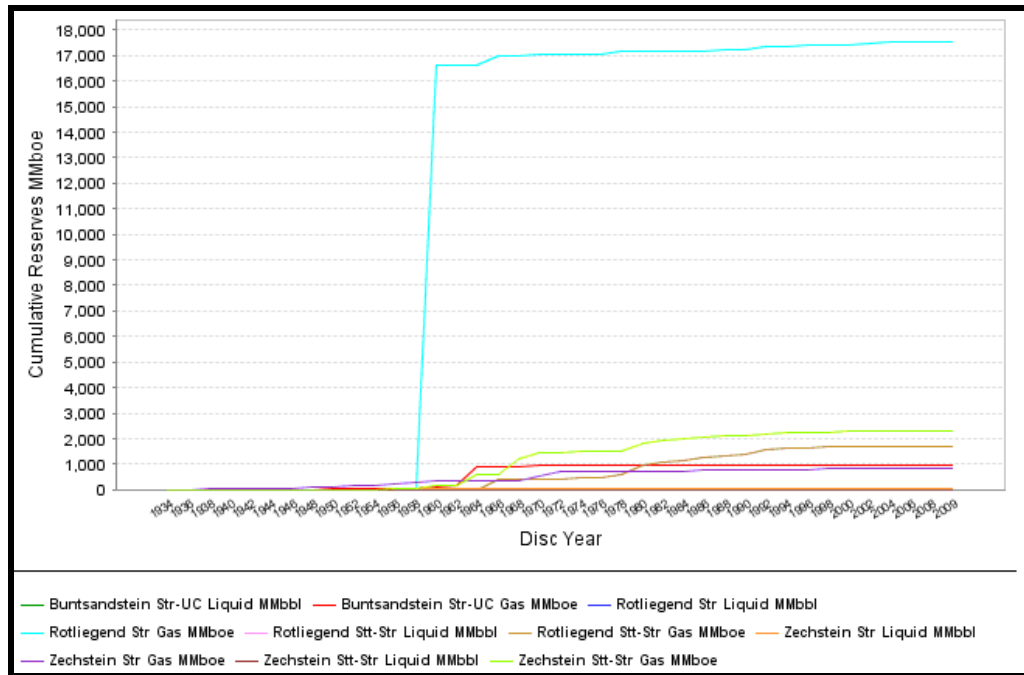


**Figure 2.9.** Northwest German Basin, chart showing cumulative liquid and gas reserves per play between 1934 and 2009. Stt: stratigraphic; Str: structural (IHS, 2009).

Carboniferous stratigraphic and structural plays also have gas potential where Carboniferous channel sandstones are overlain by Rotliegend shales and evaporitic rocks. Accumulations could exist either in structural closures or lithologic boundaries where gas was entrapped stratigraphically. Carboniferous is comparatively unexplored in the region (Gautier, 2003).

## CHAPTER 3

### DATA

This section covers the basic geological data obtained from seismic and borehole data which is required for modeling studies. Since, seismic interpretation is not the main objective of this study, brief information about the interpretation procedure and obtained results are presented in this chapter.

#### 3.1 Seismic Data

The discovery of the Groningen Field initiated an intense exploration and production activity in Netherlands. More than half of on- and offshore Netherlands is covered with high quality 3D seismic data. Thanks to early commencement of 3D seismic data acquisition, some of which are already public, this study could be done.

Seismic reflections originate from interfaces between layers that show sufficient density-velocity contrasts. Each seismic layer in the subsurface has its own acoustic impedance. The *acoustic impedance* is defined as the product of *density* and *velocity* of a rock layer. Formation velocity and density depend on the mineral composition and the granular nature of the rock matrix, cementation, porosity, fluid content, and environmental pressure. Depth of burial and geologic age also have an effect on acoustic impedance especially due to lithification processes that include compaction and cementation. It is important to remember that different lithologic units (for instance a shale and a sand) can have similar acoustic impedance (density\*velocity) values, depending on the porosity distribution, fluid contents and degree of compaction (Veeken, 2007) (Figure 3.1). Therefore, lithology cannot be directly deduced from the seismic reflection data alone. For this reason, picking of horizons

are based mainly on the geometry of the reflections and well ties that are mostly characteristic seismic reflections of major geologic events.

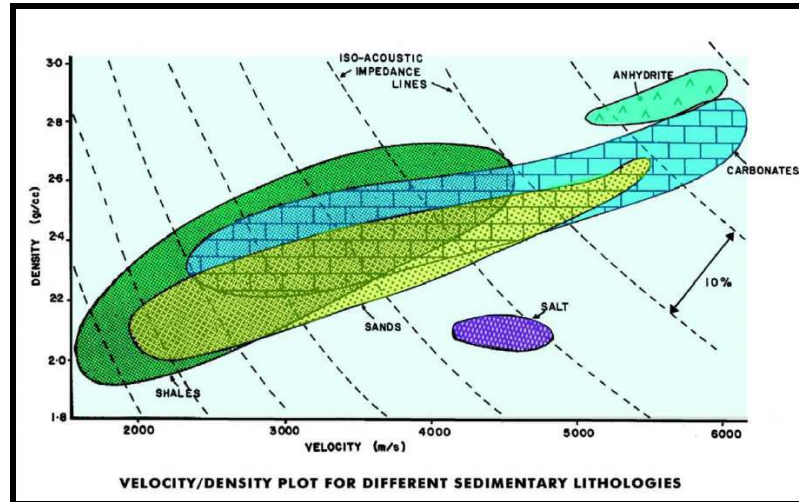


**Figure 3.1.** Interval velocity vs. lithology cross plot. The lithologies are overlapping. Therefore, direct identification from the P-wave velocities is difficult. Thus, additional information is necessary for discrimination (Veeken, 2007).

Workflow followed during the data preparation and interpretation of the model by using Petrel is shown below:

- Data loading; introduction of seismic volume and borehole data,
- Picking of seismic horizons using formation tops obtained from well data,
- Fault interpretation and generation of fault surfaces,
- Velocity model preparation by using interval velocities,
- Time to depth conversion of interpreted horizons and fault surfaces,
- Choosing representative boreholes and seismic lines to be used for basin modeling.

### 3.2 Seismic Interpretation

Seismic volume in SEG-Y format and wireline logs from the wells in ASCII and LIS-LAS format were loaded to Petrel. Since the wireline log data are in depth domain, and seismic data is in time domain (two-way-travel time (TWT)), using interval velocities obtained from the borehole seismic data (Table 3.1), the well tops were converted from depth to time domain in order to match the formation tops with the seismic data. Interval velocity is the velocity of a specific layer of rock, calculated from acoustic logs. The accuracy of the interval velocity calculations depends on the thickness of the interval over which they are computed (Veecken, 2007).

**Table 3.1.** Interval velocities used for the time to depth conversion of the seismic volume (Van Dalfsen et al., 2006).

Age	Symbol	Formation	Interval velocity (m/s)
Tertiary	N	North Sea Group	1981.3
Late Cretaceous	CK	Chalk Group	3250.0*
Lower Cretaceous	KN	Rijnland Group	3053.0
Triassic	RN	Upper Germanic Trias Group	2550.0
	RB	Lower Germanic Trias Group	3671.8
Late Permian	ZE	Zechstein Group	4700.4
Late Permian	RO	Rotliegend Group	4056.1
Carboniferous	DC	Limburg Group	4500.0

\*3784.3 m/s in the reference data.

Based on formation tops obtained from well data and literature information verifying these tops, the main horizons are interpreted. Triassic was not interpreted, since it was not continuous throughout the study area and not crucial for the model. It was treated with the Lower Cretaceous Rijnland Group (Figure 3.2 and 3.3).

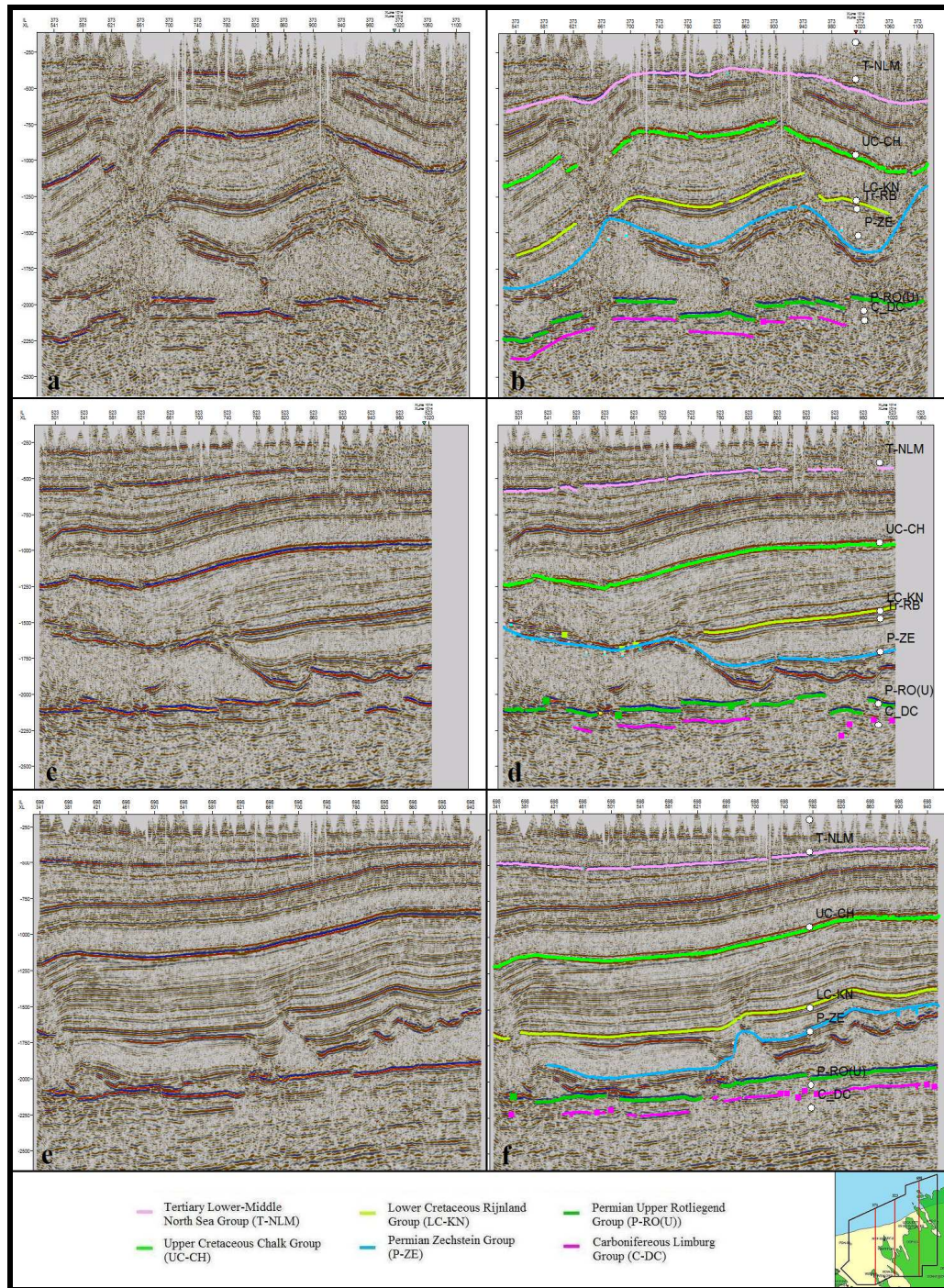


**Figure 3.2.** (a-b) Inline 373, (c-d) inline 523, (e-f) inline 698, raw and interpreted seismic sections. Note that inline and crossline intervals are 25 m.

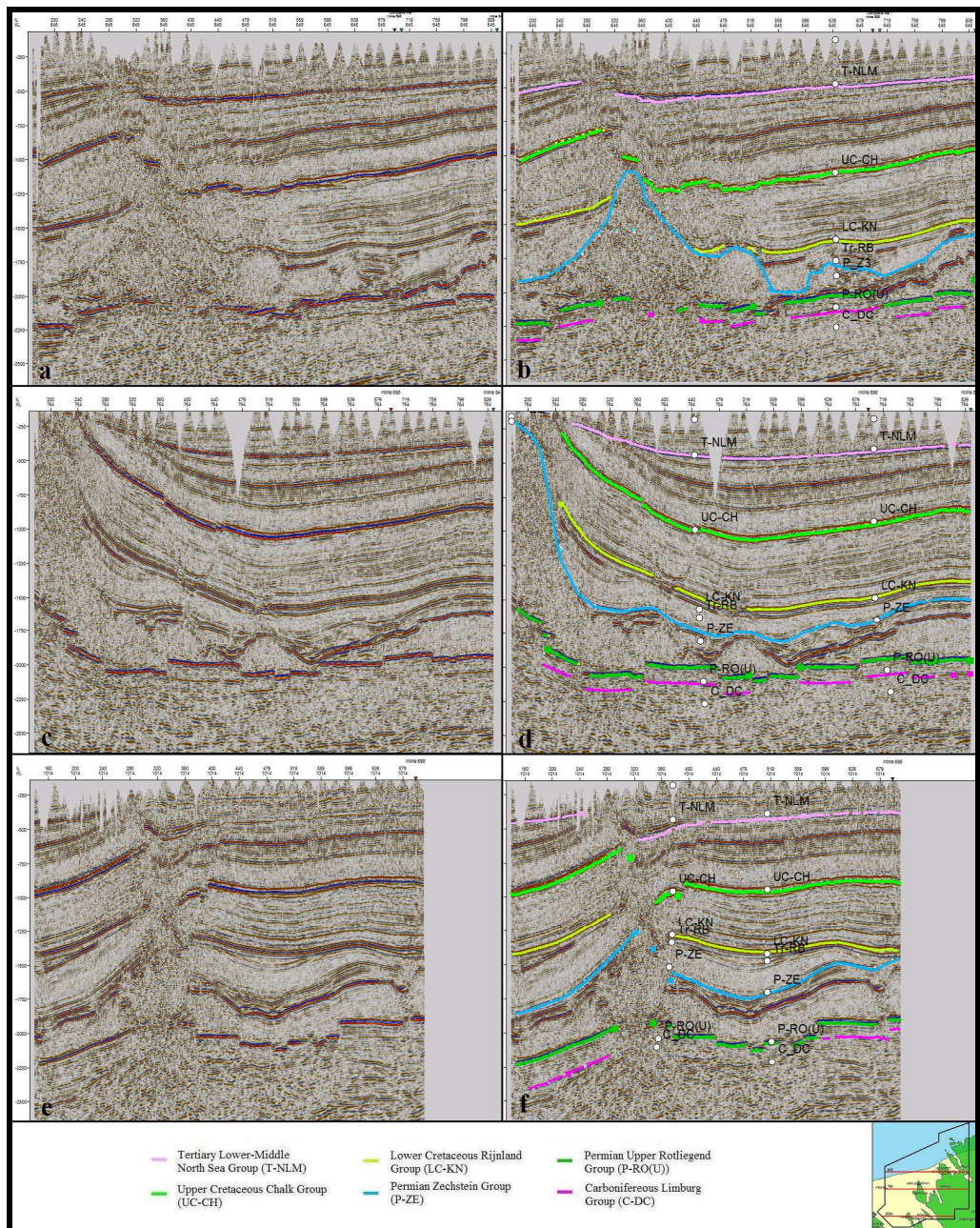


**Figure 3.3.** (a-b) Crossline 645, (c-d) crossline 764, (e-f) crossline 1014, raw and interpreted seismic sections. Note that inline and crossline intervals are 25 m.

It is observed that major unconformities in the study area have angular character by which they can be easily distinguished on the seismic. In Figure 3.6, the Early Permian unconformity that resulted from Variscan Orogeny, Late Jurassic unconformity that is related to Kimmerian inversion due to the opening of the North Atlantic and led to the erosion of whole Jurassic (Altena Group) and most of Triassic units, and Late Cretaceous unconformity between the Chalk and North Sea Groups due to the effect of Laramide inversion are shown.

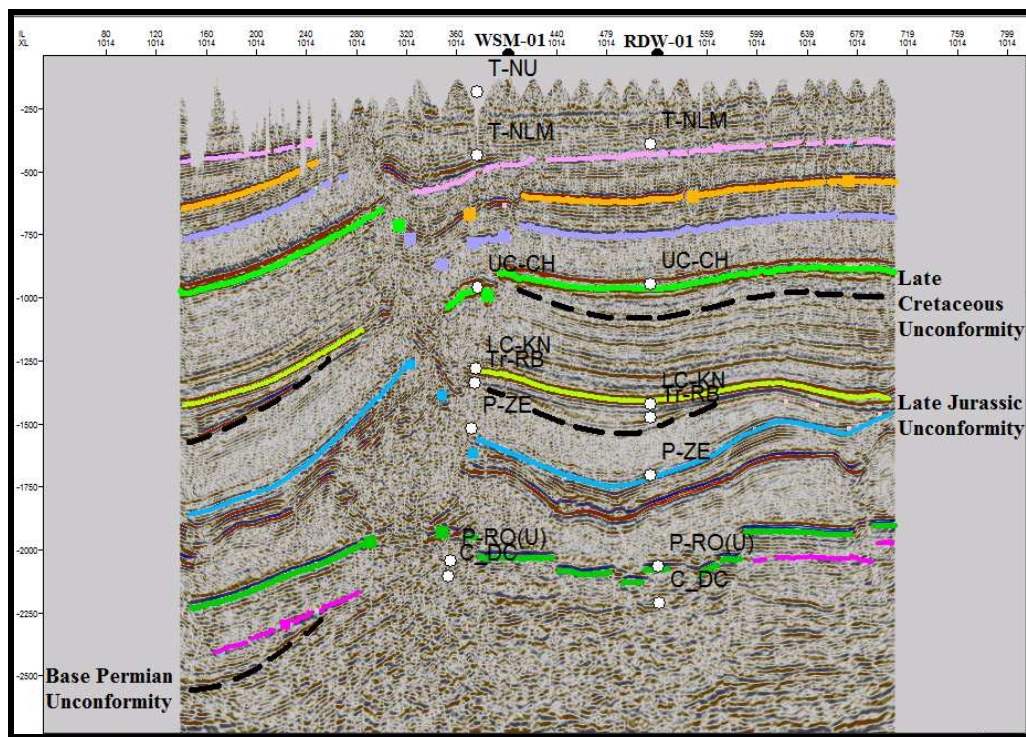


**Figure 3.4.** Major unconformities in the study area (Abbreviations and location of the seismic section are same as Figure 3.2).

Although, numerous small-scale faults are encountered in the seismic data, for the sake of simplicity and objectives of the study, only major Permian and the faults that are thought to have effect on the petroleum migration are interpreted. Most of the Permian faults are oriented NW-SE as seen on Figure 3.5.

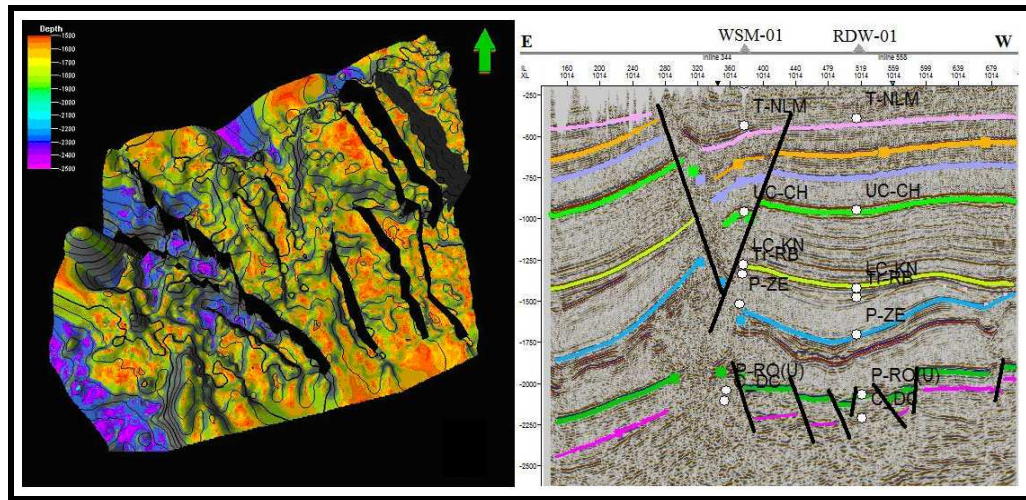


**Figure 3.5.** (a) Perspective view of alignments of Permian faults, arrow shows North and (b) a representative cross-section illustrating the Permian and younger faults. Location of the seismic section is same as Figures 3.2.

The interval velocity values were also used for time to depth conversion of seismic data as they were obtained from the sonic logs except for Chalk Group (Table 3.1). Instead of 3784.3 m/s for the Chalk Group, 3250.0 m/s was used in order to have better fit with the well tops and reflections on the seismic. The interval velocities depicted in Table 3.1 are representative for whole area of Netherlands and southern North Sea Basin. However, in some areas, values can show small differences due to lateral lithology and/or thickness changes.

The conversion is simply made by using the equation;  $x = vt$  where *distance* (depth) is equal to *velocity* multiplied by *time*. Time in seismic is two-way-time (TWT), therefore, half of the time value is multiplied with velocity. The time surfaces/grids (maps created from horizon interpretations) are converted to depth by multiplying time with half of the interval velocities. Same procedure was just reversed for depth to time conversion of well tops, as well (Figure 3.6).

Having identified some horizons that were significant for understanding the geology and the prospectivity of the area, the next step was to map them. These maps were used with the interval velocities of the formations for establishing velocity model (Figure 3.7) and then time to depth conversion of seismic volume (Figure 3.8).

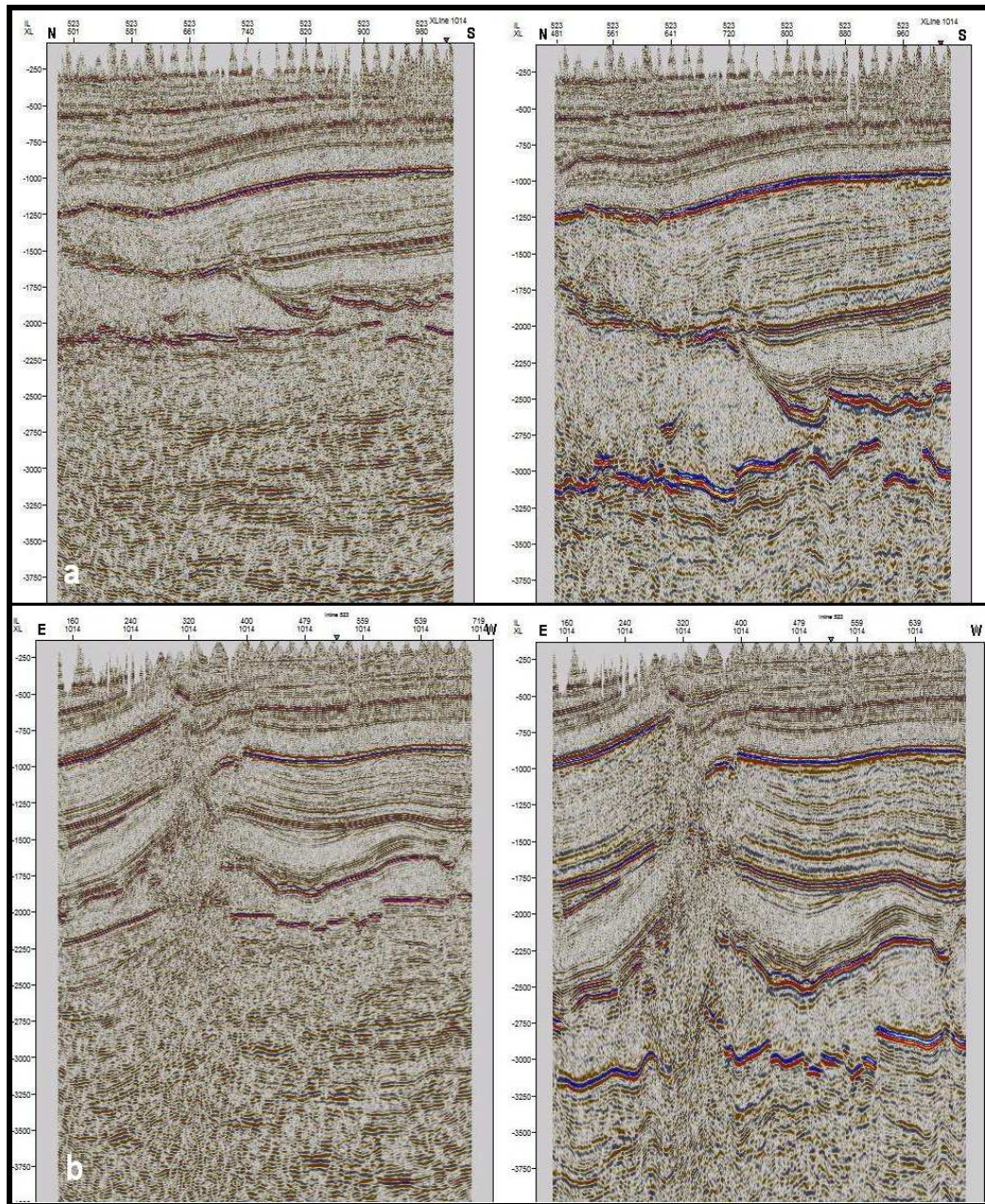


**Figure 3.6.** (a) Inline 523 and (b) crossline 1014 in time and depth respectively. Location and scale of the seismic sections are same as Figure 3.2.

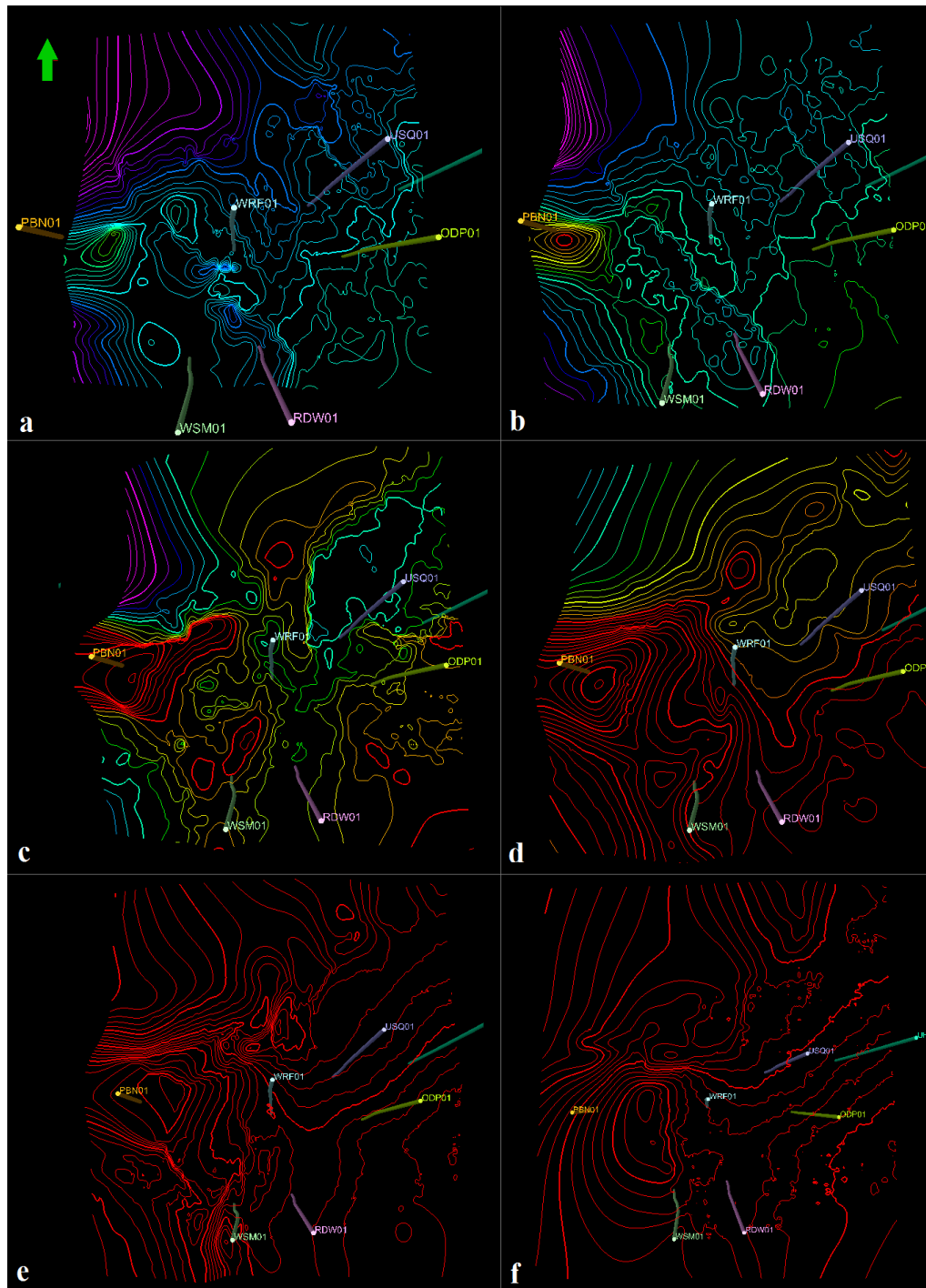


**Figure 3.7.** Velocity model maps (a) top Carboniferous, (b) top Rotliegend, (c) top Permian, (d) top Rijland, (e) top Chalk and (f) top North Sea Group. Green arrow shows North.

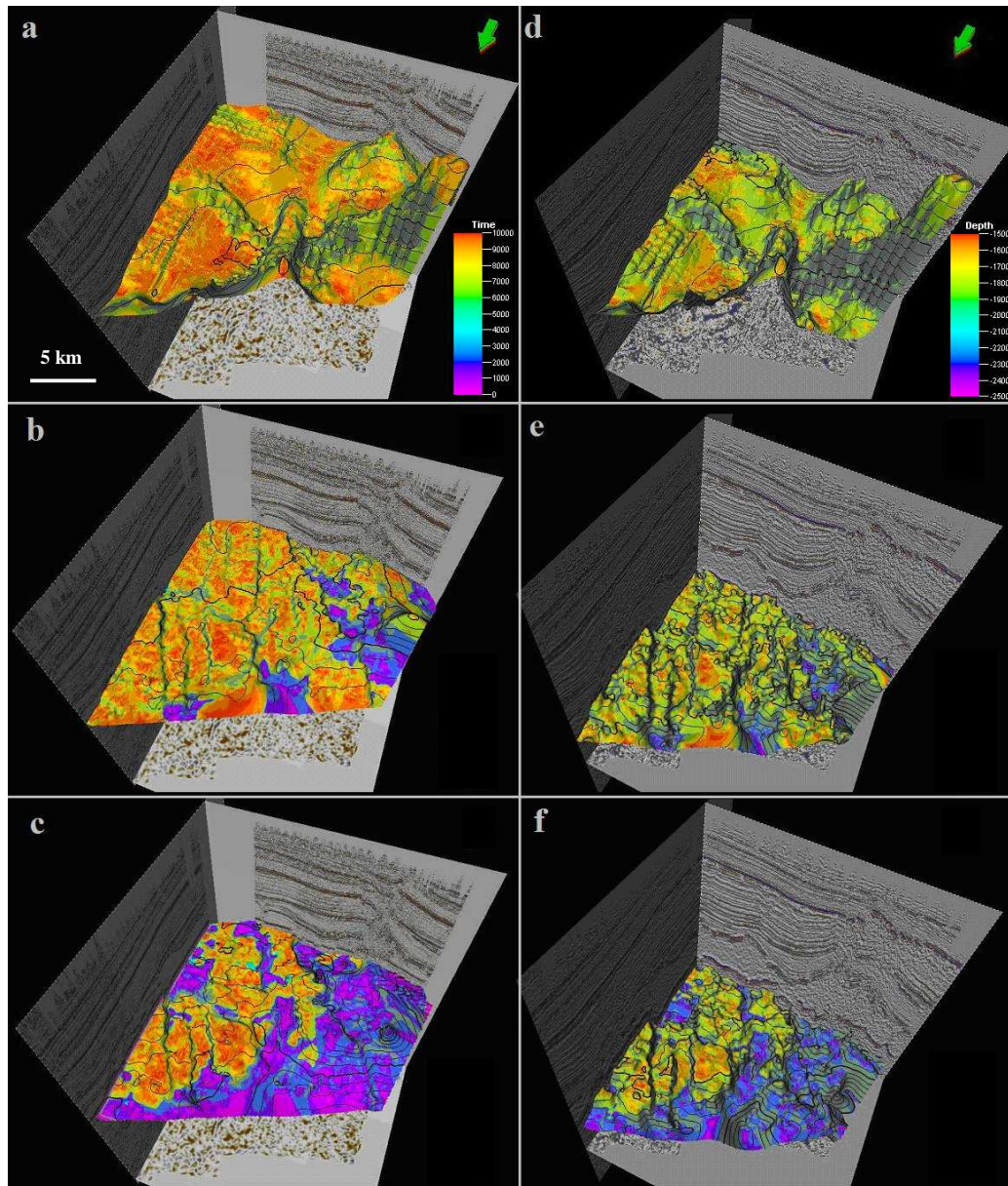


**Figure 3.8.** Time and depth maps of interpreted horizons (a-c) time maps of Top Permian (top Zechstein), top Rotliegend, and top Carboniferous and (d-f) depth maps of same horizons, respectively. Horizontal axes are x5 exaggerated. Green arrows show North (see Appendix B, for their higher resolution versions).

In addition to the Carboniferous and Permian rocks, the overburden units were also interpreted. The resultant time and depth maps are shown in Figure 3.9.

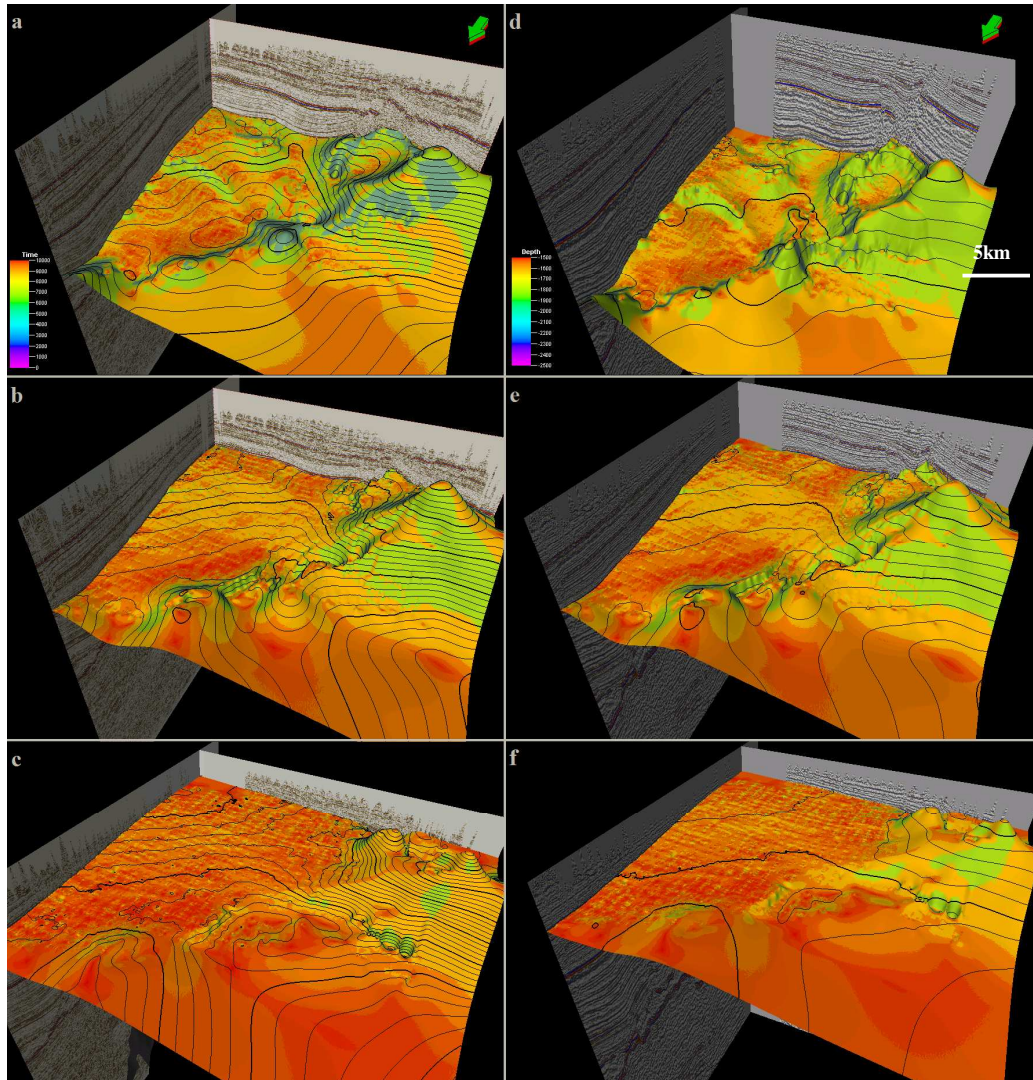


**Figure 3.9.** (a-c) Time maps of base Rijnland, Chalk and North Sea Groups and (d-f) their corresponding depth maps. Arrows show North (see Appendix B for their higher resolution versions).

## CHAPTER 4

### 1D MATURITY MODELING

#### 4.1 Introduction and Data Processing

The aim of 1D modeling is to determine burial and thermal history of source rock as well as timing of hydrocarbon generation. The essential inputs of maturity modeling is paleo-heat flow that source rock has been subjected to, quantity and quality of organic matter in the sediments (total organic carbon, maturity indicators and hydrogen index) and kinetic equations for the calculation of kerogen conversion to oil and gas (Burnham and Sweeney, 1991).

In the modeling process, first of all, lithology, age and thickness of each rock unit are determined for the software to assign porosity, density and permeability of units. If there is measured porosity, density or permeability data, they can be used for calibration of the assigned data. Lithology determination is very important since it controls all petrophysical properties including compaction rates, thermal conductivities and heat capacities. In this study, present day heat-flow is entered to adjust present day temperature by finding the acceptable fit between measured and calculated present-day temperatures as a second step. Then, paleoheat flow and geologic events during erosion and non-deposition periods are adjusted by calibrating with thermal indicators (Waples, 1994).

The present-day temperature and reconstruction of temperature history is crucial for the evaluation of the petroleum potential of a basin since temperature is the most sensitive parameter in hydrocarbon generation. Paleo-temperature is not measurable; therefore, maturity indicators are used for the estimation of this parameter. Maturity indicators are function of the thermal history through complex kinetics, frequently

influenced by the type of organic matter. Kinetics of kerogen decomposition controls the amount and composition of hydrocarbons generated (Tissot et al., 1987).

Several trials are performed during the optimization process of the model to be as consistent and correct as possible. In cases when many uncertainties are present in the model parameters, sensitivity analysis is performed.

There are two boreholes chosen for 1D maturity modeling; RDW-01 and USQ-01 which are located in the study area. Lithology of the intervals and rock properties were obtained from these boreholes (Figure 4.1).

The scale of erosion influences the generation, migration, and accumulation of hydrocarbon. Thus, estimating the amount of erosion is essential in the analysis of hydrocarbon-bearing basins. Amounts of erosion were acquired from borehole Roode-Til-1 (ROT-1) in the Groningen Gas Field except for the source rock interval (Figure 4.1).

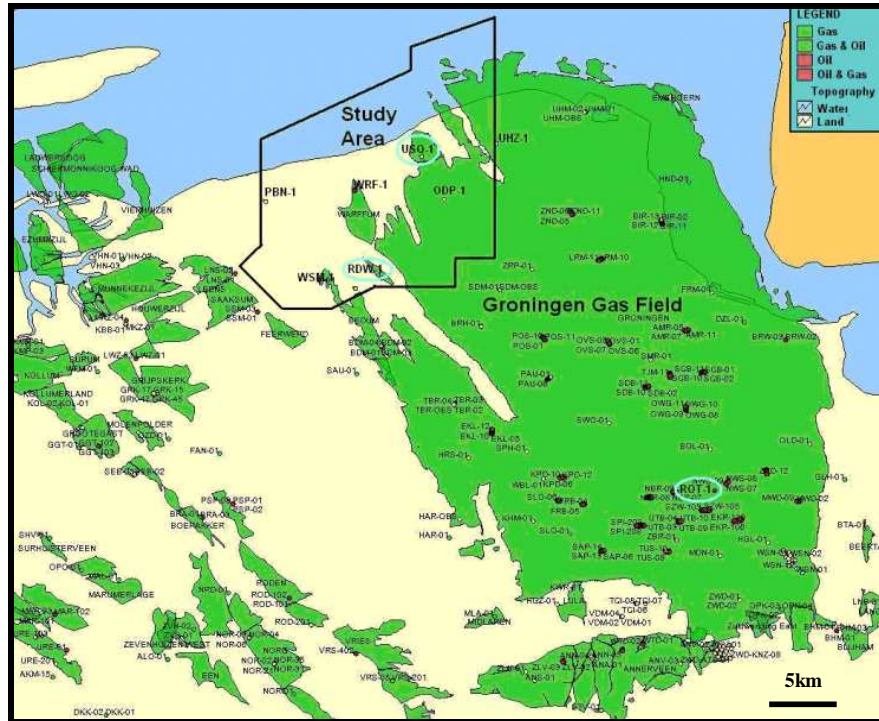


**Figure 4.1.** Map showing the Groningen Gas Field and study area. Boreholes used in the model are highlighted by circles (IHS, 2009).

The quality of the simulation is strongly dependent on the boundary conditions. Paleo-water depth (PWD), sediment-water interface temperature (SWIT) and heat flow (HF) are the boundary conditions that were set in the model.

## 4.2 Inputs of the Model

### 4.2.1 Geological Data

Rock unit lithology, ages and thickness from boreholes (Table 4.1), geochemical data from literature were obtained and input for modeling purpose.

Erosion values have been obtained from a neighboring well ROT-1 by direct proportion method (Figure A.1 and Table A.1 in Appendix A) where there are regional unconformities. However, the thickness of Carboniferous source rock and erosion above this interval is estimated according to stratigraphic scheme of the source rock (Figure 1.5) because this interval was not totally penetrated by any well. Estimation of source rock thickness is also evaluated under sensitivity analysis in Section 5.3.

**Table 4.1.** Stratigraphic and age data from wells RDW-1 and USQ-1 (intervals are same as Figure 3.2, Q stands for Quaternary).

Interval	Thickness RDW-1 (m)	Thickness USQ-1 (m)	Age (ma) FROM	Age (ma) TO	Lithology
Q	0	152	1.7	0	Clays, silts, fine- to coarse-grained sands and sandstones
T_NS	928	959	60	1.7	Clays, silts, fine- to coarse-grained sands and sandstones
UC_CH	773	932	98	64	Mainly limestones (chalk), also marls and claystones
LC_KN	81	109	136	98	Argillaceous and marly deposits, sandstone beds
Tr_RB	418	200	245	172	Silty claystones, evaporites, carbonates, sandstones and siltstones
P_ZE	854	543	258	245	Evaporites and carbonates
P_RO	298	315	264	258	Coarse and fine-grained elastic sediments
C-DC	1250	1250	318	310	Fine-grained siliciclastic sediments and coal seams

#### **4.2.2 Geochemical and Thermal Data**

The Westphalian source rock has type III kerogen in the study area. Most of the geochemical data was obtained from Ruurlo well (RLU-1) which cuts Westphalian A and B in South Limburg area, Lower Saxony Basin (Veld et al., 1993) (Figure 1.2).

Vitrinite reflectance values were used as maturity indicator to adjust the thermal history. Vitrinite reflectance ranges between 1.19% and 8.44% according to Jurisch and Kroos (2008), 0.7% and 6.1% according to IHS (2009) and 0.89% and 1.45% according to Veld et al. (1993) (Table A.2 in Appendix A) in the region. There are also Netherlands' maturity maps of Westphalian A/B boundary showing vitrinite reflectance values between 1.41% and 1.80% and Top Carboniferous showing vitrinite reflectance values between 1.01% and 1.40% for the study area (Figures A.2 and A.3 in Appendix A) (NL Oil and Gas Portal, on-line, 2009).

Average TOC was assumed to be 4% by Veld et al. (1993). The hydrogen index (HI) of the Westphalian shale ranges between 121 and 246 mg HC/g TOC (Veld et al., 1993) (Table A.2 in Appendix A). In the model, average HI of 171 mg HC/g TOC and 4% TOC were used as proposed by Veld et al. (1993).

Present-day heat flow and paleo-heat flow values were obtained from Verweij (2003) (Figure A.4 in Appendix A). Vitrinite reflectance values from Netherlands maturity maps (Figures A.2 and A.3 in Appendix A) were used to calibrate paleo-heat flow values (NL Oil and Gas Portal, on-line, 2009).

There are three kinetic models in PetroMod software for the coal source rock, type III kerogen of North Sea. The result of each kinetic model is presented in Section 5.3 as part of sensitivity analysis.

#### **4.2.3 Boundary Conditions**

As mentioned earlier, paleo-water depth (PWD), sediment-water interface temperature (SWIT) and heat flow (HF) are the boundary conditions that were set (Table 4.2). SWIT is calculated using PetroMod software, based on Wygrala (1989). PWD and HF is obtained from Verweij (2003).

**Table 4.2.** Boundary conditions.

Age (Ma)	PWD (m)	Age (Ma)	SWIT (°C)	Age (Ma)	HF (mW/m <sup>2</sup> )
318	0	318	25	318	71
258	10	258	24	310	55
245	40	245	25	263	83
139	60	139	23	251	82
90	125	90	22	150	71
60	75	60	20	143	78
0	0	0	7	97	75
				75	70
				72	62
				57	75
				0	64

### 4.3 Calibrations

The porosity calibration was possible since there were studies carried out in well RDW-1. Measured porosity values of RDW-1 well and calculated porosity values show match (Figure 4.2). Since there is no porosity data from the well USQ-1, porosity calibration was not possible.

Temperature data from two different depths (obtained from well RDW-1 and temperature map of Netherlands) were used to adjust the present-day heat flow. 64- mW/m<sup>2</sup> heat flow value was used for the first run. Further trials resulted in 71 mW/m<sup>2</sup> for RDW-1 and 69 mW/m<sup>2</sup> for USQ-1 as the best fit with measured temperatures (Table 4.2 and Figure 4.3).

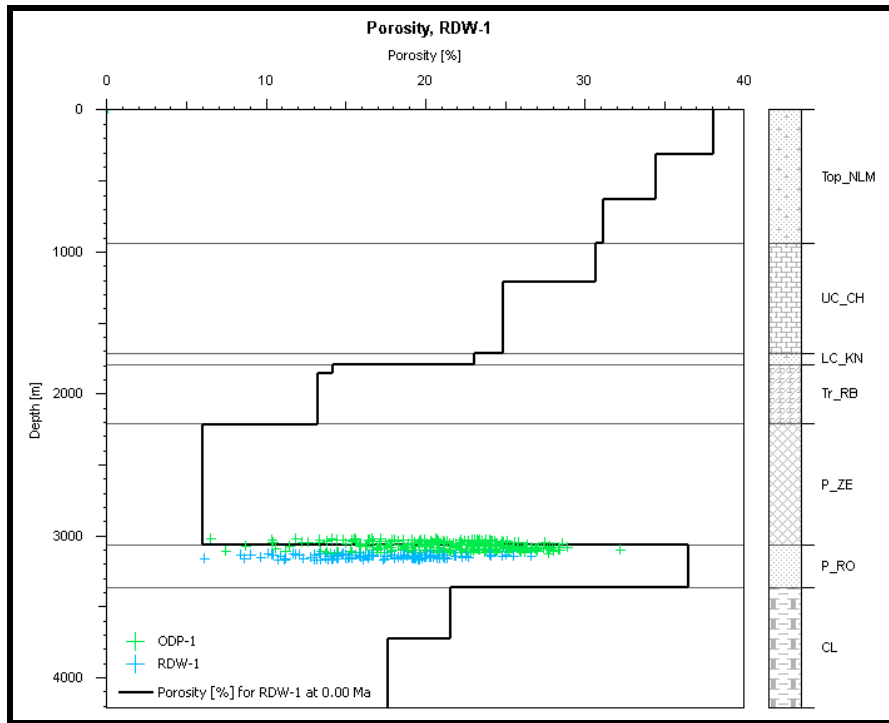


**Figure 4.2.** Porosity calibration of RDW-1 well.

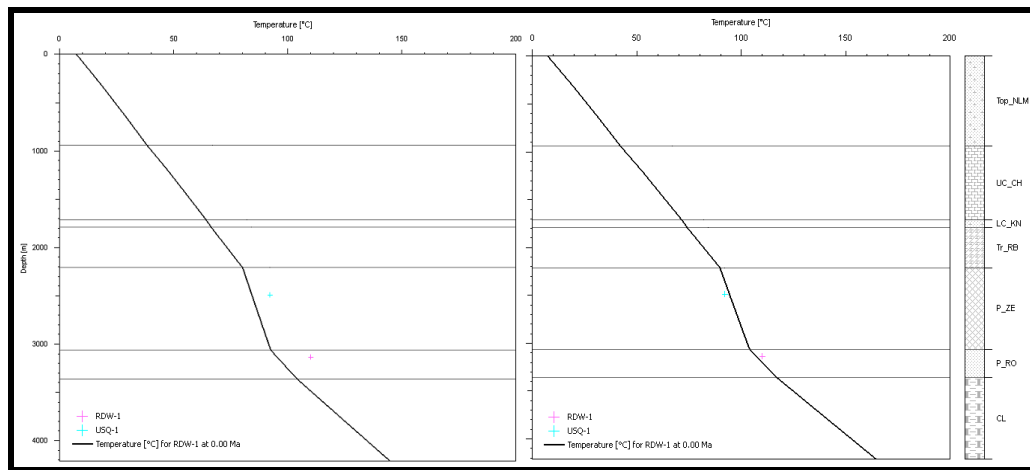


**Figure 4.3.** Heat-flow calibration with temperature; (a) before calibration, (b) after calibration.

Since the study area experienced several deformation phases, heat flow is variable in geological time; showing increase at the times of rifting and decrease in the post-rift phases expectedly. Several thermal maturity indicators exist that can be used for the calibration of paleo-heat flow. Since there are only vitrinite reflectance values obtained from literature, paleo-heat flow has been calibrated with the maturity values from two different depths (Table 4.3). There is small difference between the calibrated paleo-heat flow values of RDW-1 and USQ-1 wells (Table 4.4 and Figures 4.4 - 4.5).

**Table 4.3.** Vitrinite reflectance ( $R_o$ ) values used for calibration (NL Oil and Gas Portal, online, 2009).

Depth (m)	$R_o$ (%)	Min $R_o$ (%)	Max $R_o$ (%)
3500	1.6	1.41	1.8
3000	1.2	1.01	1.4

**Table 4.4.** Obtained and calibrated paleo-heat flow values (\*Verweij, 2003) (HF: Heat flow).

Age (Ma)	HF obtained from literature* ( $mW/m^2$ )	RDW-1 HF Final ( $mW/m^2$ )	USQ-1 HF Final ( $mW/m^2$ )
318	71	93	91
310	55	77	75
263	83	105	103
251	82	104	102
150	71	93	91
143	78	100	98
97	75	97	95
75	70	92	90
72	62	84	82
57	75	97	95
0	64	71	69

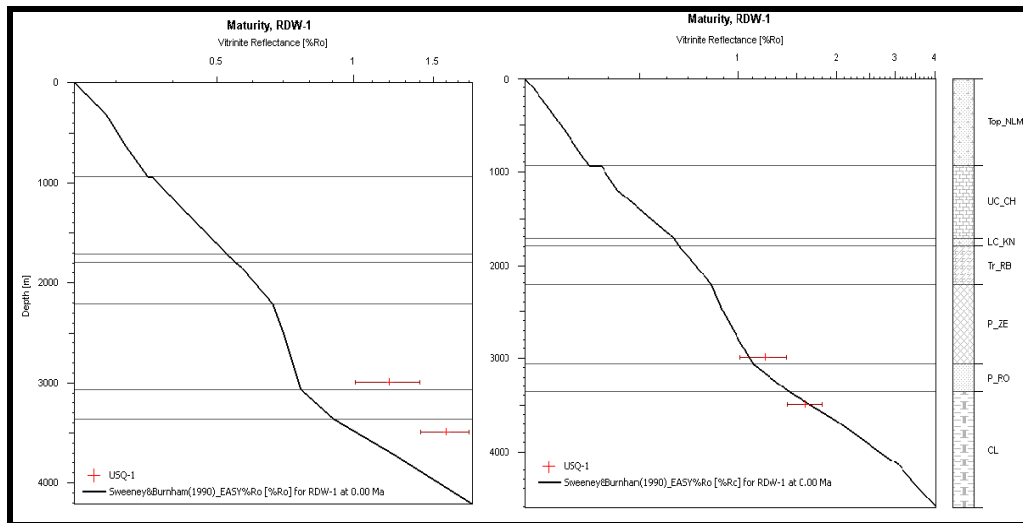


**Figure 4.4.** Maturity-paleoheat flow match of RDW-1 before and after calibration respectively.

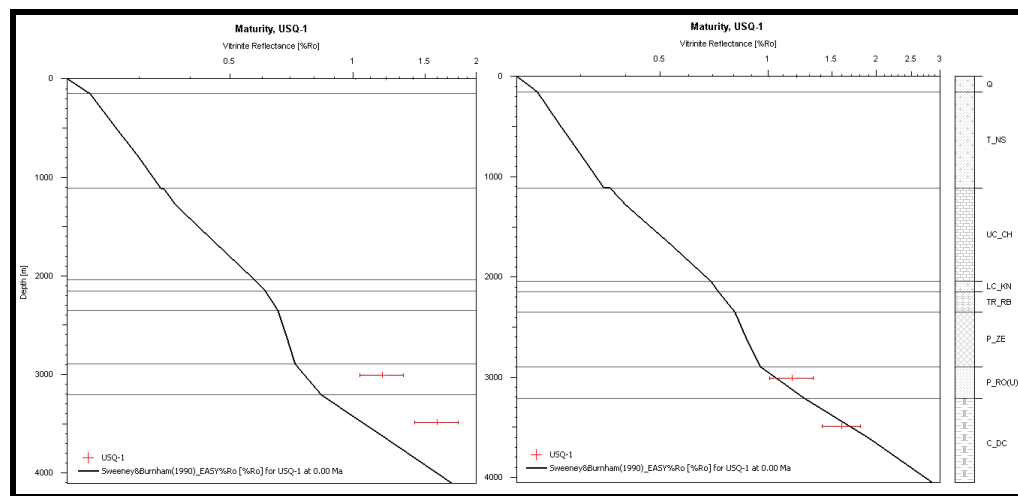


**Figure 4.5.** Maturity-paleoheat flow match of USQ-1 before and after calibration respectively.

#### **4.4 Sensitivity Analysis**

Sensitivity and uncertainty analysis in basin modeling is necessary to quantify the value of data, in other words, to quantify the reliability of the model. Uncertainties exist concerning the geologic concept of a model, its assumptions and its input parameters (Wenderbourg and Trabelsi, 2003). The aim is to model the closest possible one to the reality.

In this study, model was run by using different kinetic models and source rock thickness to see the effects on the results and their consistency with the previous studies. Sensitivity analysis was only applied to the well RDW-1.

##### **4.4.1 Kinetic Model Selection**

The complex reactions that cause formation of hydrocarbon from source rock as a result of breakdown of the kerogen are controlled by temperature and the activation energy of the particular reaction. Activation energies of each reaction, thus the kinetic model of each kerogen type are established from laboratory and field studies (Allen and Allen, 2005). Therefore, the kinetic model selection of the model is very important for the understanding of the hydrocarbon generation and expulsion.

The kinetic models for North Sea and type III source rocks that can be used in our study in the software PetroMod software include Ungerer (1990), Behar et al. (1997) and Vandenbroucke et al. (1999). These kinetic models were all derived from studies on Jurassic coals of the North Sea. Since, there is no kinetic model for Westphalian source rock in PetroMod software, the model results of three kinetic models were compared and evaluated. In the Figures 4.6 – 4.8, hydrocarbon zonation of the source rock in time as a result of different kinetic models is shown together with the burial history of the study area.

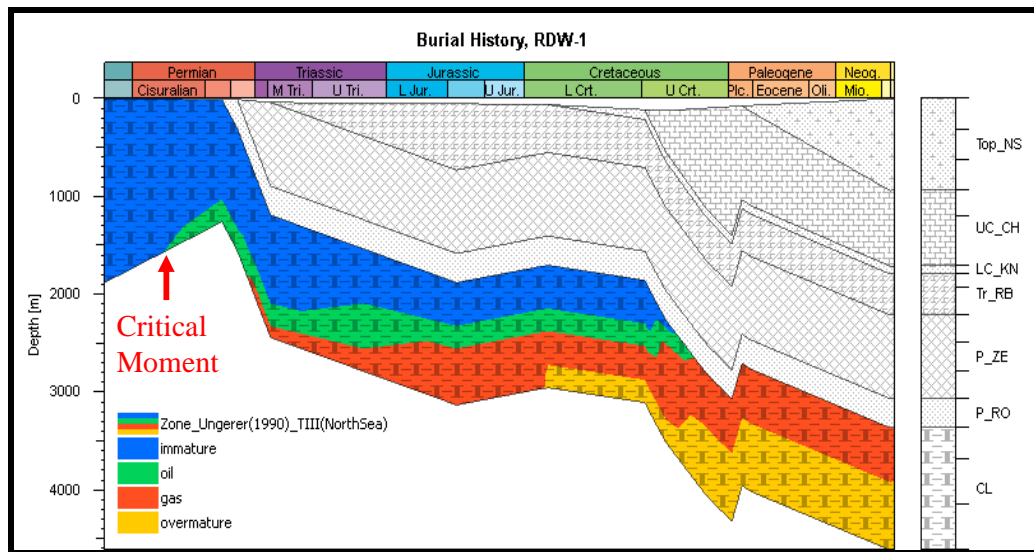


**Figure 4.6.** Burial history and hydrocarbon zones with kinetic model of Ungerer (1990).

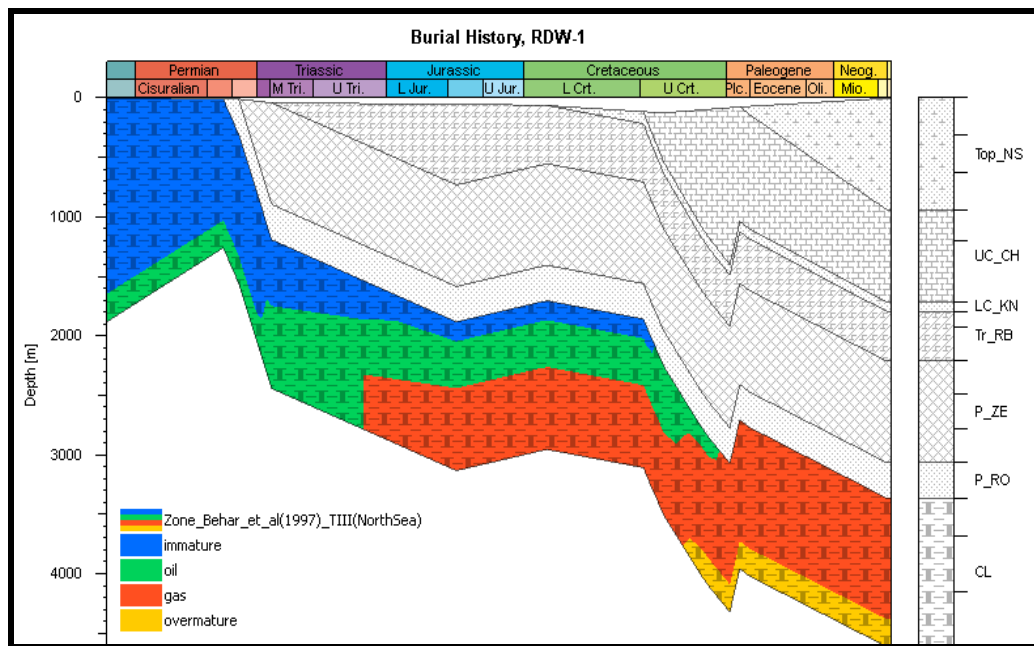


**Figure 4.7.** Burial history and hydrocarbon zones with kinetic model of Behar et al. (1997).

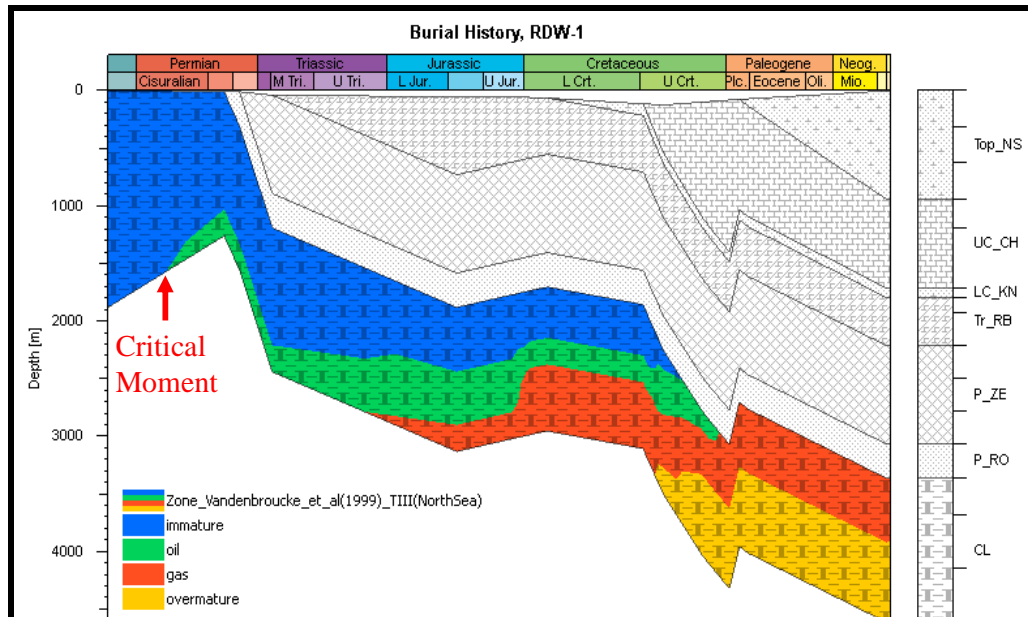


**Figure 4.8.** Burial history and hydrocarbon zones with kinetic model of Vandembroucke et al. (1999).

The results of Ungerer's (1990) and Vandembroucke et al. (1999) kinetic models show almost same critical moment with little difference in hydrocarbon zonation (Figures 4.6 & 4.8). Kinetic model of Behar et al. (1997) shows earlier time of hydrocarbon generation (Figure 4.7). Since the Vandembroucke et al. (1999) study is more recent compared to Ungerer's which also gave consistent results with the previous studies (e.g. Gautier, 2003), it is used in this study for the modeling.

#### 4.4.2 Source Rock Thickness Selection

Source rock thickness is obtained from the stratigraphic chart (Figure 1.5). Thickness of Westphalian A is between 500-1500 m and Westphalian B is between 200-600 m in the chart. Thus, source rock thickness is assumed to be changing between 700 m, to 2100 m with an average of 1250 m. Westphalian C and D are not taken into account because they are eroded in the study area (Figure 2.3).

In order to determine the suitable source rock thickness for the final model, the minimum, average and maximum thickness values are compared (Figures 4.9 – 4.11).

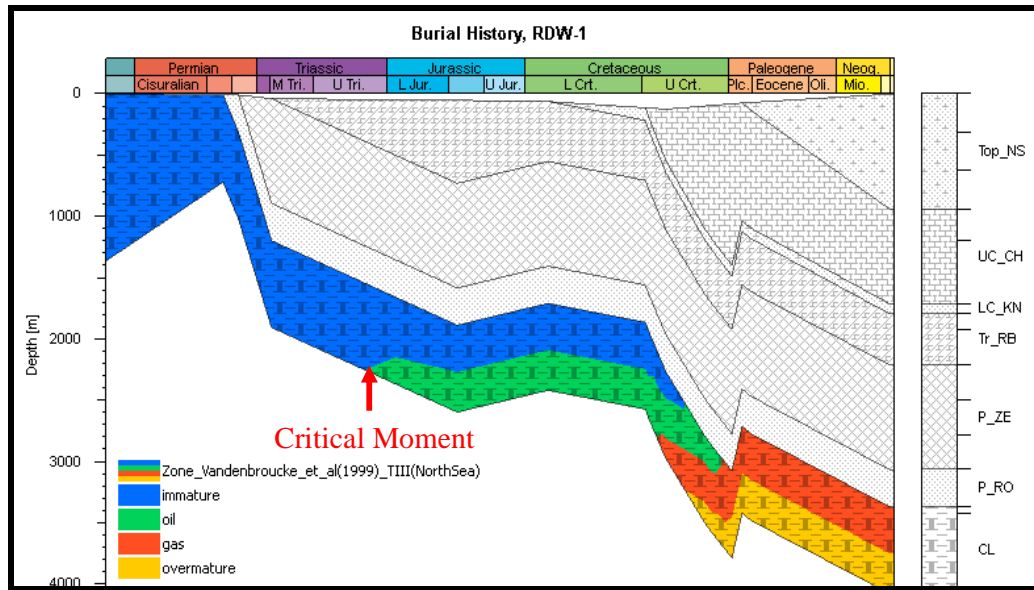


Figure 4.9. Burial history and hydrocarbon zones with 700 m source rock thickness.

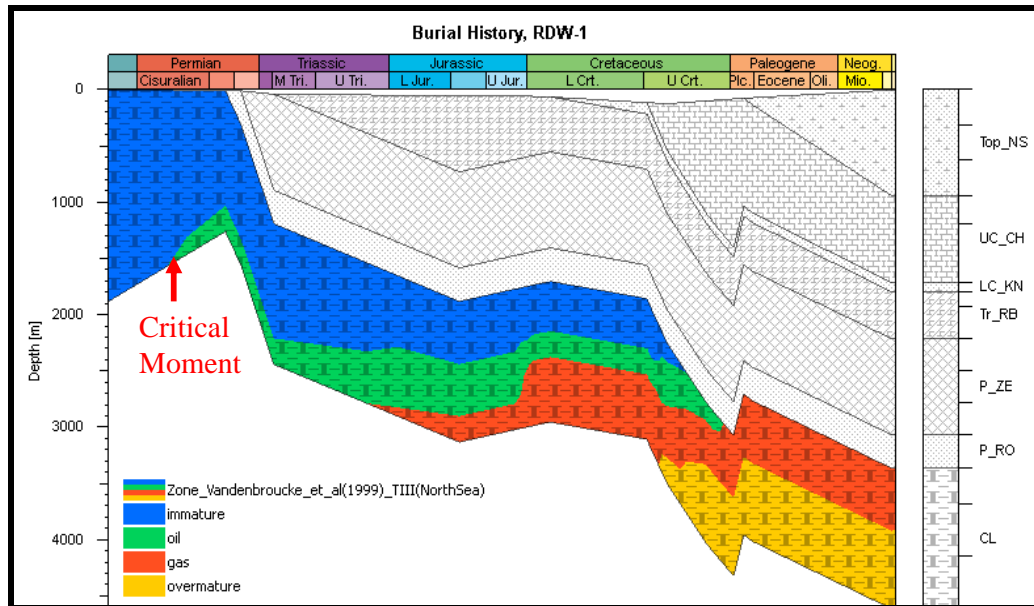
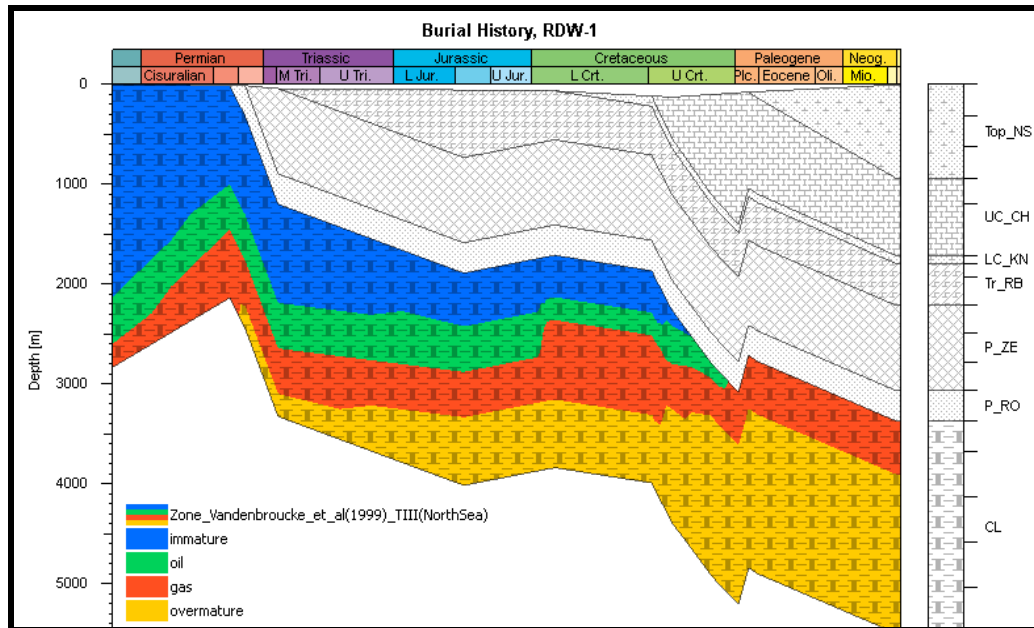


Figure 4.10. Burial history and hydrocarbon zones with 1250 m source rock thickness.



**Figure 4.11.** Burial history and hydrocarbon zones with 2100 m source rock thickness.

The thickness of the source rock affects the critical moment because of its effect on temperature. As seen in Figure 4.10, average thickness of 1250 m is consistent with the previous studies (e.g. Gautier, 2003). Therefore, it is used in this study for the modeling.

#### 4.5 1D Modeling Results

The model was run with aforementioned kinetic model based on Vandenbroucke et al. (1999) and source rock thickness as 1250m. 1D model results indicate that the main phase of hydrocarbon generation and expulsion from the Westphalian source rock began 172 Ma and continues until present (Figure 4.12). Results of all trials show that source rock is in mature to overmature and producing gas in present-day. The maturation is interpreted according to the kinetic model of Vandenbroucke which was obtained from Jurassic coal interval in North Sea as mentioned previously. As seen on Figures 4.12 & 4.13, the tectonic events have more impact on the nature and timing of hydrocarbon generation.

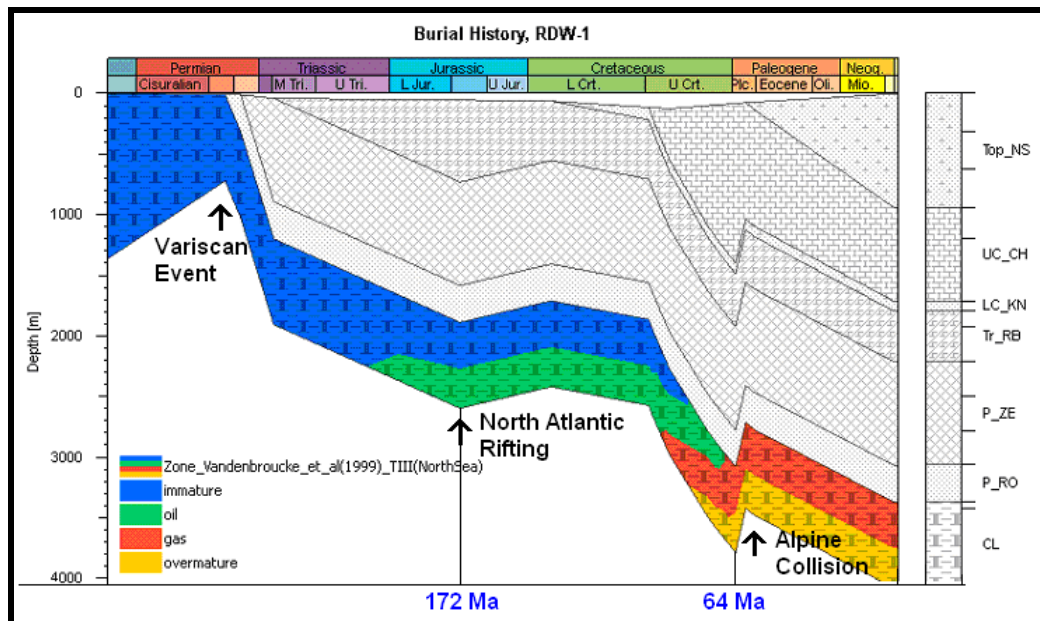


**Figure 4.12.** Burial history and hydrocarbon zones.

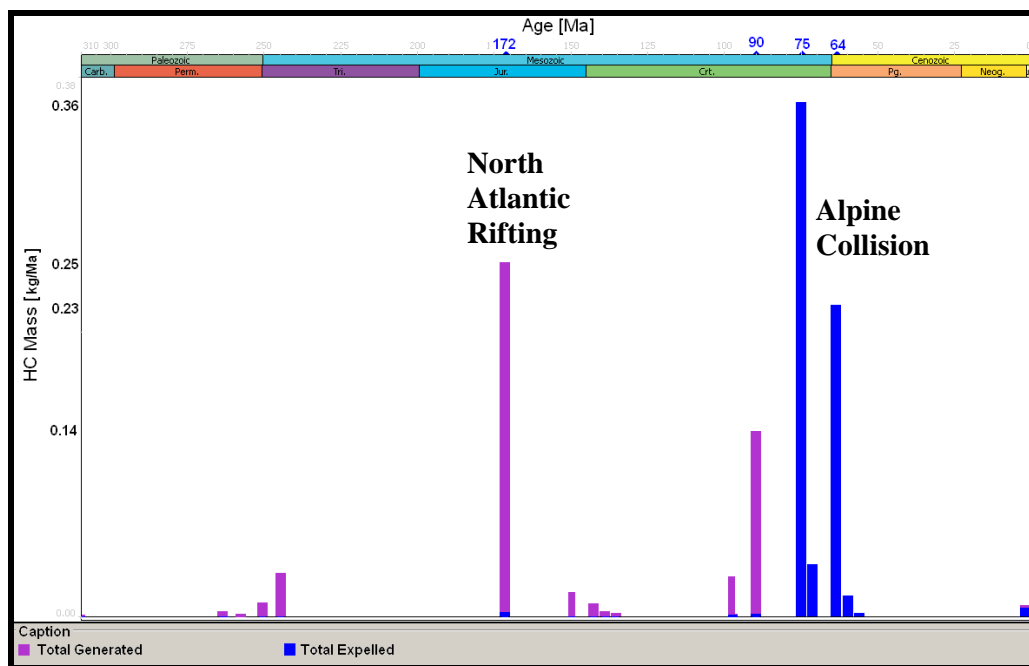


**Figure 4.13.** Graph showing time of total generated and expelled hydrocarbon from RDW-1 well. Note that the main hydrocarbon generation is during the Jurassic rifting phase and the main expulsion is during Alpine collision.

# CHAPTER 5

## 2D BASIN MODELING

### 5.1 Introduction and Data Processing

The 2D modeling has been carried out to have a more comprehensive understanding of the petroleum system in the area. In addition to 1D model results, 2D model gives results about possible distribution of the hydrocarbon. For this purpose, PetroMod software applications for data building; PetroBuilder, model run; Simulator and display; Viewer 2D have been used. The sequence that was followed during data preparation for simulation is as follows (Figure 5.1).

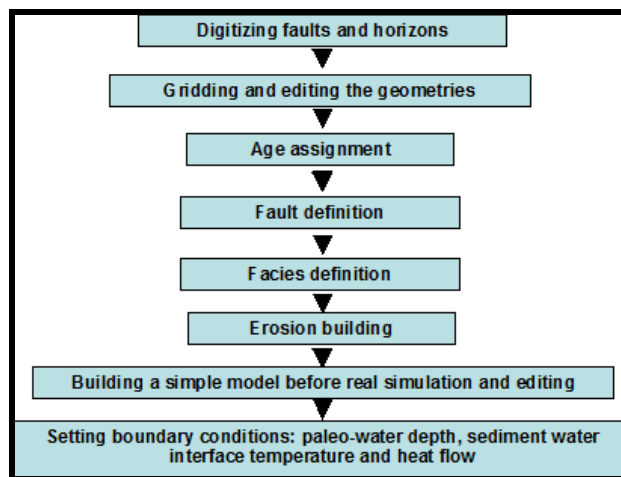


**Figure 5.1:** Data processing sequence in PetroBuilder (PetroMod, Tutorial Version 11, 2009).

One of the representative cross-sections of the region was chosen for the model and interpreted horizons and faults in Petrel (Chapter 3) have been loaded as image on seismic section and digitized in PetroMod software. After assigning the lithology, age and thickness of the rock units, erosion model has been built and boundary conditions have been set. Before simulation, it is possible to visualize the 2D burial history to see the possible inconsistencies and/or mismatches on the geometry. Model has been run after setting the calculation method, hydrocarbon migration method and the number and kinds of overlays such as kinetic calibration model(s) in Simulator. Simulator is the essential interface of the PetroMod software. It simulates the deposition of each layer from bottom to top and re-compact to obtain present-day geometry. This approach is called forward modeling. Results have been displayed in Viewer 2D.

The model run has been carried out several times until reaching an acceptable optimization value showing the geometrical consistency between defined input data and modeled present day section.

## **5.2 Inputs of the Model**

### **5.2.1 Geophysical, Geological and Geochemical Data**

Seismic crossline 1014 was used as the representative cross-section of the area. The fault and horizon interpretations were digitalized and gridded in PetroBuilder (Figure 5.2).

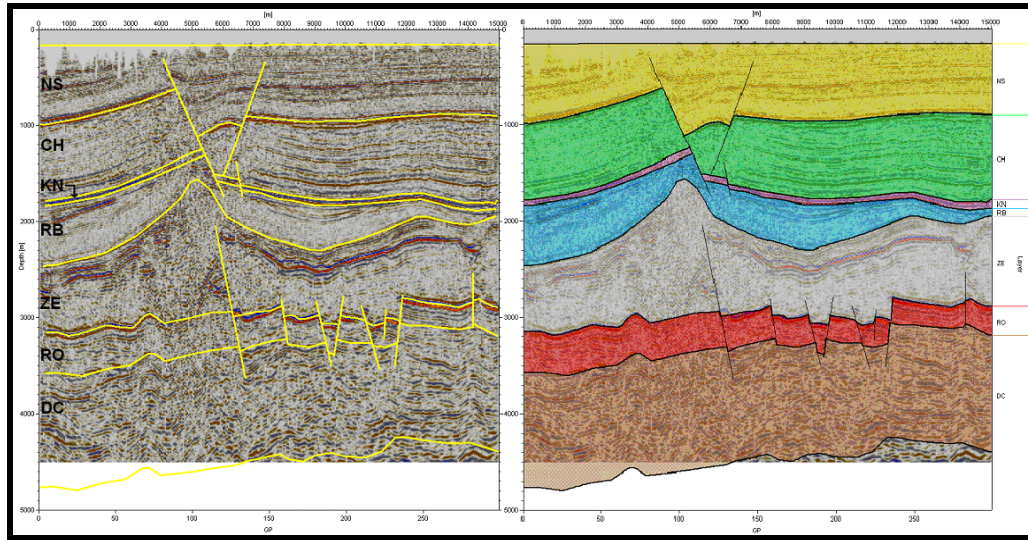


**Figure 5.2.** Crossline 1014 used for modeling purpose, pre-grid and grid-based sections respectively (abbreviations are same as Figure 3.2).

Age assignment of the layers is same as 1D modeling section (Table 4.1).

Faults were defined as sealing. In practice, fault activities coincide with the time of erosion. Thus, it was very hard to determine the duration of these activities. It is also known in the area that there is no hydrocarbon accumulation other than in the Permian carbonates intercalated with Zechstein salts and Rotliegend sandstones. This can be as a result of either the sealing faults or lack of suitable traps above this section. Presence of salt above these carbonates and Rotliegend sandstones is possibly the main factor preventing the faults to leak.

Facies definition; lithology, age and thickness of the layers were defined same as 1D model (Table 4.1).

Erosion model was built according to geological history of the region at three boundaries as it was interpreted in 1D model (Figure 5.3). The erosion amounts were also kept same as 1D model (Figure A.1 and Table A.1 in Appendix A).

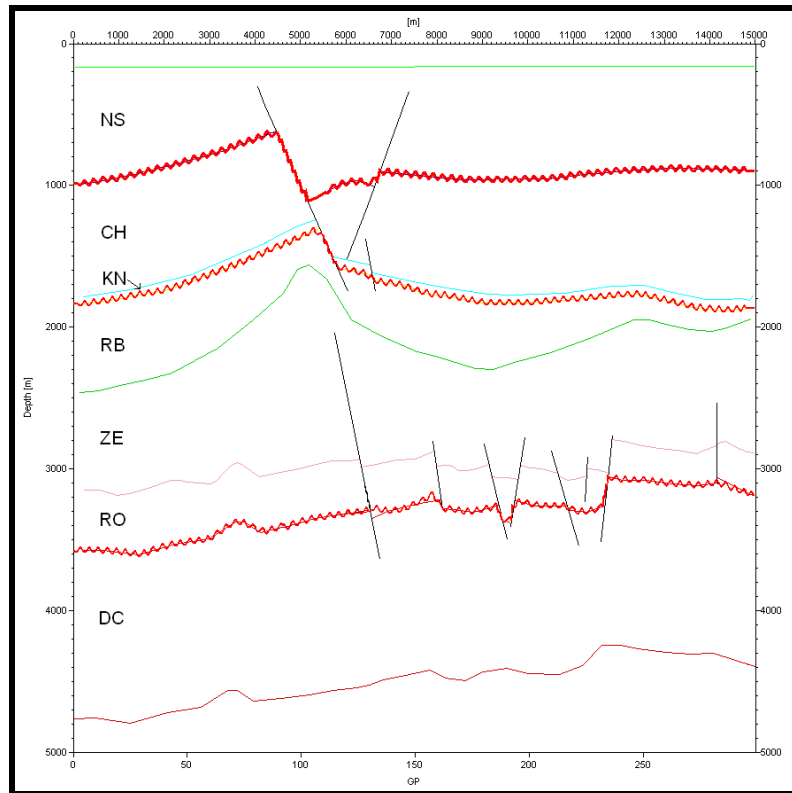


**Figure 5.3.** Erosion building (Red zigzag lines show unconformities).

In PetroMod software, it is possible to simulate salt movement in time. However, since salt is the sealing element of the petroleum system of the region and since it only shows local diapirism in the area (Figure 3.7), its movement was ignored in the model.

Simulation tool of PetroBuilder was used to preview the evolution of the basin for checking the geometries. Intersections of some horizons and faults were edited by using this tool. It was also possible to observe and evaluate the consistency of the time of uplifts and subsidence on the simulation preview. Erosions are observed from 310 Ma to 258 Ma, 172 Ma to 136 Ma and 72 Ma to 60 Ma. Other periods are characterized by the time of deposition and subsidence (Figure 5.4).

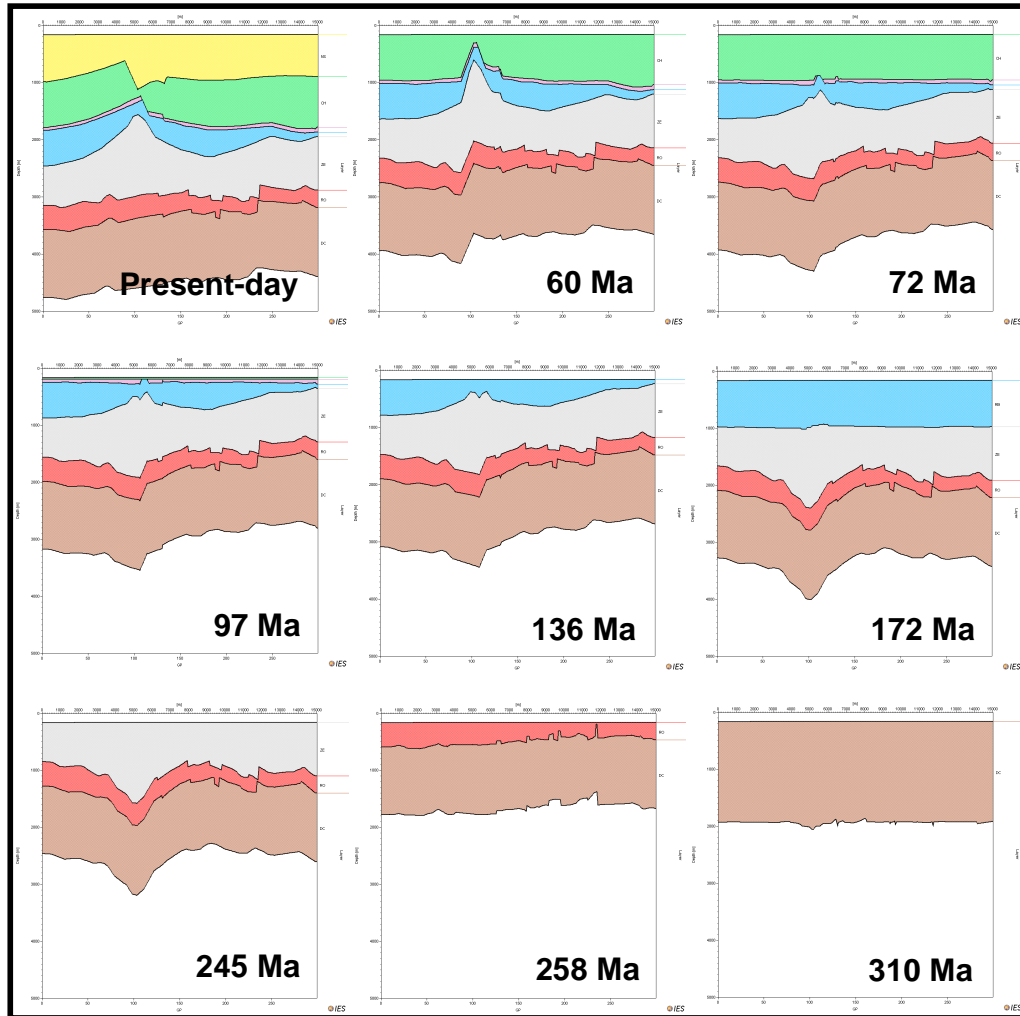


**Figure 5.4.** Simulation preview showing the evolution of the basin in time.

Boundary conditions were entered as 1D model (Table 4.2).

There are two wells cutting the cross-section used for calibration of the model by software; RDW-1 and WSM-1.

### **5.2.2 Simulation – Model Run**

The selection of the migration method is the most important decision of the model before simulation for the understanding of the migration trend. Hybrid (Darcy + Flowpath) method is set in this study as it is advised in PetroMod, Tutorial Version 11 (2009). This method takes into account calculation of fluid flow through porous media, buoyancy driving migration and percolation.

Calibration method and kinetic model were chosen as 1D model; Sweeney & Burnham, 1990 and Vandenbroucke et al., 1999 respectively.

The model was run after setting above mentioned inputs and parameters. The optimization value as a result of the model run was 0.4036% after five trials. Optimization value shows geometrical consistency between input and modeled section if the value is less than 1%.

### **5.3 2D Model Results**

The observed organic thermal maturity measurements in the study area indicate that the Westphalian source rock is at a mature to overmature stage as in the case of 1D model. The maturity of the Westphalian source rock increases gradually towards the west due to change in depth of burial. Measured maturity indices show gradual increase in thermal maturity with depth (Figure 5.5). There is no other defined sequence younger than Westphalian that had the capability to expel hydrocarbon in the study area. However, Namurian intervals (Figure 1.5) that has the capability to produce hydrocarbon was ignored in this study since this interval is totally overmature and known as source of Nitrogen (N<sub>2</sub>) in the area (Balen et al., 2000; Jurisch and Krooss, 2008).

The 2D model predicted that the Upper Rotliegend sandstone reservoirs are filled with gas condensate (Figure 5.5). Condensate forms when the wet gas yields accumulation of liquid in reservoir conditions that is changing into gas in surface conditions since the pressure drops below dewpoint. Dewpoint here is equal to the initial reservoir pressure.

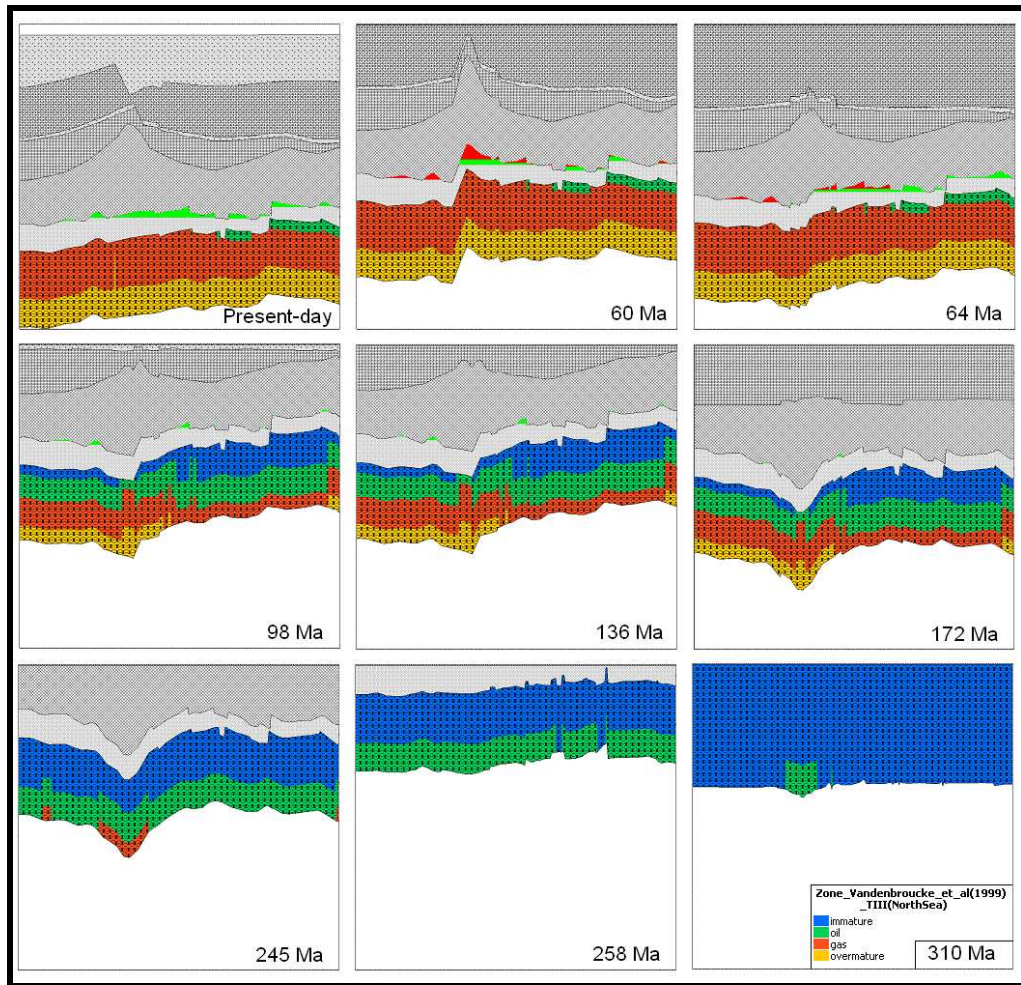


**Figure 5.5.** 2D model results of hydrocarbon zonation and accumulations in geological time.

Composition of the accumulated hydrocarbon has been calculated under subsurface conditions. As seen in the Figure 5.6, accumulated liquid in reservoir conditions changes into gas when flashed to surface conditions in the model result. In addition, the volume of accumulated hydrocarbons were calculated by assuming a lateral 1 km width of the reservoir in million barrels (MMbbls) for oil and million cubic meter (Mm<sup>3</sup>) for gas.

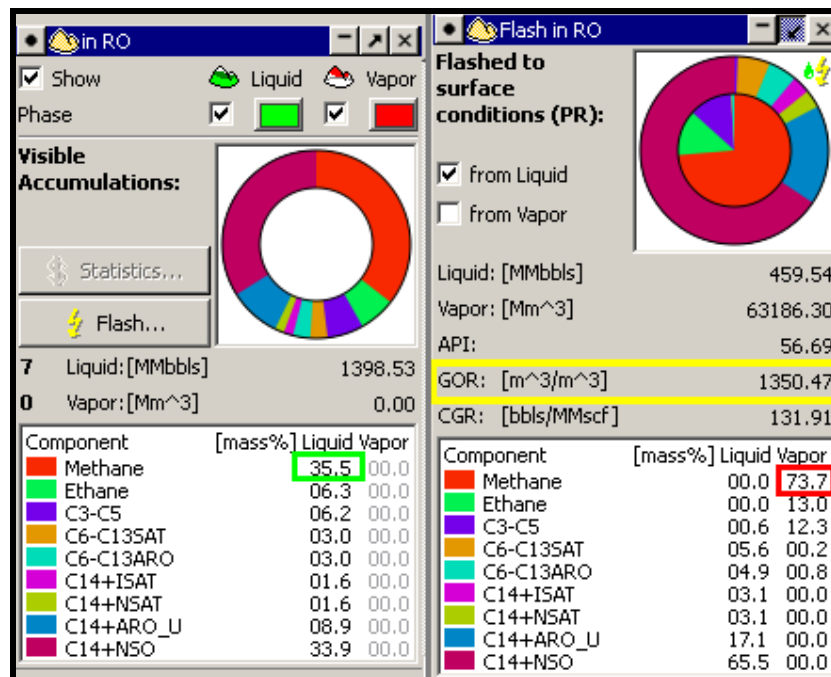


**Figure 5.6.** Accumulations in reservoir and surface conditions respectively.

The gas-oil ratio (GOR) has been used for the classification of the petroleum. GOR as a result of model is 1350.47 m<sup>3</sup>/m<sup>3</sup> which is within the gas condensate interval according to Table 5.1.

**Table 5.1.** Classification of petroleum (Hantschel and Kauerauf, 2009).

Class	GOR (m <sup>3</sup> /m <sup>3</sup> )	Composition
Dry Gas		CH <sub>4</sub> + other light gas comp. only
Wet Gas	> 10000	mainly CH <sub>4</sub> + other light gas comp.
Gas Condensate	570...10000	< 12.5 mol % C <sub>7+</sub>
Volatile Oil	310...570	12.5...20 mol % C <sub>7+</sub>
Black Oil	< 310	> 20 mol % C <sub>7+</sub>

Model results show that the main phase of hydrocarbon generation and expulsion from the Westphalian source began at 172 Ma and continues until present-day. After the initiation at 172 Ma, there is also significant amount of expulsion in 64 Ma (Figure 5.7). The model also predicts that the hydrocarbon migration is in short range vertically in up-dip direction (Figure 5.8).

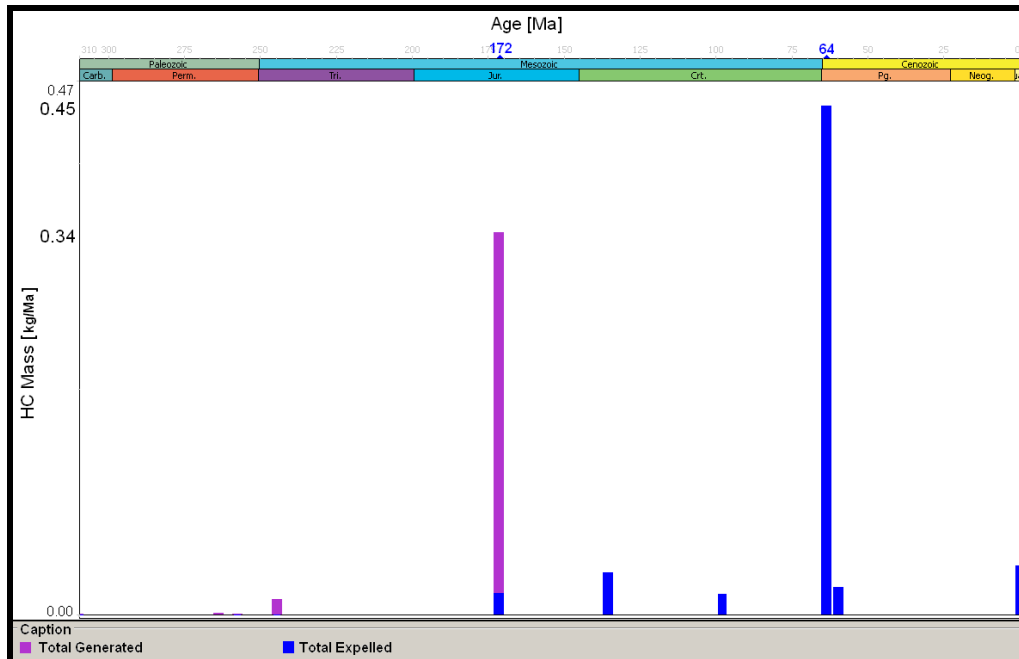


**Figure 5.7.** Graph showing total hydrocarbon generated and expelled as a result of 2D model.

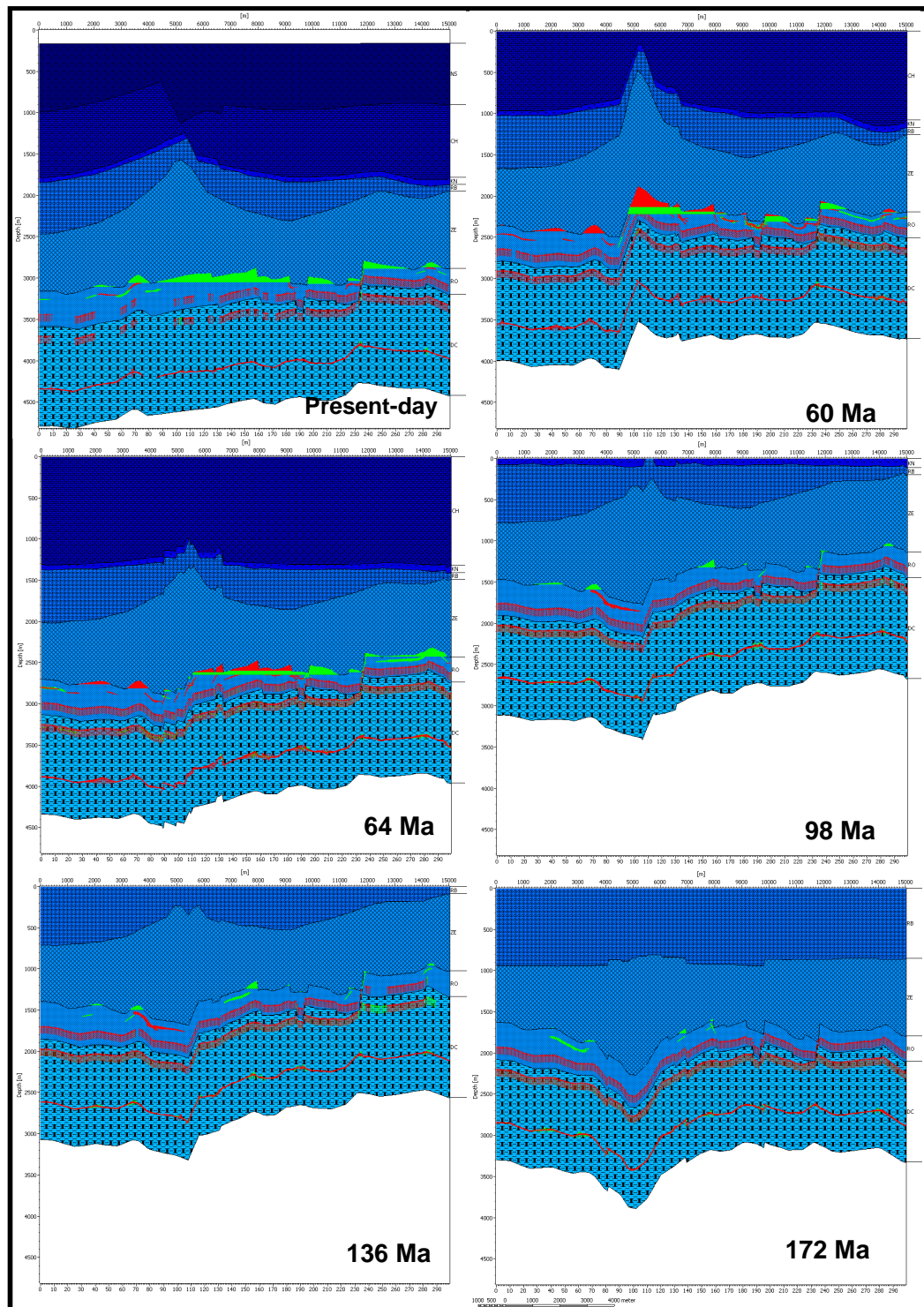


**Figure 5.8.** Migration pathways and accumulation of hydrocarbon. Red arrows show the up-dip migration.

## CHAPTER 6

### SUMMARY AND CONCLUSIONS

In this study, the petroleum system of a part of South Permian Basin is characterized and modeled. In order to accomplish this, geochemical, geophysical and geological studies are combined which include 3D seismic volume, borehole data and literature information which are used for the reconstruction of the geological history of the study area. Thermal maturation history, timing of hydrocarbon generation, expulsion and accumulation in the study area are predicted from model results.

The models were performed in 1D and 2D. Although, the parameters are same in both models, there are slight differences between the results. Both model results show that Westphalian source is mature to overmature recently. The accumulations in the reservoirs are gas condensate. Main generation and expulsion of hydrocarbon was at 172 Ma and 64 Ma which corresponds to main tectonic events in the region and are characterized by uplift and subsidence in the area.

Since the Westphalian source rock are overlain by fluvio-aeolian sandstone reservoirs of Upper Rotliegend, migration was assumed to be directly from source into the reservoir. Zechstein salt is the main seal rock in the basin forming a convenient trap at the time of accumulation. It seems that all the necessary elements of a petroleum system and processes (Figure 6.1) worked in the region tractably and resulted in the accumulations of hydrocarbons in the study area which is being one of the largest gas field in western Europe.

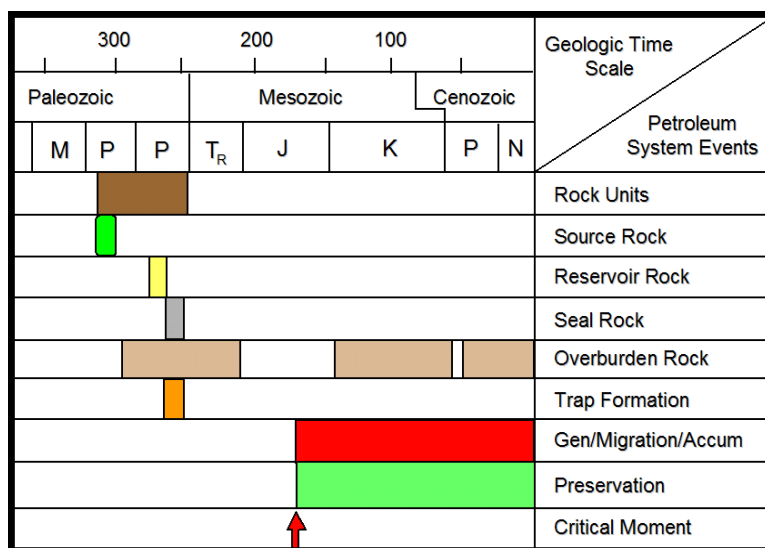


**Figure 6.1.** Petroleum system event chart of the study area.

The results are compatible with the Groningen Gas Field in which most of the wells are producing gas and gas condensate from the Carboniferous-Rotliegend Petroleum System.

In summary, most known traps were formed pre-Zechstein and critical moment for the hydrocarbon generation-migration-accumulation of petroleum commenced during Middle Jurassic and continues to the present. The timing of peak of hydrocarbon generation varies spatially and has begun after trap formation. Since migration trends of hydrocarbon are short range and hydrocarbon was migrated vertically from highly pressured area toward lower pressured zones, both early and late migration enhances the prospectivity of the porous Upper Rotliegend reservoirs. Prospective hydrocarbon traps may occur in the southwestern regions of the basin due to shallower depth of burial. Exploration risks decrease where the structural highs are available as a result of Zechstein salt movement. The wells that have no production (but have hydrocarbon shows) within the study area can be explained by locally inadequate reservoir quality.

## REFERENCES

Allen, P. A. and Allen, J. R. (2005). *Basin analysis principles and applications*. Blackwell Scientific Publications, London, p. 451.

Balen, R.T., Bergen, F., Leeuw, C., Pagnier, H., Simmelink, H., Wees, J.D. and Verweij, J.M. (2000). *Modeling the the hydrocarbon generation and migration in the West Netherlands Basin, the Netherlands*. Netherlands Journal of Geosciences 79 (1), pp. 29-44.

Buggenum, J.M. and den Hartog Jager, D.G. (2007). *Silesian in Geology of the Netherlands* edited by Th.E. Wong, D.A.J. Batjes & J. de Jager. Royal Netherlands Academy of Arts and Sciences.

Burnham, A.K. and Sweeney, J.J. (1991). *Modeling the maturation and migration of petroleum in Source and Migration Processes and Evaluation Techniques* edited by R.K. Merrill. Treatise of Petroleum Geology Handbook of Petroleum Geology, American Association of Petroleum Geologists, pp. 55-64.

Burrus, J., Espitalie, J., and Rudkiewivz, J., (1995). *Integrated basin modeling: From theory to practical applications*. Short course Notes, Am. Assoc. Petrol Geologists, p. 169.

Cornford, C. (1998). *Source rocks and hydrocarbons of the North Sea in Petroleum Geology of the North Sea* edited by K.W. Glennie. Blackwell Science, Oxford, pp. 376-462.

Gerling, P., Geluk, M. C, Kockel, F., Lokhorst, A., Lott, G. K. & Nicholson, R. A. (1999a). *'NW European Gas Atlas' - new implications for the Carboniferous gas plays in the western part of the Southern Permian Basin in Petroleum Geology of Northwest Europe: Proceedings of the 5th Conference* edited by FLEET, A. J. & BOLDY, S. A. R.. ©Petroleum Geology '86 Ltd. Published by the Geological Society, London, pp. 799-808.

Gerling, P., Kockel, F. and Krull, P. (1999b). Das Kohlenwasserstoff-Potential des Präwestfals im norddeutschen Becken - Eine Synthese, *DGMK-Forschungsbericht, Hamburg* 433, p. 107.

Gautier D.L. (2003). *Carboniferous-Rotliegend Total Petroleum System Description and Assessment Results Summary*. US Geological Survey Bulletin 2211.

Geluk, M.C. (2007). *Permian in Geology of the Netherlands* edited by Th.E. Wong, D.A.J. Batjes & J. de Jager. Royal Netherlands Academy of Arts and Sciences.

Geluk, M.C., Dusar, M. And Vos W. (2007). *Pre-Silesian in Geology of the Netherlands* edited by Th.E. Wong, D.A.J. Batjes & J. de Jager. Royal Netherlands Academy of Arts and Sciences.

Gent, H.W., Back, S., Urai, J.L., Kukla, P.A. and Reicherter, K. (2008). *Paleostresses of the Groningen area, the Netherlands—Results of a seismic based structural reconstruction*. *Tectonophysics* 470, pp. 147–161.

Glennie, K.W. (1998). *Petroleum geology of the North Sea: basic concepts and recent advances*. Blackwell Science, Oxford.

Gras, R. and Geluk, M.C. (1999). *Late Cretaceous – Early Tertiary sedimentation and tectonic inversion in the southern Netherlands*. *Netherlands Journal of Geosciences* 78, pp. 1-19.

Grötchsh, J. and Steenbrink, J. (2009). Presentation: *The Groningen Gas Field, 50 years of history – and a long future to come*. Retrieved from: [www.nlog.nl](http://www.nlog.nl) on 17 January 2010.

Hantschel, T. and Kaurauf, A.I. (2009). *Fundamentals of Basin and Petroleum Systems Modeling*. Springer, p. 476.

IHS Energy (2009). Retrieved from [www.ihsenergy.com](http://www.ihsenergy.com) on 22 November 2009.

Jager, J. (2007). *Geological Development in Geology of the Netherlands* edited by Th.E. Wong, D.A.J. Batjes & J. de Jager. Royal Netherlands Academy of Arts and Sciences.

Jager, J. and Geluk, M.C. (2007). *Petroleum Geology in Geology of the Netherlands* edited by Th.E. Wong, D.A.J. Batjes & J. de Jager. Royal Netherlands Academy of Arts and Sciences.

Jurisch, A., Krooss, B.M. (2008). *A pyrolytic study of the speciation and isotopic composition of nitrogen in carboniferous shales of the North German Basin*. *Organic Geochemistry* 39, pp. 924–928.

Kombrink, H. (2008). *The Carboniferous of the Netherlands and surrounding areas; a basin analysis*. Thesis in Faculty of Geosciences, Utrecht University.

Magoon, L.B. and Dow, W.G. (1994). *The Petroleum System – From Source to Trap*. AAPG Memoir 60, pp. 3-24.

Magoon, L.B. (2009). *History of the Petroleum System Concept*. AAPG Hedberg Research Conference, May 3-7, 2009 - Napa, California, U.S.A. Retrieved from <http://www.searchanddiscovery.net/abstracts/html/2009/hedberg/abstracts/extended/magoon/magoon.htm> in 2009.

Mccann, T., Pascal, C., Timmerman, M. J., Krzywirc, P., Lopez-Gomez, J., Wetzels, A., Krawczyk, C.M., Rieke, H. and Lamarche, J. (2006). *Post-Variscan (end Carboniferous–Early Permian) basin evolution in Western and Central Europe* in *European Lithosphere Dynamics* edited by Gee, D. G. & Stephenson, R. A.. Geological Society, London, Memoirs 32, pp. 355–388.

NL Oil and Gas Portal (2009). Retrieved from [www.nlog.nl](http://www.nlog.nl) on 10 November 2009.

PetroMod, Tutorial Version 11 (2009). Retrieved from [http://www.ies.de/index.php?option=com\\_content&task=view&id=35&Itemid=57](http://www.ies.de/index.php?option=com_content&task=view&id=35&Itemid=57) on 23 February 2010.

Tissot, B. P., Pelet, R. and Ungerer, Ph. (1987). *Thermal History of Sedimentary Basins, Maturation Indices, and Kinetics of Oil and Gas Generation*. AAPG Bulletin Volume 71.

Van Adrichem Boogaert, H.A. and Kouwe, W.F.P. (compilers) (1994). *E. Triassic (Lower and Upper Germanic Triassic Groups) in Stratigraphic nomenclature of the Netherlands*. Revision and update by RGD and NOGPA. Mededelingen Rijks Geologische Dienst 50, pp. 1-28.

Van Dalfsten, W., Doornenbal, J.C., Dortland S., Gunnink, J.L. (2006). *A comprehensive seismic velocity model for the Netherlands based on lithostratigraphic layers*. Netherlands Journal of Geosciences 85 (4), pp. 277-292.

Van Wees, J.D., Stephenson, R.A., Ziegler, P.A., Bayer, U., McCann, T., Dadlez, R., Gaupp, R., Narkiewicz, M., Bitzer, F. & Scheck, M. (2000). *On the origin of the Southern Permian Basin, Central Europe*. Marine and Petroleum Geology 17, pp. 43-59.

Veeken, P.C.H. (2007). *Chapter 2: The Seismic Reflection Method and Some of Its Constraints in Seismic Stratigraphy, Basin Analysis and Reservoir Characterisation* edited by K. Helbig and S. Treitel. Elsevier.

Veld, H., Fermont, W.J.J. and Jegers L.F. (1993). *Organic petrological characterization of Westphalian coals from The Netherlands: Correlation between Tmax, vitrinite reflectance and hydrogen index*. Geochemistry Vol.20, No.6, pp.659-675.

Verweij, H. (2003). *Fluid flow systems analysis on geological timescales in onshore and offshore Netherlands*. Netherlands Institute of Applied Geosciences – National Geological Survey.

Waples, D.W. (1994). *Maturity modeling: Thermal indicators, Hydrocarbon generation, and oil cracking in The petroleum system – from source to trap* edited by Magoon, L.B. and Dow, W.G.. AAPG Memoir 60.

Wendebourg, J. and Trabelsi, K. (2003). *Sensitivity and uncertainty analysis in basin modeling to quantify the value of data*. Beicip-Franlab publications.

Ziegler, P.A. (1982). *Geological Atlas of Western and Central Europe*. The Hague: Shell Internationale Petroleum Maatschappij B.V. Elsevier Scientific Publishing Company, p. 130.

# APPENDIX A

## LITERATURE DATA USED IN THE MODEL

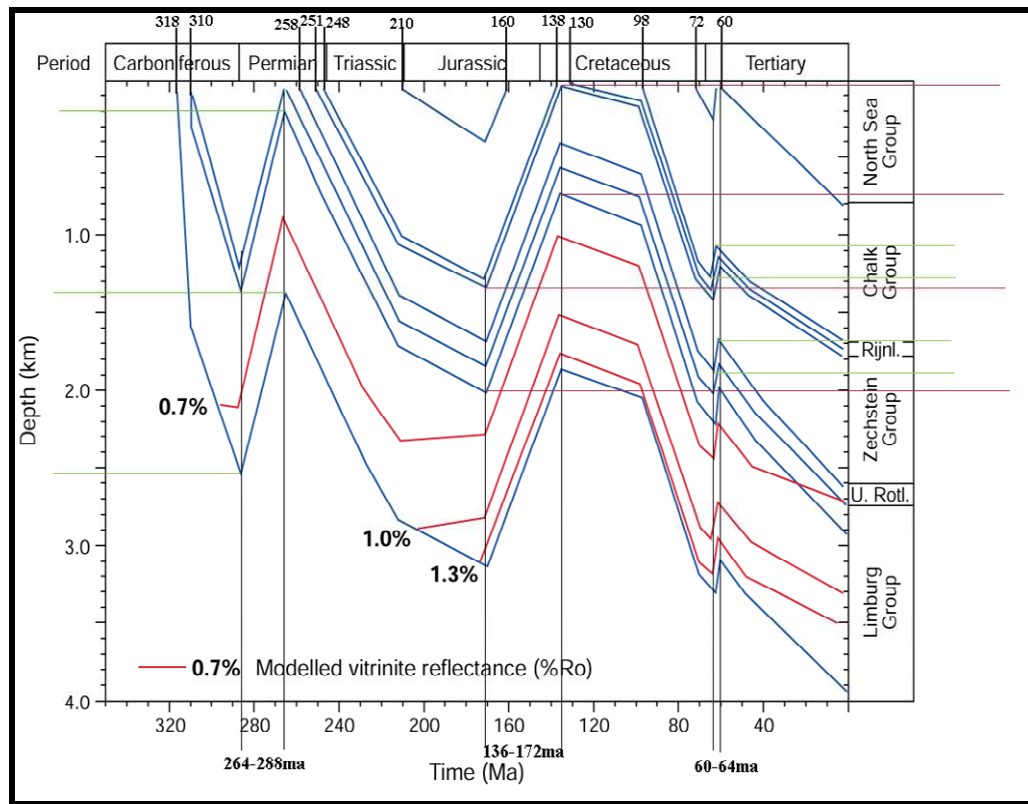


Figure A.1. Burial history with maturity evolution of ROT-1

**Table A.1.** Erosion amounts from reference well ROT-1 and calculated erosions for RDW-1 and USQ-1 wells.

Interval	Average Thicknesses Cut by Wells	Thickness in Roode-Till-1	Erosion in Roode-Till-1	Thickness in RDW-1	Erosion in RDW-1	Thickness in USQ-1	Erosion in USQ-1
Q	151	?		0		152	
NS	735	800		938		959	
UC-CH	780	900	220 (64-60ma)	773	256	932	212
LC-KN	115	50?100		81		109	
Tr-RB	279	50?0	1250 (172-136ma)	418	150	200	313
P-ZE	767	800		854		543	
P-RO(U)	277	150		298		315	
C-DC	116	1250	1175 (310-264ma)	1250	600	1250	600

**Table A.2.** Vitrinite reflectance (Rm) and hydrogen index (HI) values from Ruurlo well (Veld et al., 1993).

Ruurlo (RLO-1), n=39					
Depth	%Rm	HI (mg HC/g TOC)	Depth	%Rm	HI (mg HC/g TOC)
813.80	0.96	220	1194.31	1.26	178
826.83	0.89	187	1212.35	1.31	171
832.44	1.02	193	1213.89	1.21	163
852.07	1.02	190	1235.53	1.29	147
860.23	0.99	198	1238.87	1.16	184
870.11	1.05	184	1260.62	1.27	147
888.73	1.01	191	1262.43	1.26	129
912.91	1.02	204	1270.15	1.33	180
954.71	1.11	156	1287.31	1.33	154
997.00	1.05	181	1293.14	1.21	145
999.57	0.97	228	1301.67	1.32	135
1042.82	1.07	195	1309.83	1.30	164
1050.46	1.05	172	1310.72	1.35	154
1055.95	1.02	246	1347.59	1.37	148
1066.88	1.04	190	1372.38	1.40	129
1112.68	1.18	183	1378.10	1.21	144
1116.14	1.10	186	1435.81	1.41	132
1185.60	1.15	190	1454.80	1.47	121
1188.52	1.09	160	1478.82	1.45	129
1192.18	1.23	147	<b>Average HI</b>		<b>171</b>

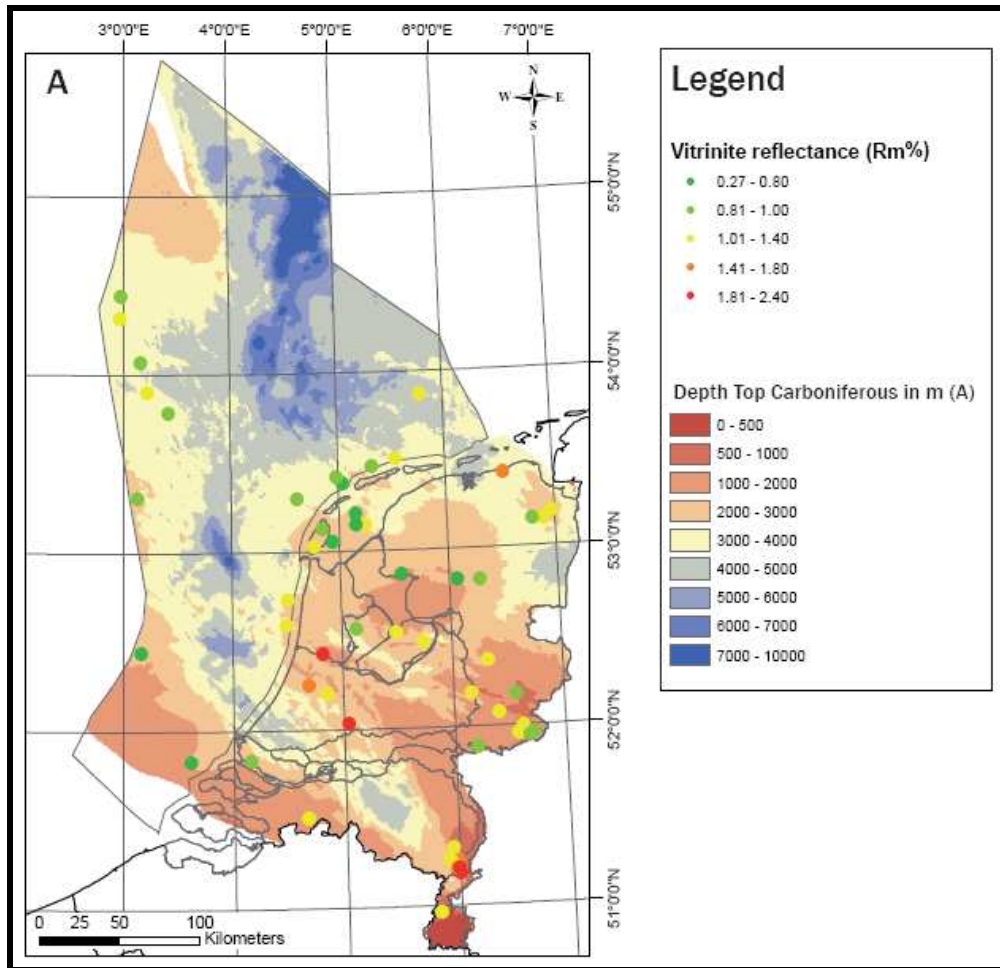


**Figure A.2.** Maturity map of Westphalian A/B boundary (IHS, 2009).

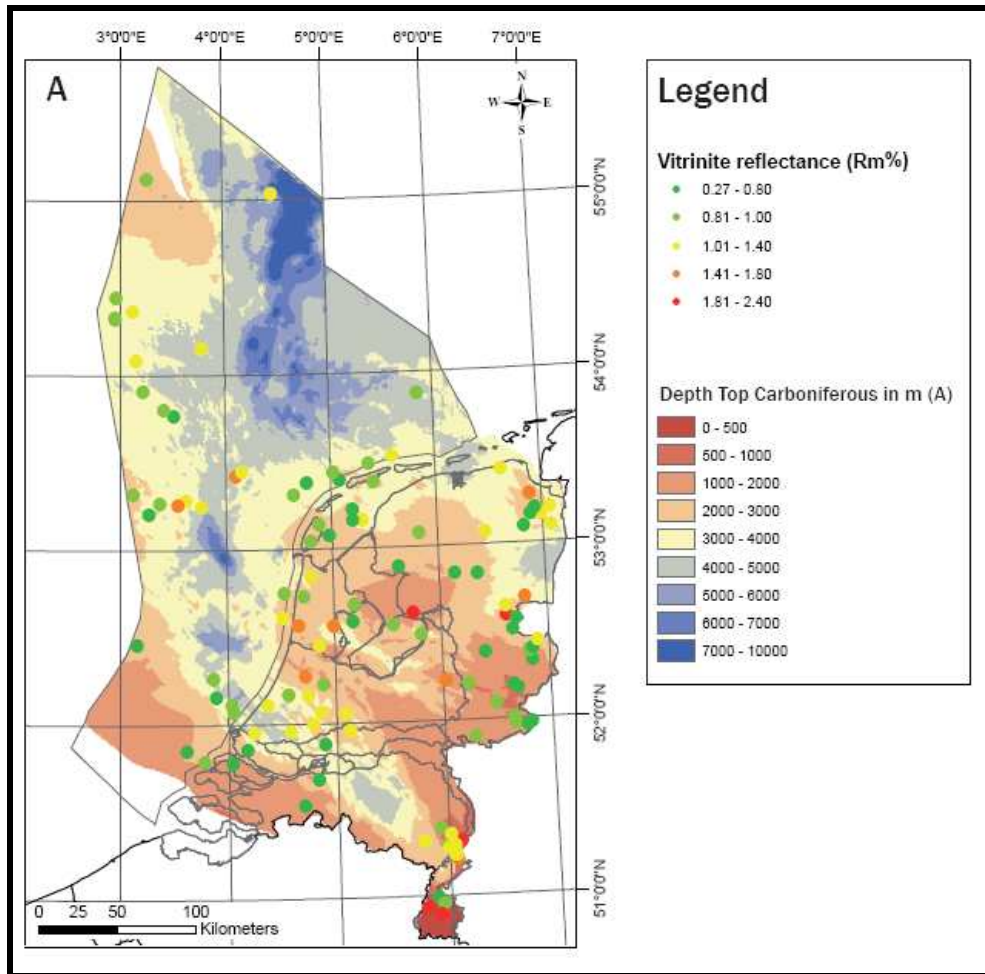


**Figure A.3.** Maturity map of Top Carboniferous (IHS, 2009).

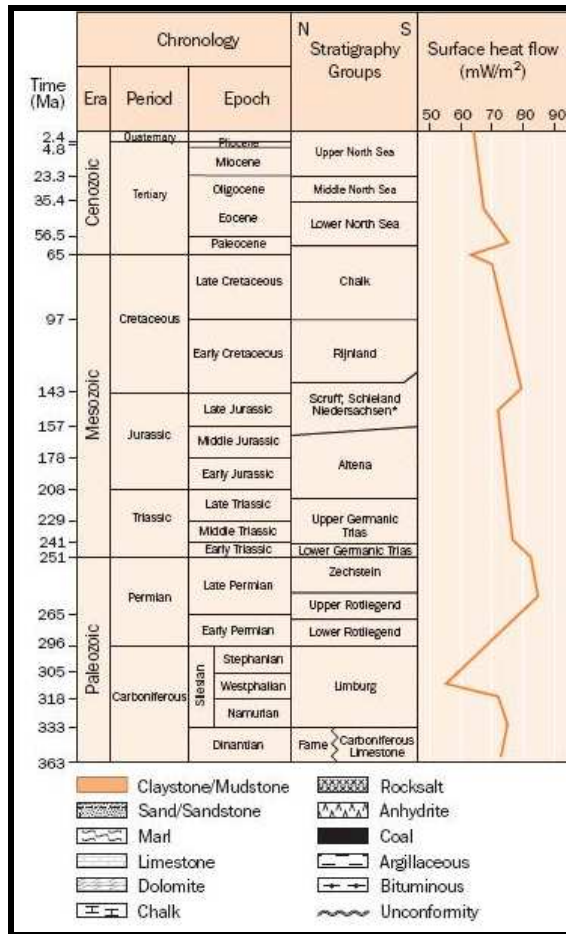


**Figure A.4.** Heat flow history in onshore and offshore Netherlands (Verweij, 2003).

## APPENDIX B

### INTERPRETED HORIZONS MAPS

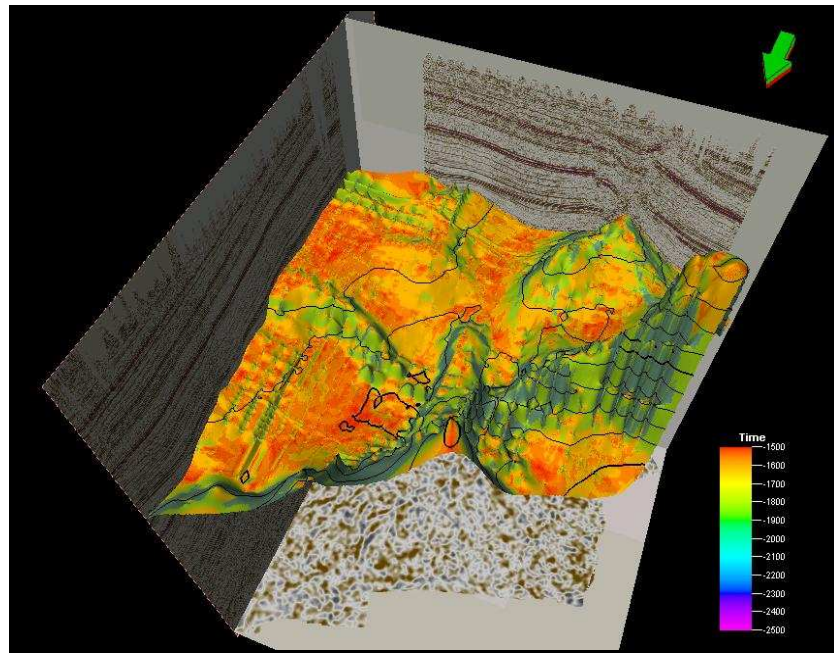


**Figure B.1.** Map of Top Permian (top Zechstein) in time.

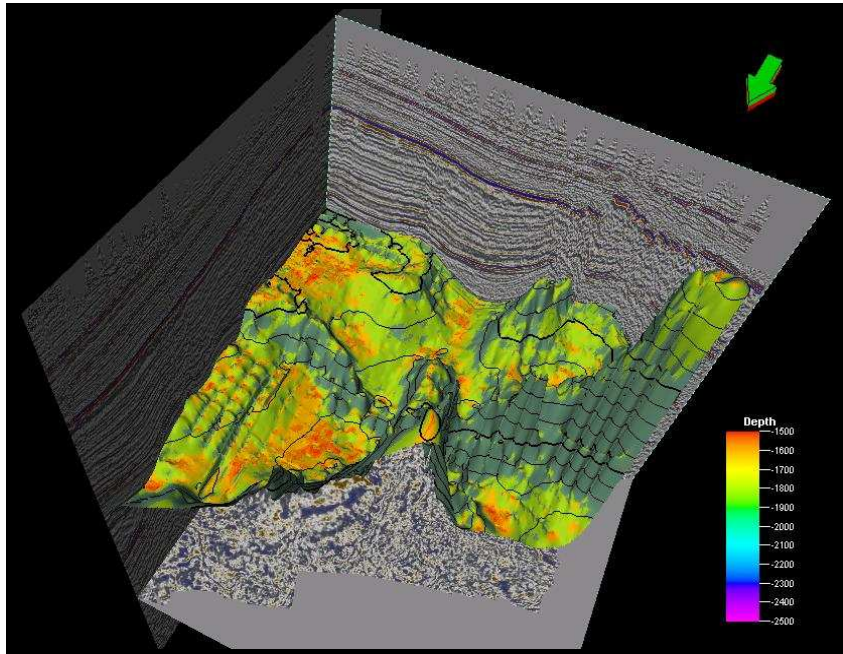


**Figure B.2.** Map of Top Permian (top Zechstein) in depth.

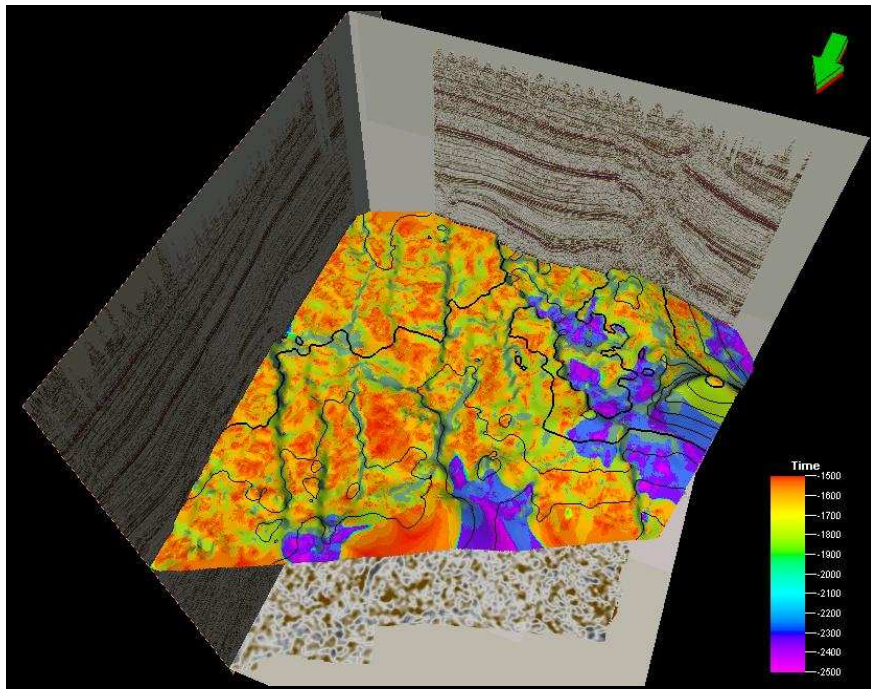


**Figure B.3.** Map of Top Rotliegend in time.

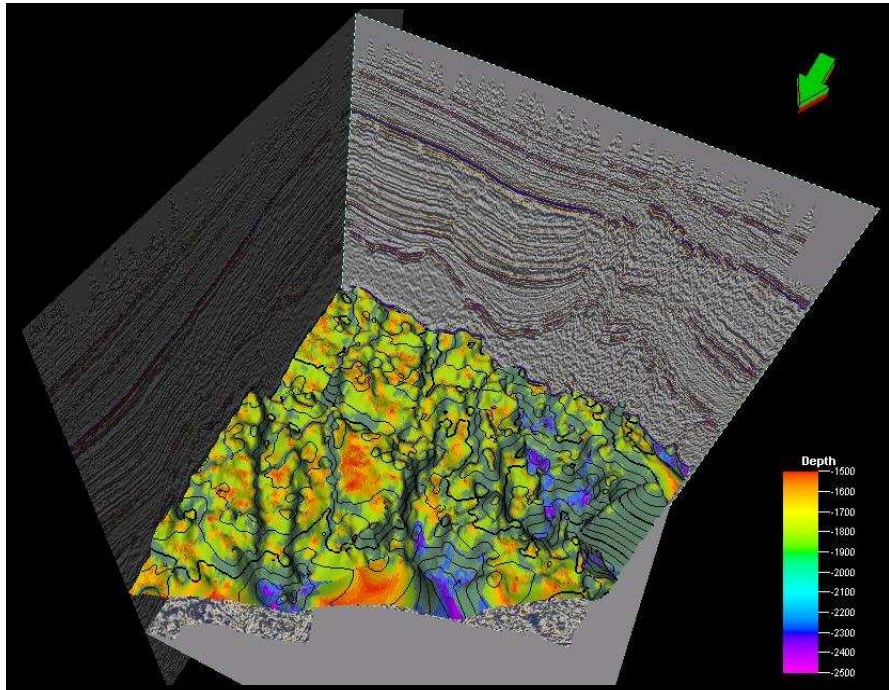


**Figure B.4.** Map of Top Rotliegend in depth .

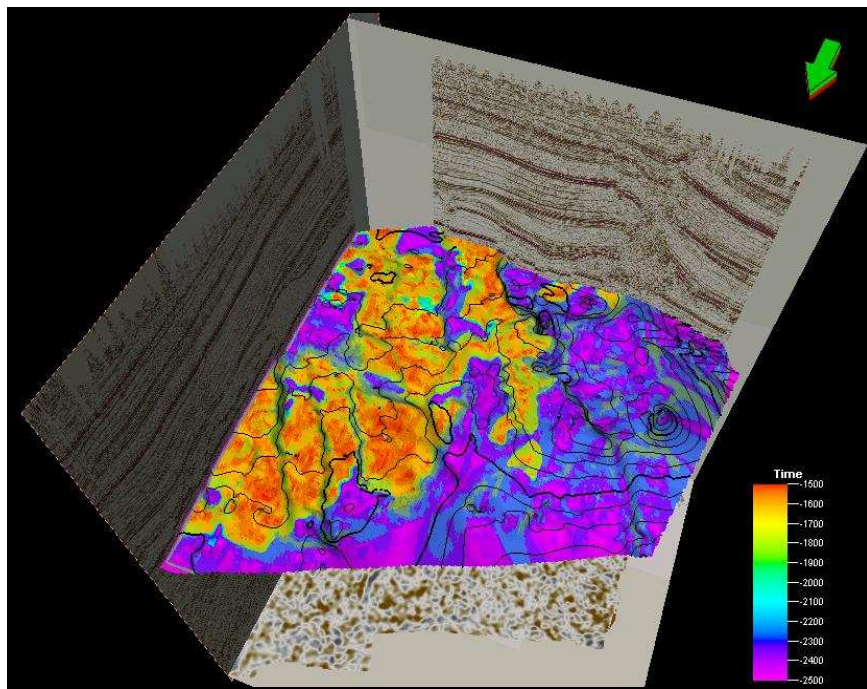


**Figure B.5.** Map of Top Carboniferous in time.

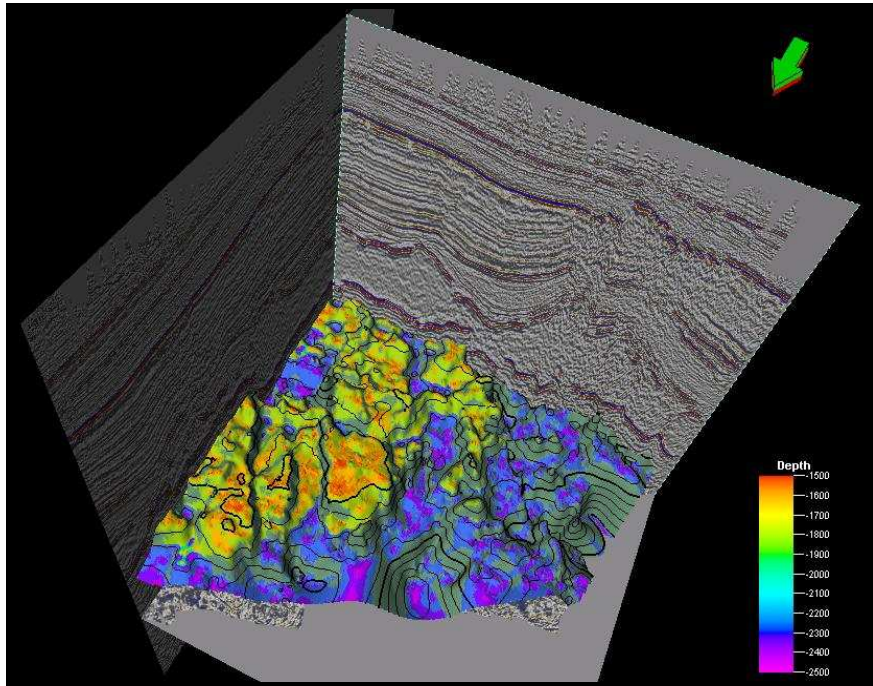


**Figure B.6.** Map of Top Carboniferous in depth.

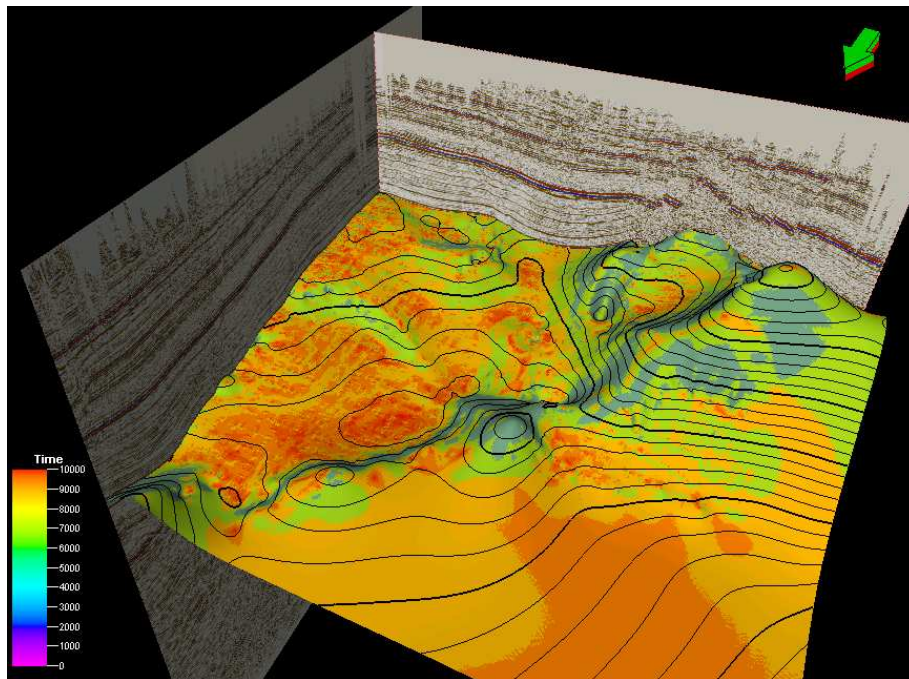


**Figure B.7.** Map of Top Rijnland Group in time.

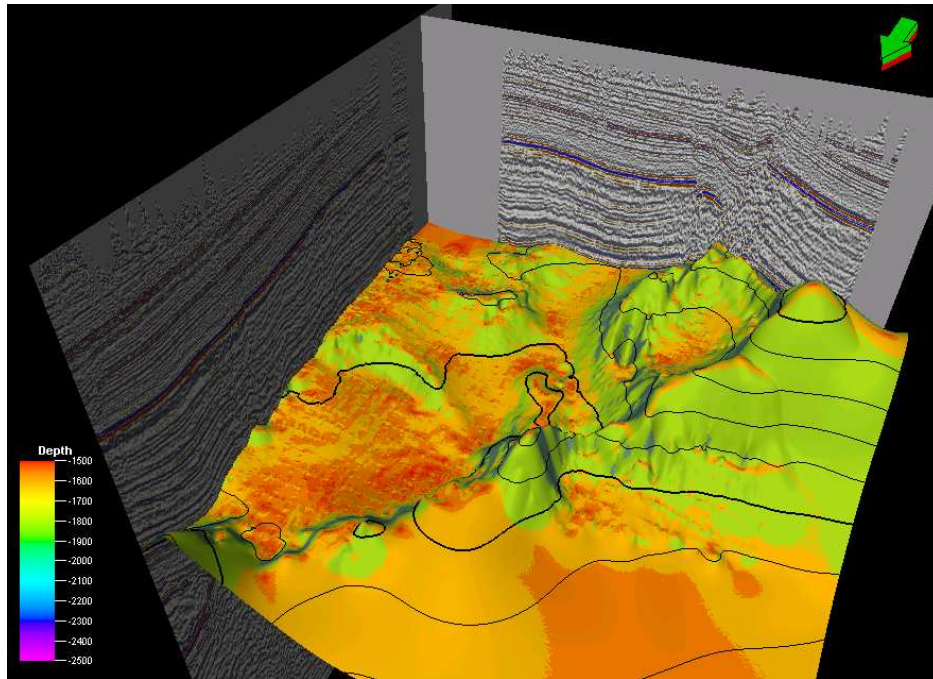


**Figure B.8.** Map of Top Rijnland Group in depth.

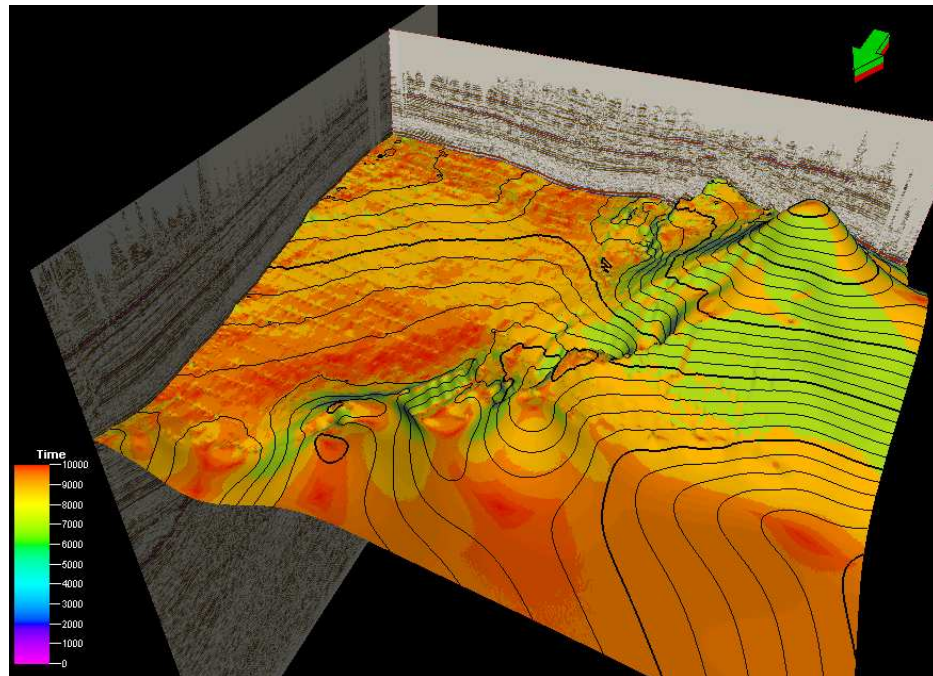


**Figure B.9.** Map of Top Chalk Group in time.

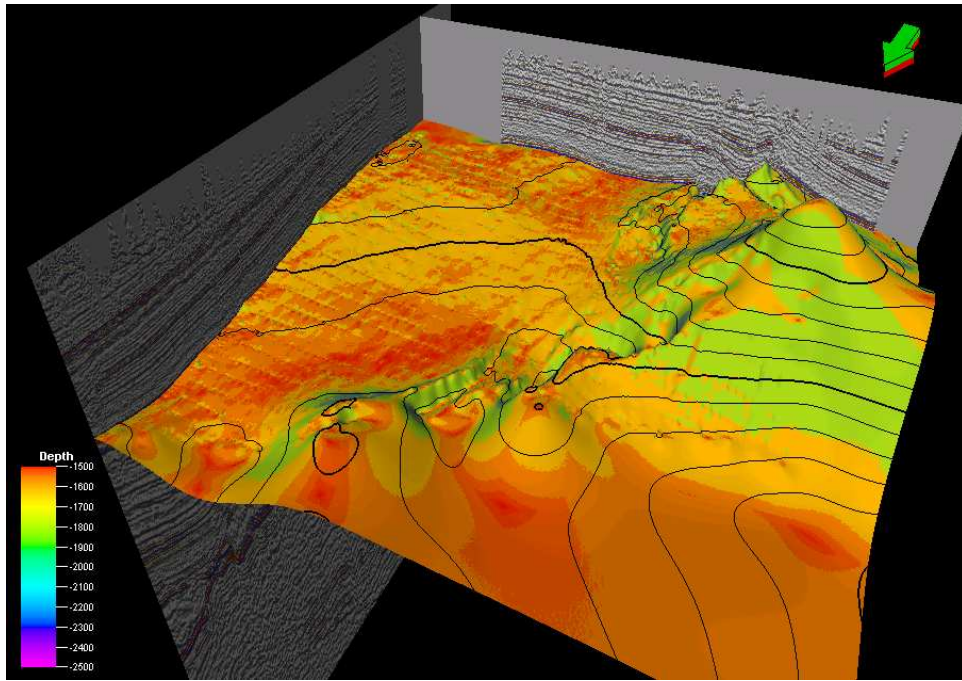


**Figure B.10.** Map of Top Chalk Group in depth.

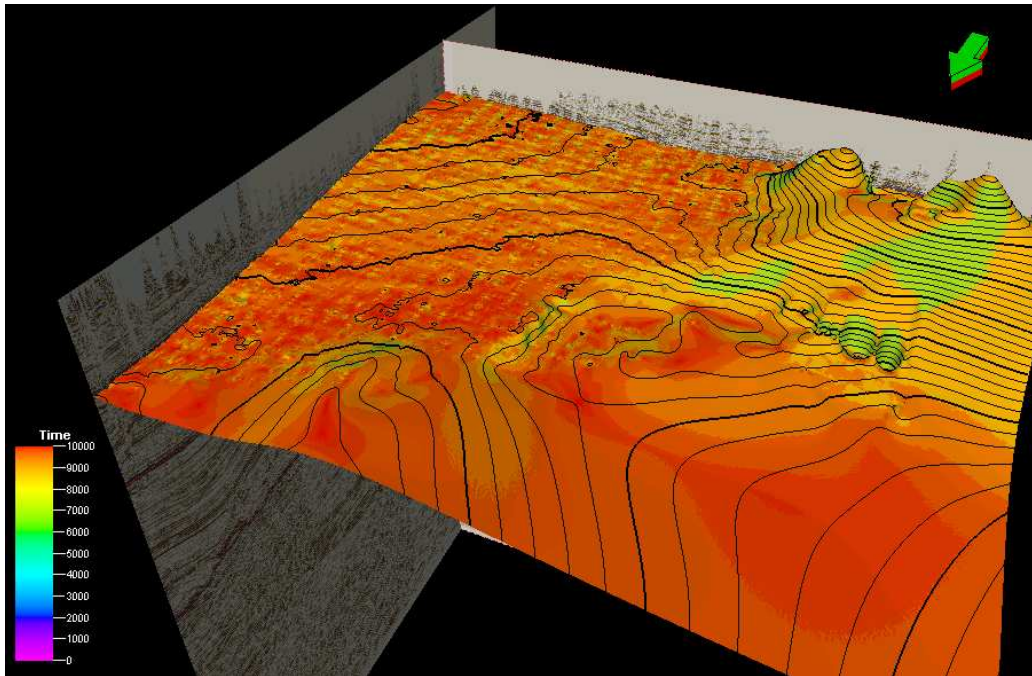


**Figure B.11.** Map of Top North Sea Group in time.

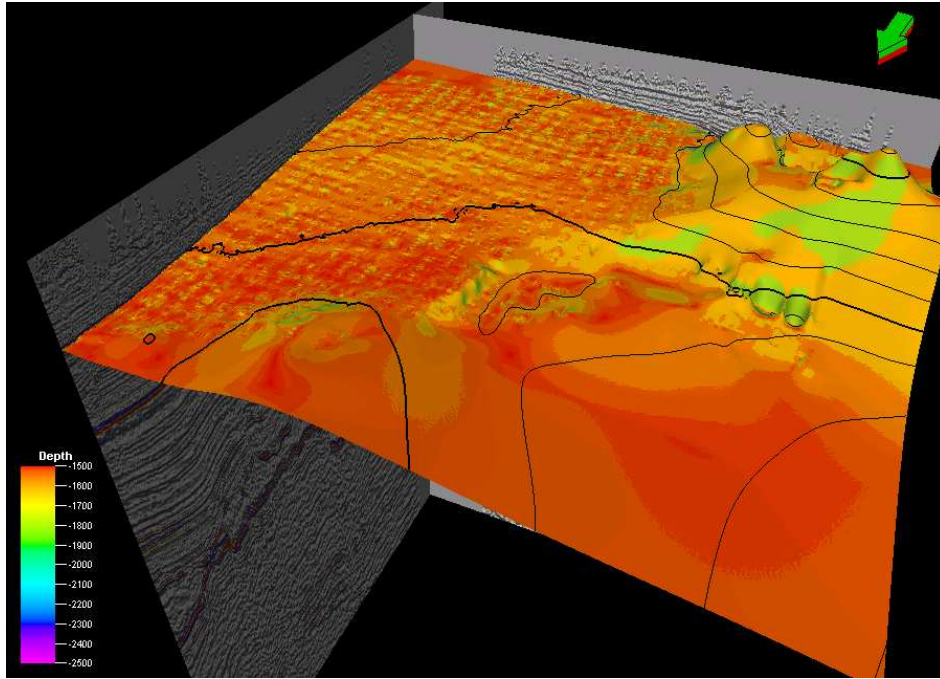


**Figure B.12.** Map of Top North Sea Group in depth.